

**UNCLASSIFIED**

---

**AD 282 125**

*Reproduced  
by the*

**ARMED SERVICES TECHNICAL INFORMATION AGENCY  
ARLINGTON HALL STATION  
ARLINGTON 12, VIRGINIA**



---

**UNCLASSIFIED**

NOTICE: When government or other drawings, specifications or other data are used for any purpose other than in connection with a definitely related government procurement operation, the U. S. Government thereby incurs no responsibility, nor any obligation whatsoever; and the fact that the Government may have formulated, furnished, or in any way supplied the said drawings, specifications, or other data is not to be regarded by implication or otherwise as in any manner licensing the holder or any other person or corporation, or conveying any rights or permission to manufacture, use or sell any patented invention that may in any way be related thereto.

282 125

282 125

62-4-5

**U. S. A R M Y**  
**TRANSPORTATION RESEARCH COMMAND**  
**FORT EUSTIS, VIRGINIA**

CATALOGED BY ASTIA

AS AD NO.

NOX

TCREC TECHNICAL REPORT 62-36

**HOVERING STATIC STABILITY  
AND PERFORMANCE EXPERIMENTS  
ON THREE-DIMENSIONAL ANNULAR JET MODELS**

Task 9R99-01-005-02

Contract DA 44-177-TC-709

November 1961

**prepared by:**

AERONUTRONIC  
A Division of Ford Motor Company  
Ford Road,  
Newport Beach, California

ASTIA  
RECEIVED  
AUG 16 1962  
TISIA C



#### DISCLAIMER NOTICE

When Government drawings, specifications, or other data are used for any purpose other than in connection with a definitely related Government procurement operation, the United States Government thereby incurs no responsibility nor any obligation whatsoever; and the fact that the Government may have formulated, furnished, or in any way supplied the said drawings, specifications, or other data is not to be regarded by implication or otherwise as in any manner licensing the holder or any other person or corporation, or conveying any rights or permission, to manufacture, use, or sell any patented invention that may in any way be related thereto.

#### ASTIA AVAILABILITY NOTICE

Qualified requesters may obtain copies of this report from

Armed Services Technical Information Agency  
Arlington Hall Station  
Arlington 12, Virginia

This report has been released to the Office of Technical Services, U. S. Department of Commerce, Washington 25, D. C., for sale to the general public.

The information contained herein will not be used for advertising purposes.


The findings and recommendations contained in this report are those of the contractor and do not necessarily reflect the views of the Chief of Transportation or the Department of the Army.

HEADQUARTERS  
U. S. ARMY TRANSPORTATION RESEARCH COMMAND  
Fort Eustis, Virginia

The contemplated Army missions for Ground Effect Machines require that the ground clearances be greater and the overall machine dimensions be smaller, leading to a higher value of  $h/d$  ratio than has usually been investigated for air cushion concepts. Since the annular jet and plenum chamber configurations normally become unstable at  $h/d$  ratios above 0.05 to 0.1, this investigation was undertaken to determine the static stability of a generalized annular jet in hovering and forward flight and to evaluate various modifications which would improve the stability. In addition to stability, data were generated on control forces and performance.

The results of this investigation indicate that inherent stability can be achieved in the GEM at the operating heights believed to be necessary for overland use.

FOR THE COMMANDER:

  
KENNETH B. ABEL  
1st Lt., TC  
Assistant Adjutant

APPROVED BY:

  
WILLIAM D. HINSHAW  
Project Engineer

Publication No. U-1443  
Dated 10 November 1961

SPECIAL PROGRAMS OPERATIONS

Submitted to:

U. S. Army Transportation Research Command  
Fort Eustis, Virginia

CONTRACT NO. DA 44-177-TC-709

# TECHNICAL REPORT

HOVERING STATIC STABILITY AND PERFORMANCE  
EXPERIMENTS ON THREE-DIMENSIONAL ANNULAR  
JET MODELS

Prepared by:

*B. H. Carmichael*

B. H. Carmichael

Approved by:

*M. F. Southcote*

M. F. Southcote, Manager  
Air Transportation

AERONUTRONIC

A DIVISION OF *Ford Motor Company*

FORD ROAD/NEWPORT BEACH, CALIFORNIA

## TABLE OF CONTENTS

	<u>PAGE</u>
LIST OF ILLUSTRATIONS	1
LIST OF SYMBOLS	4
SUMMARY	6
INTRODUCTION	8
TEST FACILITY	9
MODEL AND INSTRUMENTATION DESCRIPTION	10
DATA REDUCTION PROCEDURE	12
EXPERIMENTAL RESULTS	23
1.    LONGITUDINAL STABILITY	23
A.    SIMPLE PERIPHERAL JET MODELS	23
B.    SHAPED BASES	25
C.    SKIRTED AND FLAP SEGMENTED MODELS	26
D.    JET SEGMENTED MODELS	27
2.    LATERAL STABILITY	53
A.    SIMPLE PERIPHERAL JET MODELS	53
B.    SHAPED BASES	54
C.    SKIRTED AND FLAP SEGMENTED MODELS	54
D.    JET SEGMENTED MODELS	54
3.    QUALIFICATION OF THE STABILITY RESULTS	79
A.    RESPONSE OF THE FLOW SUPPLY	79
B.    POSSIBLE CONTRIBUTIONS NOT MEASURED IN THESE TESTS	79
4.    PERFORMANCE ASPECTS	80
A.    EFFECT OF TILT ON LIFT	80
B.    COST OF STABILIZATION	81
ACKNOWLEDGEMENTS	88
BIBLIOGRAPHY	89

## LIST OF ILLUSTRATIONS

	<u>PAGE</u>
1. Hovering Test Facility (Photograph 10520).	13
2. Available and Required Pressure vs. Flow.	14
3. Three-Dimensional Model Bases (Photograph 10217).	15
4. Vertical Peripheral Jet Model Drawing.	16
5. 45° Inclined Peripheral Jet Model Drawing.	17
6. Shaped Base Model Drawing.	18
7. Skirted and Flap Segmented Model Drawing.	19
8. Centerline Jet Segmented Model Drawing.	20
9. Corner Lobe Jet Segmented Model Drawing.	21
10. Concentric Jet Segmented Model Drawing.	22
<u>(A) Longitudinal Stability</u>	
11. Vertical Peripheral Jet Model - Base + Jet Center of Pressure Shift.	30
12. Vertical Peripheral Jet Model - Base Center of Pressure Shift.	31
13. Vertical Peripheral Jet Model - Jet Center of Pressure Shift.	32
14. 45° Inclined Peripheral Jet Model - Base + Jet Center of Pressure Shift.	33
15. 45° Inclined Peripheral Jet Model - Base Center of Pressure Shift.	34
16. 45° Inclined Peripheral Jet Model - Jet Center of Pressure Shift.	35
17. Static Longitudinal Hovering Stability - Vertical vs. 45° Inclined Jet.	36
18. Height-Pitch Angle Stability Boundaries - Vertical vs. 45° Inclined Jet.	37
19. Effect of Base Shaping on Base + Jet Center of Pressure Shift.	38
20. Effect of Base Shaping on Base + Jet Center of Pressure Shift.	39



LIST OF ILLUSTRATIONS, continued...

	<u>PAGE</u>
21. Effect of Skirt and Flaps on Base + Jet Center of Pressure Shift.	40
22. Effect of 5% Length Skirt and Flaps on Static Longitudinal Hovering Stability	41
23. Centerline Jet Segmented Model - Base + Jet Center of Pressure Shift.	42
24. Centerline Jet Segmented Model - Base Center of Pressure Shift.	43
25. Centerline Jet Segmented Model - Jet Center of Pressure Shift.	44
26. Corner Lobe Jet Segmented Model - Base + Jet Center of Pressure Shift.	45
27. Corner Lobe Jet Segmented Model - Base Center of Pressure Shift.	46
28. Corner Lobe Jet Segmented Model - Jet Center of Pressure Shift.	47
29. Concentric Jet Segmented Model - Base + Jet Center of Pressure Shift.	48
30. Concentric Jet Segmented Model - Base Center of Pressure Shift.	49
31. Concentric Jet Segmented Model - Jet Center of Pressure Shift.	50
32. Effect of Jet Segmentation on Static Longitudinal Hovering Stability.	51
33. Effect of Jet Segmentation on Height-Pitch Angle Stability Boundaries.	52
<u>(B) Lateral Stability</u>	
34. Vertical Peripheral Jet Model - Base + Jet Center of Pressure Shift.	57
35. Vertical Peripheral Jet Model - Base Center of Pressure Shift.	58
36. Vertical Peripheral Jet Model - Jet Center of Pressure Shift.	59
37. 45° Inclined Peripheral Jet Model - Base + Jet Center of Pressure Shift.	60
38. 45° Inclined Peripheral Jet Model - Base Center of Pressure Shift.	61
39. 45° Inclined Peripheral Jet Model - Jet Center of Pressure Shift.	62
40. Static Lateral Hovering Stability - Vertical vs. 45° Inclined Jet.	63
41. Effect of Base Shaping on Base + Jet Center of Pressure Shift.	64

LIST OF ILLUSTRATIONS, continued . . .

	<u>PAGE</u>
42. Effect of Base Shaping on Base + Jet Center of Pressure Shift	65
43. Effect of Skirt and Flaps on Base + Jet Center of Pressure Shift	66
44. Effect of 5% Length Skirt and Flaps on Static Lateral Hovering Stability	67
45. Centerline Jet Segmented Model - Base + Jet Center of Pressure Shift	68
46. Centerline Jet Segmented Model - Base Center of Pressure Shift	69
47. Centerline Jet Segmented Model - Jet Center of Pressure Shift	70
48. Corner Lobe Jet Segmented Model - Base + Jet Center of Pressure Shift	71
49. Corner Lobe Jet Segmented Model - Base Center of Pressure Shift	72
50. Corner Lobe Jet Segmented Model - Jet Center of Pressure Shift	73
51. Concentric Jet Segmented Model - Base + Jet Center of Pressure Shift	74
52. Concentric Jet Segmented Model - Base Center of Pressure Shift	75
53. Concentric Jet Segmented Model - Jet Center of Pressure Shift	76
54. Effect of Jet Segmentation on Static Lateral Hovering Stability	77
55. Effect of Jet Segmentation on Height-Roll Angle Stability Boundaries	78
56. Hovering Performance - Vertical Peripheral Jet	85
57. Hovering Performance - Jet Segmented Models	86
58. Stability Improvement and Performance Cost Due to Jet Segmentation	87

# LIST OF SYMBOLS

<u>Symbol</u>	<u>Description</u>	<u>Units</u>
b	Characteristic model length (base + jets)	ft
$C_m$	Pitching moment coefficient = $M/L \cdot b$	--
$C_l$	Rolling moment coefficient = $1/L \cdot w$	--
C. P.	Center of pressure in % b or w	%
C. G.	Center of gravity (moment center in % b or w)	%
d	Effective diameter = $\sqrt{4S/\pi}$	ft
G	Ground effect power factor (see Page 81 )	--
h	Height (base to ground)	ft
HP	Jet horsepower = $P/550$	HP
l	Jet peripheral length (on jet centerline)	ft
l	Rolling moment	ft lb
L	Lift force (perpendicular to ground)	lbs
M	Pitching moment	ft lb
$P_b$	Static pressure under base	lbs/ft <sup>2</sup>
$P_j$	Static pressure in jet	lbs/ft <sup>2</sup>
$P_{tj}$	Total pressure in jet	lbs/ft <sup>2</sup>
P	Jet power = $Q \cdot \bar{P}_{tj}$	ft lbs/sec
Q	Jet flow quantity = $\int_0^l V_j t dl$	ft <sup>3</sup> /sec
$q_j$	Jet dynamic pressure = $\frac{\rho}{2} V_j^2$	lbs/ft <sup>2</sup>

LIST OF SYMBOLS, continued...

<u>Symbol</u>	<u>Description</u>	<u>Units</u>
S	Reference area (base + jet)	ft <sup>2</sup>
S <sub>b</sub>	Base area	ft <sup>2</sup>
S <sub>j</sub>	Jet area	ft <sup>2</sup>
t	Jet thickness (perpendicular to jet)	ft
V <sub>j</sub>	Jet velocity = $\sqrt{2 q_j / \rho}$	ft/sec
w	Characteristic width (base + jet)	ft

SIGN CONVENTION

M	Positive if in direction of initial rotation. Negative if in opposition to initial rotation.
l	Same as above.
L	Positive up.

## SUMMARY

Hovering static stability and performance experiments have been conducted with a series of three-dimensional annular jet models. The model planforms measured 40 by 20 inches and incorporated one-inch thick jets operated at a total pressure of 41.5 pounds per square foot. Height-length ratios of 0.05 to 0.20 were investigated.

Simple vertical and  $45^\circ$  inclined peripheral jets demonstrated static longitudinal stability at low heights and instability at high heights. The crossover point was  $h/b = 0.075$  for the vertical jet and  $h/b = 0.107$  for the  $45^\circ$  inclined jet. Static lateral instability existed for both models at all heights.

Convex and concave base shaping with a depth equal to 5% of the model length did not appreciably affect stability in either pitch or roll.

A rigid skirt together with rigid base segmenting flaps of length equal to 5% of the model length were effective in augmenting longitudinal and lateral stability when they extended two-thirds the way to the ground, but were not very effective when they extended only half way to the ground. The order of increasing effectiveness of segmenting flap configuration was, concentric, corner lobe, and centerline.

The concentric, corner lobe, and centerline jet segmented configurations were all statically stable in pitch at all heights including 20% of the length. The order given is in order of increasing stability. In roll, the first two configurations were stable at heights up to 20% of the model width, while the centerline jet segmented model was stable at all heights including 40% of the width.

All comments on stability apply to tilt angles equal to or less than one-third of the touchdown angle. At angles approaching touchdown even the centerline jet segmented model becomes unstable.

The configurations investigated were not optimized for hovering performance. The configurations are, however, representative of compromises which occur due to forward flight considerations. For these cases, the penalty in hovering performance due to jet segmentation was only 8% at height/length = 0.10 and only 4% at height/length = 0.20 for the corner lobe and centerline jet configurations. The concentric jet configuration actually had an improvement of 8% and 11.5% respectively at the same heights.

## INTRODUCTION

Contract DA 44-177-TC-709 undertaken by Aeronutronic for U. S. Army Transportation Research Command called for study of stability and control of air-cushion vehicles for overland use. The scope of the study was restricted to static stability and control investigation, and emphasized the realm of height-diameter ratios near and beyond 0.10.

The work was divided into three phases. Phase I consisted of hovering studies and experiments. Phase II covered the design and preparation of a wind tunnel model and program based on the information generated in Phase I. Phase III consisted of Test and Analysis of the wind tunnel model.

The results of Phase I are reported herein. This report is confined to stability data as outlined in the proposal (Reference 2). Extensive control investigations were conducted on the hovering rig in the same time period as part of an Aeronutronic funded program, and will be reported separately as a portion of Contract DA 44-177-TC-745.

Information from Phase II was forwarded on June 27, 1961 (Reference 3) in the form of a pre-test memorandum. The final report covering Phase III is submitted as Aeronutronic Publication No. U-1447 (Reference 4), together with the subject report.

### TEST FACILITY

The general arrangement of the Aeronutronic hovering test facility is illustrated by the photograph presented as Figure 1. Flow was supplied by a Chicago Airfoil Centrifugal Blower driven by a 30-HP, 3-phase electric motor through belts and pulleys. This unit was mounted at the top of an 11-foot tower. Figure 2 presents an envelope of maximum pressure and flow combinations available from the unit. Lines of actual flow versus supply pressure are also presented for the five different jet configuration models. The experiments were conducted at a constant jet total pressure level of 41.5 pounds per square foot.

An 8-foot by 8-foot ground board was supported on a central jack post which permitted height adjustment. The board was mounted to the jack with trunions which permitted rotation of the ground plane in pitch or roll. The ground board was locked into position by posts at four corners which were C clamped to the tower as shown in Figure 1.



### MODEL AND INSTRUMENTATION DESCRIPTION

All models in these experiments were bolted rigidly to the bottom of the long vertical duct. All force data was obtained through integration of pressure distributions picked up from the model base and jets. Various models are depicted in the photograph included as Figure 3. The central model presents a base view of the  $45^\circ$  model and includes the outer nozzle wall as well as the base. The remaining models in the photograph present a top view of several base inserts which fit concentrically within the outer nozzle wall of the basic vertical jet model. Three examples of jet segmentation are included together with a basic unsegmented base.

Figures 4 through 10 provide geometric description and instrumentation locations for the following models:

Vertical Peripheral Jet	Centerline Jet Segmented
$45^\circ$ Inclined Peripheral Jet	Corner Lobe Jet Segmented
Shaped Base	Concentric Jet Segmented
Skirted and Flap Segmented	

The static pickups indicated by O on the above drawings consisted of .065" O. D. .012" wall stainless steel tube mounted at right angles to and flush with the surface. The total head tubes indicated by X on the above drawings were made from the same tubing and mounted in the center of the jet. The mouth was located one-half inch above the bend in the tube. All tubes were gathered together in one spot just under the base top, routed vertically up the duct through a hollow tube, and then horizontally out of the duct through a hollow streamlined strut. The pressures were conducted by plastic tubing to the 50-tube water manometer shown in the background of Figure 1 and photographically recorded.

## DATA REDUCTION PROCEDURES

Each base static pressure tap was assumed to have an area of influence and to be located at the centroid of that area of influence. The base lift was obtained by summing the pressure-area products. The arms from the pressure tap to the pitch axis and roll axis were recorded. The net moments were obtained by summing the pressure-area-arm products.

Each instrumented jet location had an inner wall static tap, an outer wall static tap, and a mid jet total head tube. The two wall tap values were averaged to get the effective static pressure  $p_j$  - this was subtracted from the total head  $p_t$ ; to get the local dynamic pressure  $q_j$ . The local reaction pressure was computed  $= p_j + 2 q_j$ . The jet lift was obtained by summing the reaction pressure-area products. The lift of the  $45^\circ$  jet which was summated along the jet was multiplied by .707 to get the component perpendicular to the base. The jet moment contributions were obtained by summing the reaction pressure-area-arm products. The arms were measured as the perpendicular distance between the jet centerline and the centroid of the model planform in the plane of the base.

The total lift was found by multiplying the sum of the base lift, and the jet component perpendicular to the base by the cosine of the tilt angle. This is wind axis or lift perpendicular to the ground.

The jet velocity in ft/sec was obtained from the dynamic pressure at each jet instrumented location. The volume flow in  $\text{ft}^3/\text{sec}$  was found by summing the velocity-jet area products. The exit jet power in ft lb/sec was found by integrating the products of jet velocity, jet area, and total pressure.

The final results of the machine integrations were in the following form:

$$C_{M_{\text{total}}} = \text{Base Moment} + \text{Jet Moment} / (\text{total lift}) (\text{Model length})$$

$$C_{M_{\text{Base}}} = \text{Base Moment} / (\text{total lift}) (\text{Model length})$$

$$C_{M_{\text{Jet}}} = \text{Jet Moment} / (\text{total lift}) (\text{Model length})$$

Also the three roll coefficients non-dimensionalized with model width.

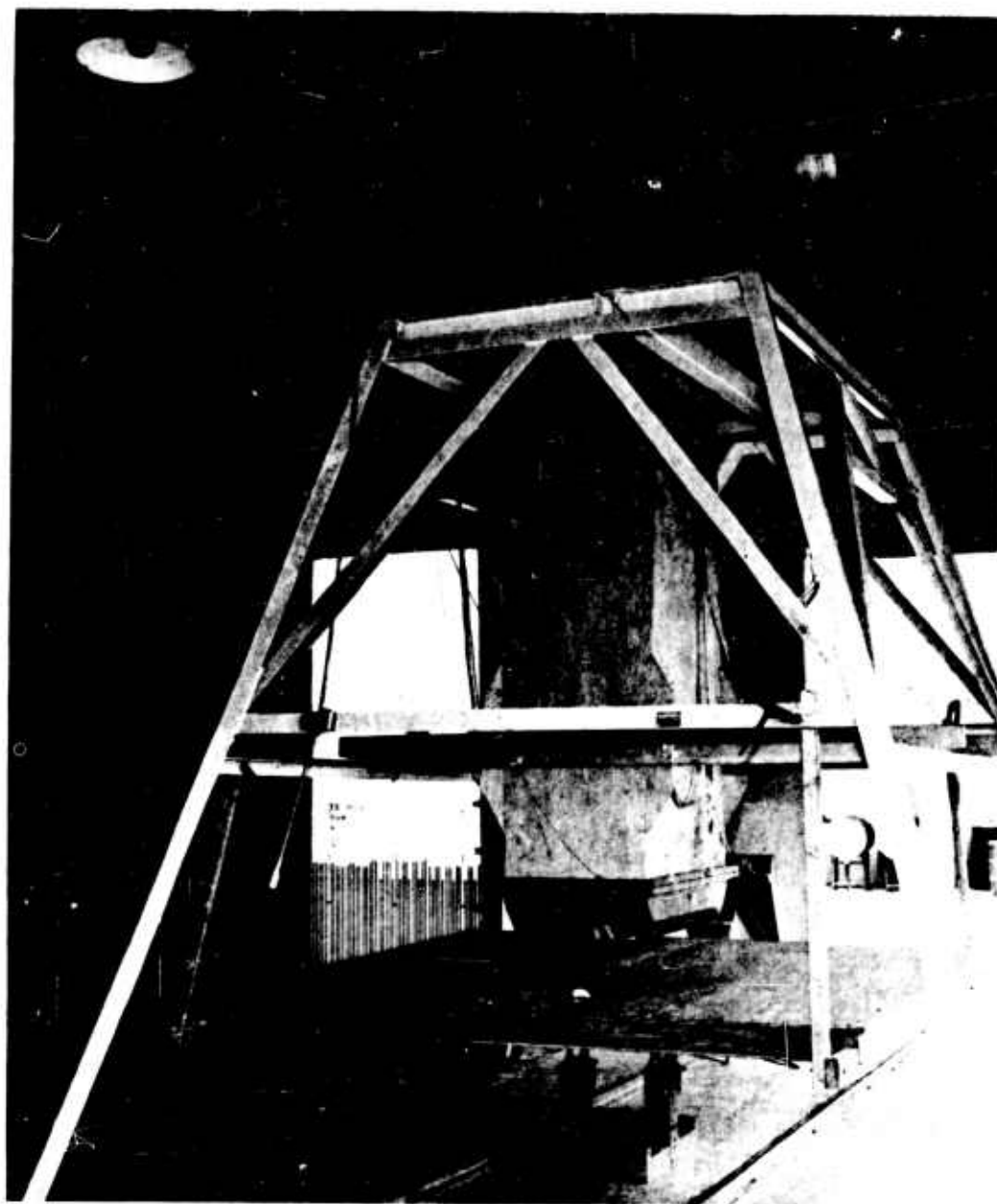
Also

Total lift in pounds.

Total volume flow in  $\text{ft}^3/\text{sec}$ .

Total jet power in HP.

Figure 1



Hovering Test Facility ((Photograph 10520))

Figure 2

# AVAILABLE AND REQUIRED PRESSURE AND FLOW

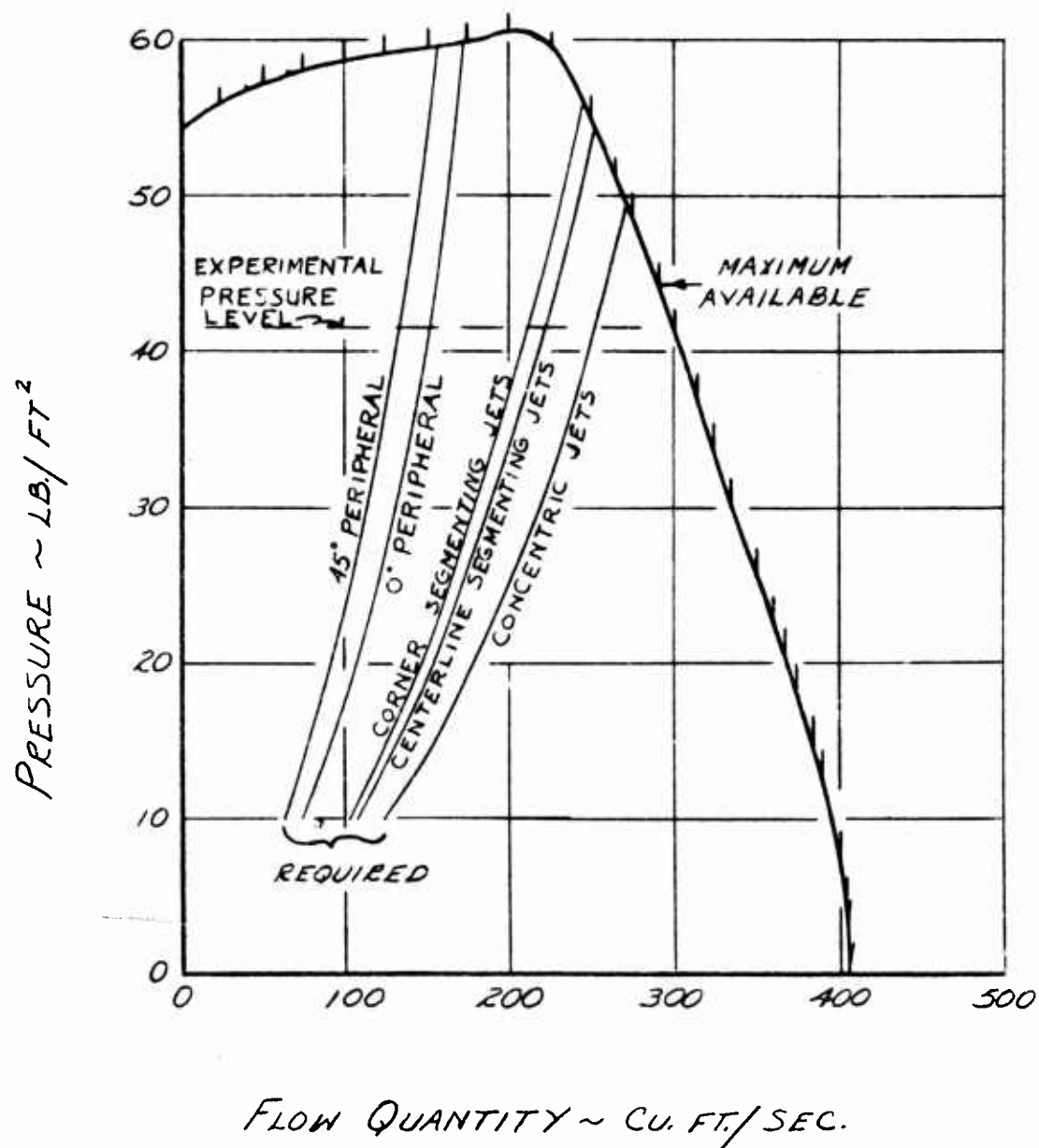
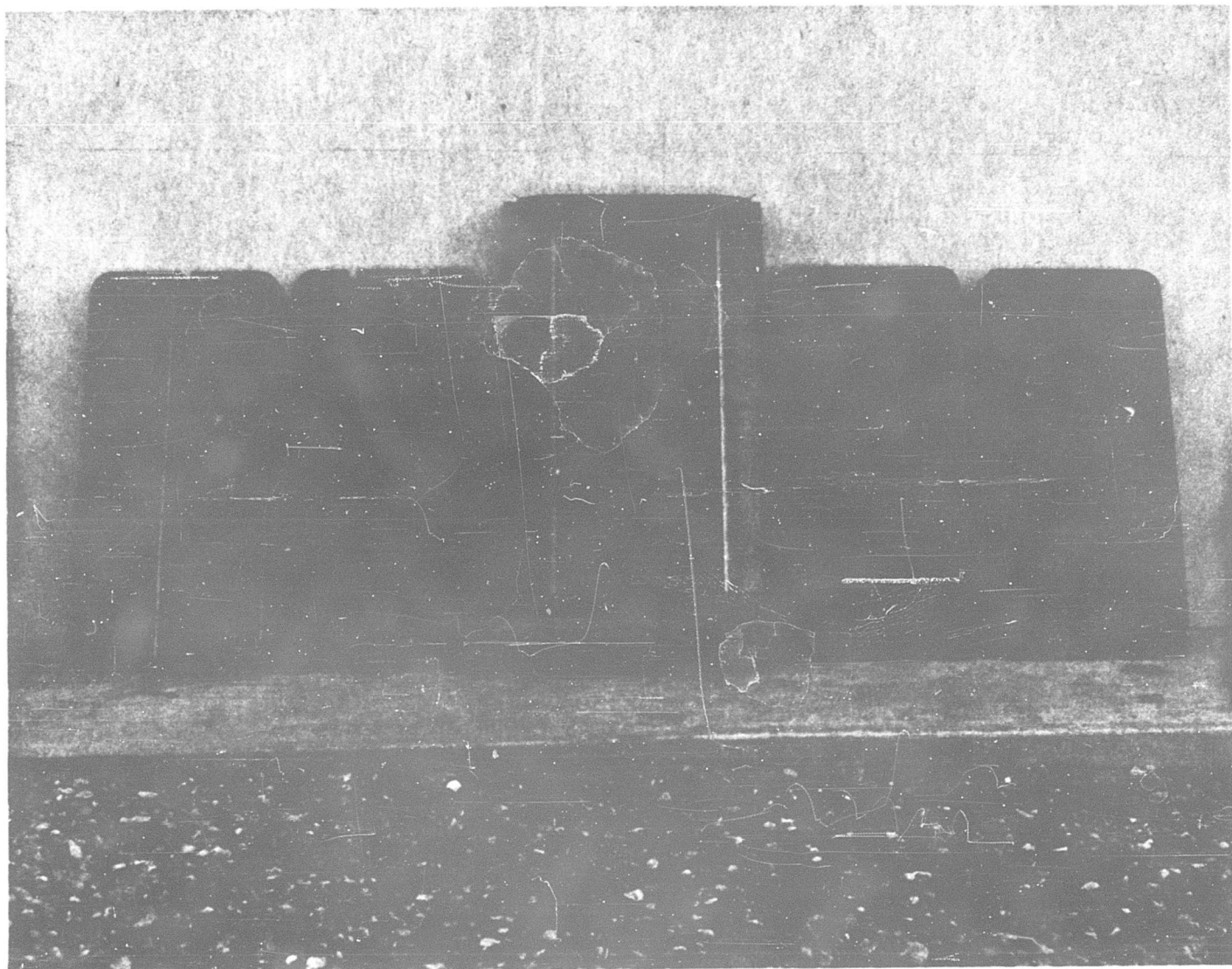
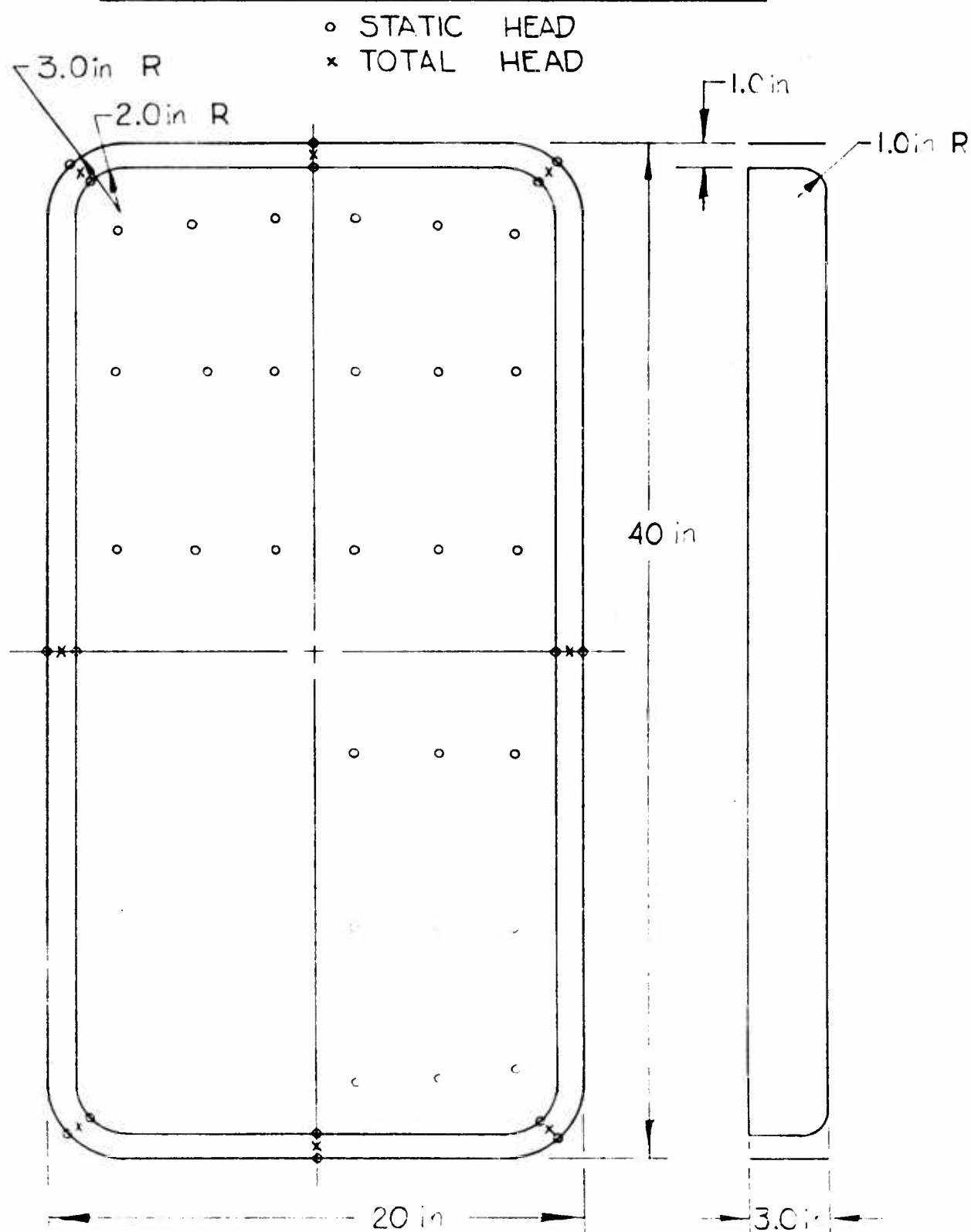
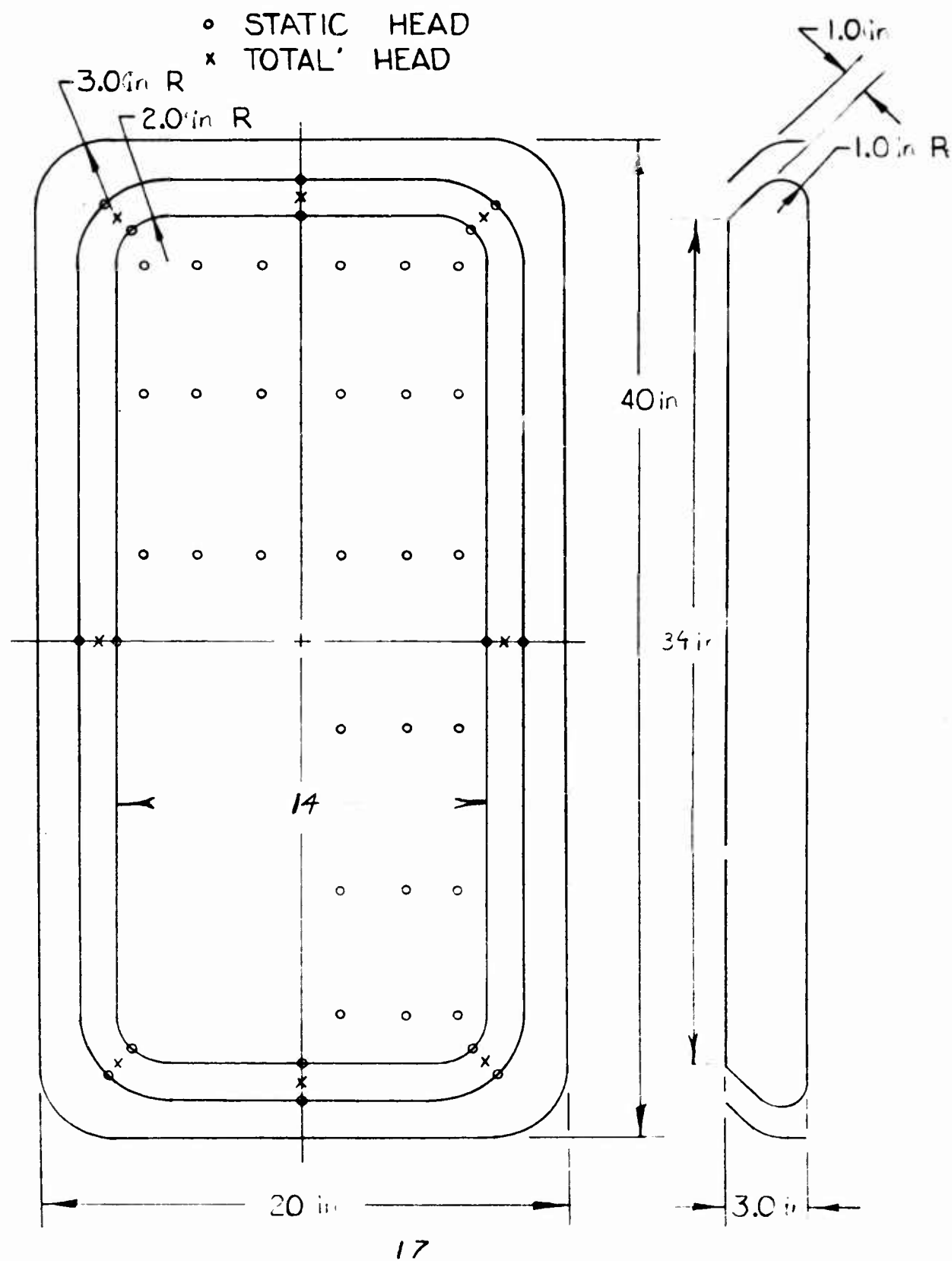


Figure 3



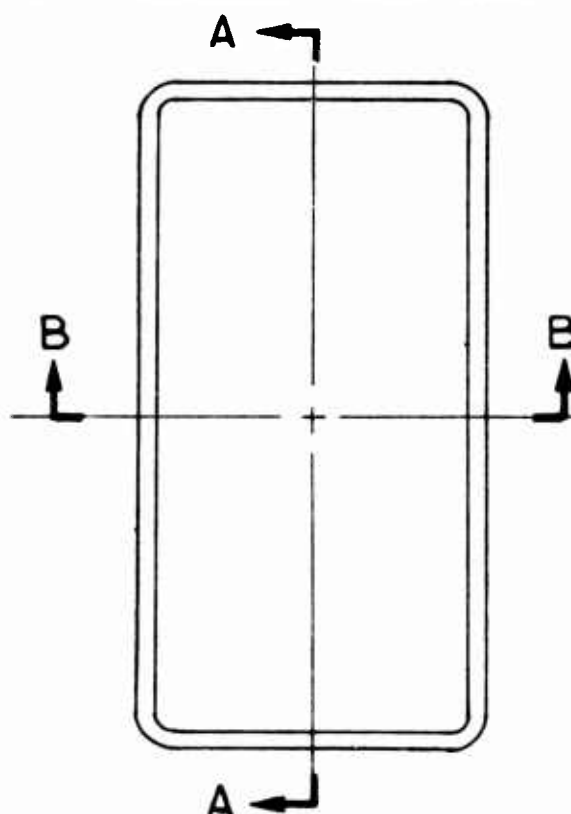
**Three-Dimensional Model Bases (Photograph 10217)**

VERTICAL PERIPHERAL JET MODEL

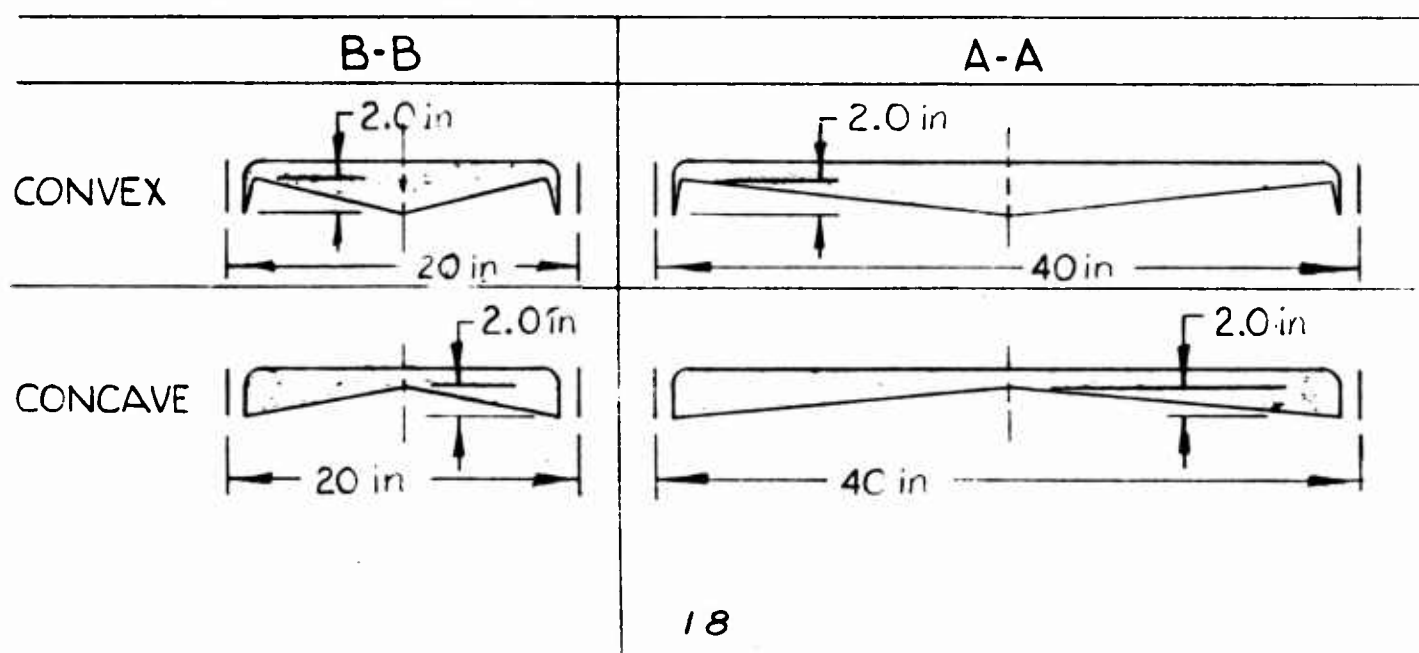
45° INCLINED PERIPHERAL JET MODEL



## SHAPED BASE MODELS

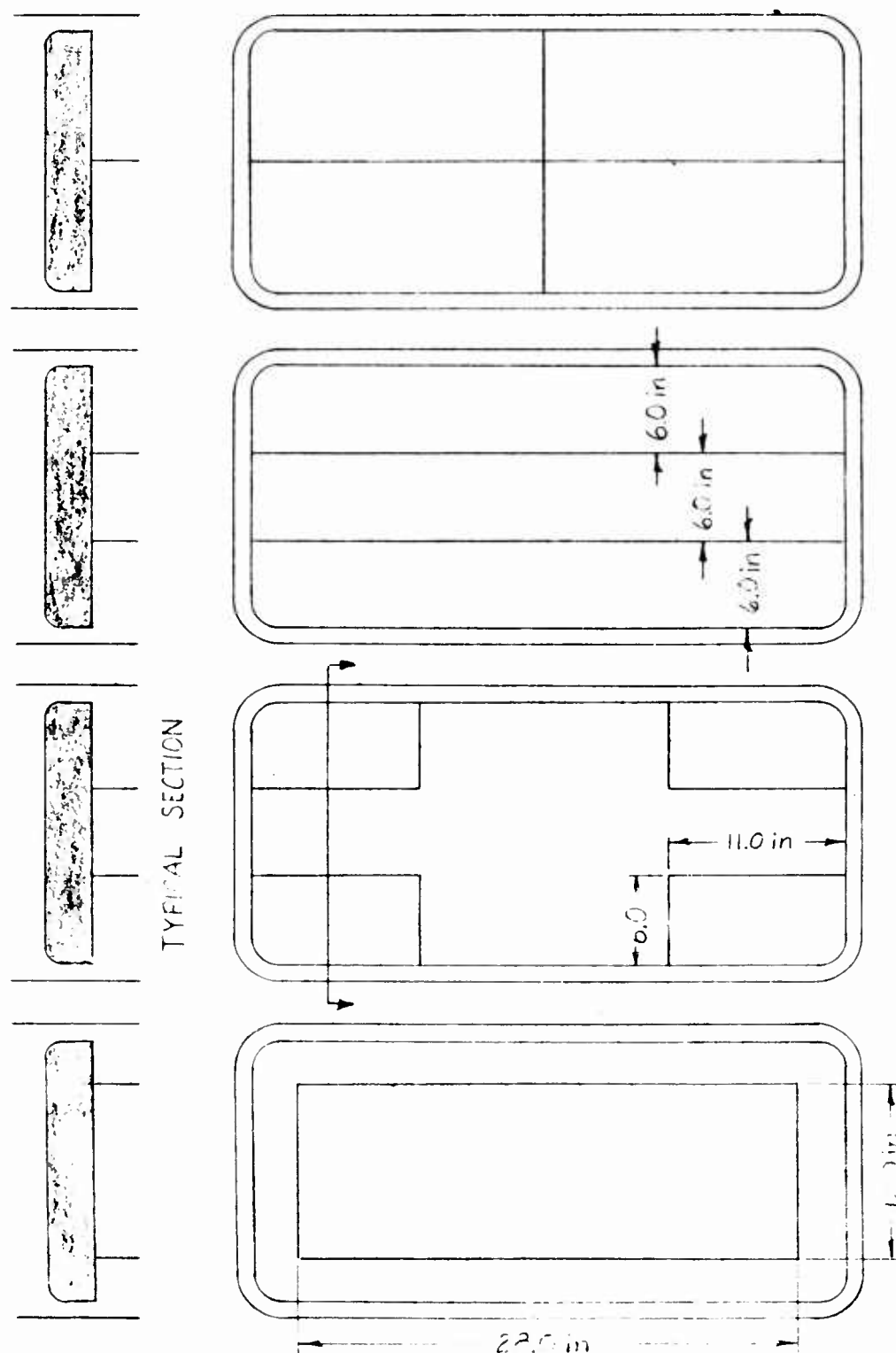


NOTE : INSTRUMENTATION AND JET CONFIGURATION IDENTICAL TO VERTICAL PERIPHERAL JET MODEL



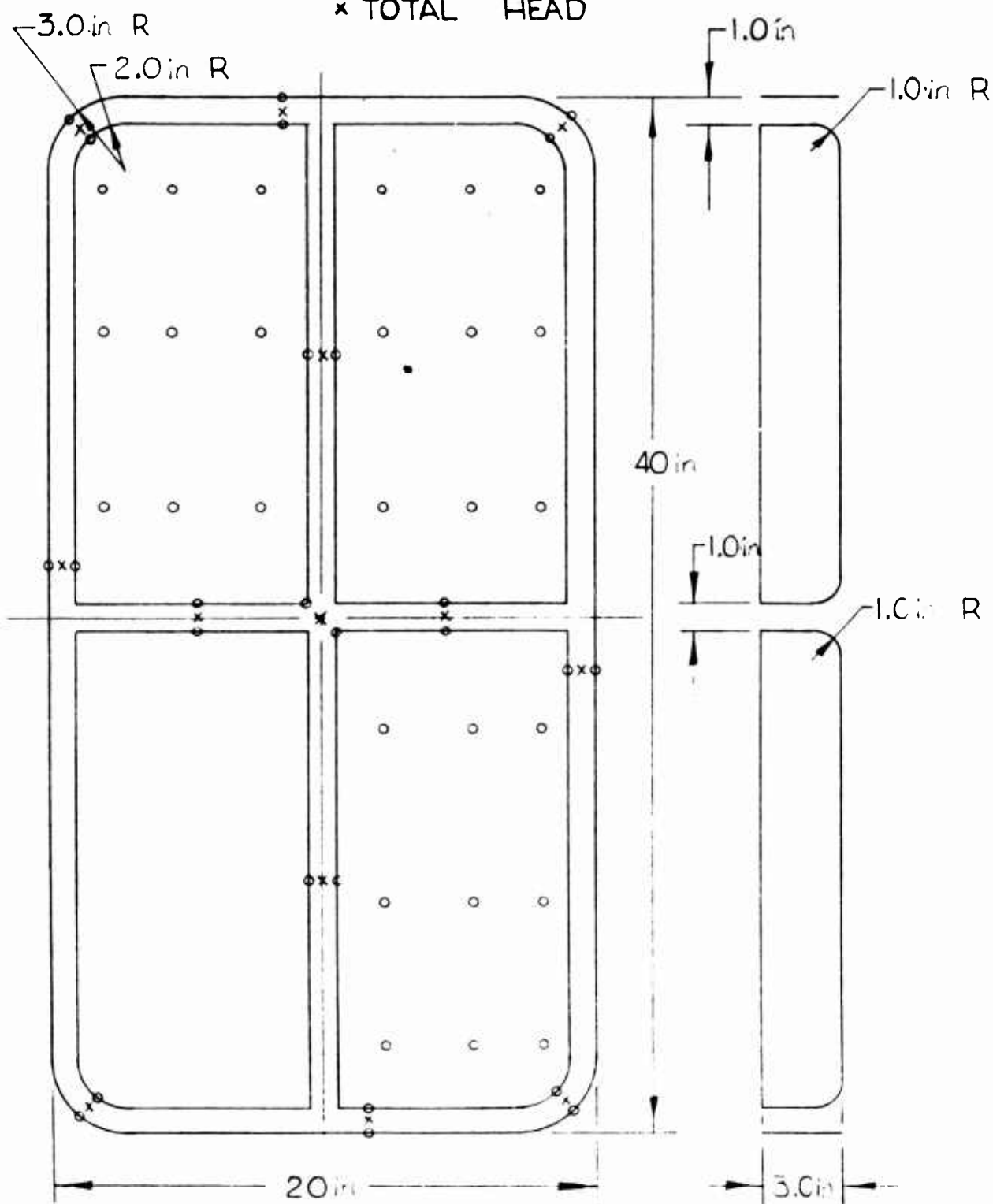
# SKIRTED AND FLAP SEGMENTED MODELS

NOTE: INSTRUMENTATION & JET CONFIGURATION  
IDENTICAL TO VERTICAL PERIPHERAL  
JET MODEL

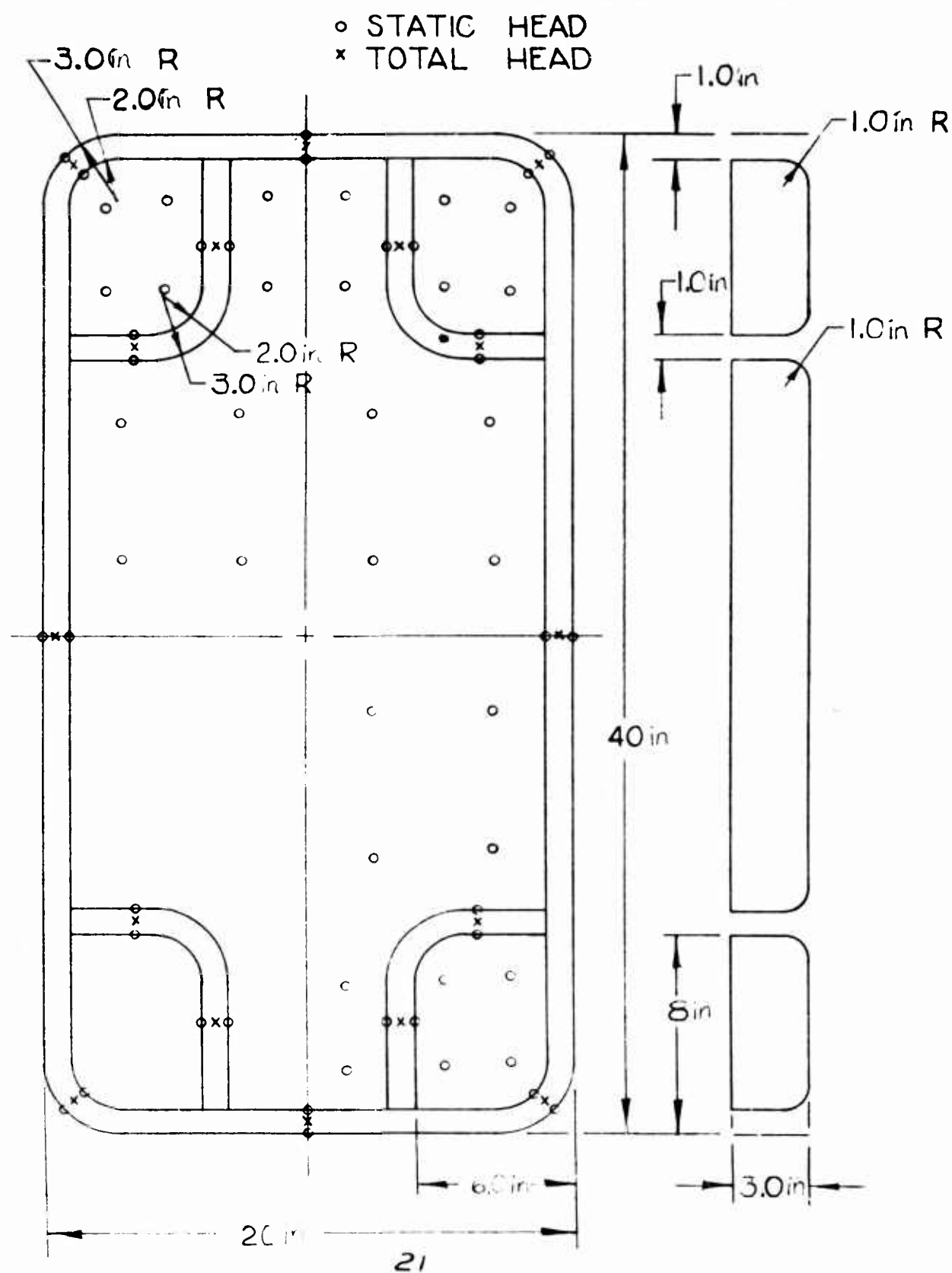


CENTERLINE JET SEGMENTED MODEL

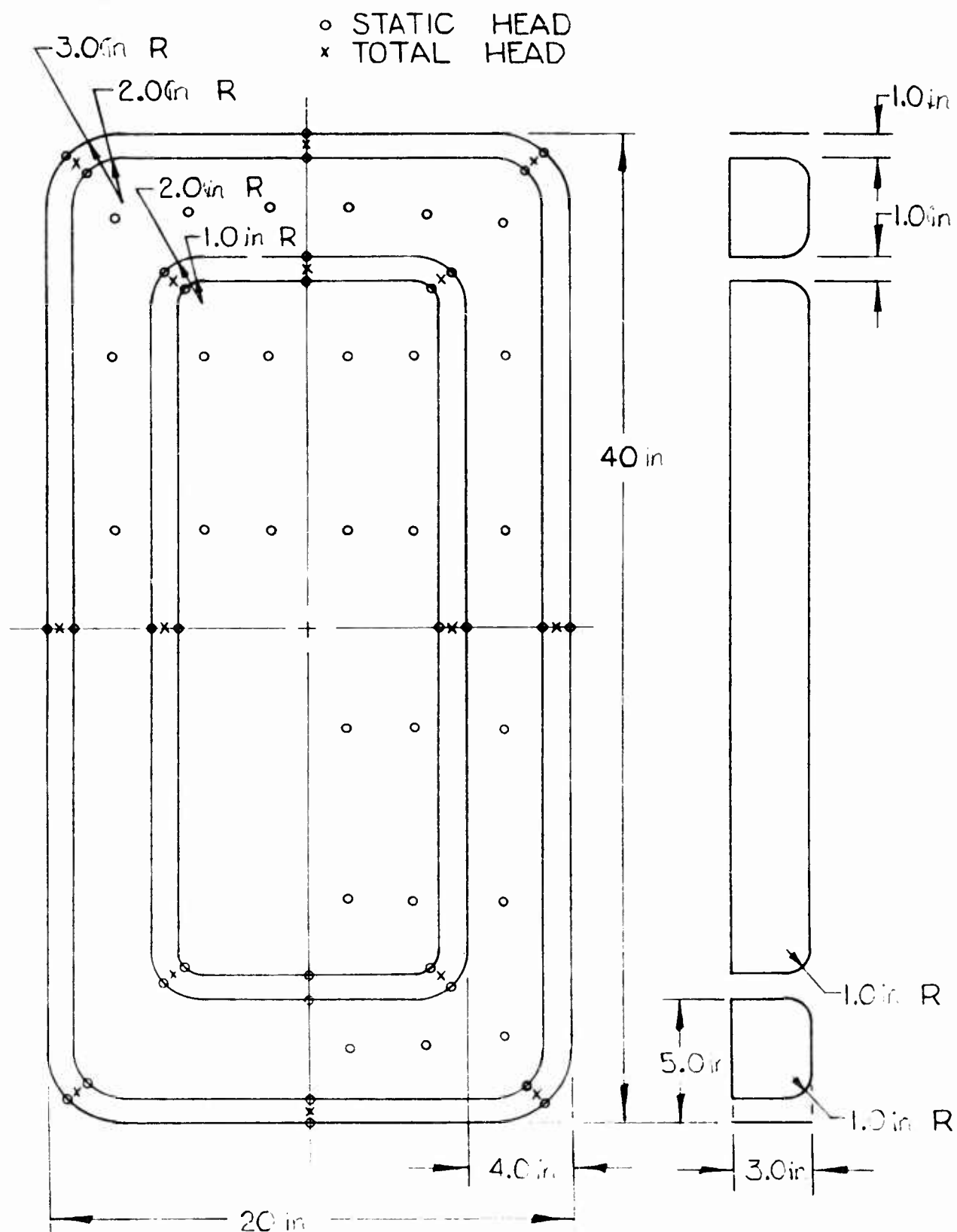
◦ STATIC HEAD  
× TOTAL HEAD



# CORNER LOBE JET SEGMENTED MODEL



# CONCENTRIC JET SEGMENTED MODEL



## EXPERIMENTAL RESULTS

### 1. Longitudinal Stability

#### a. Simple Peripheral Jet Models

The base plus jet center of pressure shift of the vertical peripheral jet model is presented in Figure 11. The small angle slopes indicate static stability at  $h/b = .05$ , neutral stability at  $h/b = .075$  and instability at larger values of  $h/b$ . At  $h/b = .05$ , the stability appears to decrease slightly at large pitch angles. At intermediate heights, the initial unstable slopes actually change to stable slopes at high pitch angles. At  $h/b = .20$ , this effect had not yet occurred at the highest angle tested.

Figure 12 reveals that the base contribution to static stability becomes increasingly stable at high angles of pitch at all heights except  $h/b = .20$ . Examination of base pressure distribution indicates a softening of the unstable pressure gradients at high angle compared to moderate angles and a large local pressure increase near the low end. The base contribution is seen to be a large portion of the total and to a first approximation describe the complete model stability.

The minor contribution of the jet is confirmed in Figure 13 at all heights except  $h/b = .05$ . Here the jet contribution becomes large at the touchdown angle. When added to the base alone C. P. shift curve, the favorable trend in slope at high angles is reversed. At moderate and high heights, the jet contribution curves are systematic indicating a slightly stable influence up to moderate pitch angles followed by a slightly unstable influence at larger pitch angles. At angles very near touchdown (not covered at the higher heights in these experiments) an appreciable unstable jet contribution similar to that observed at

$h/b = .05$  would probably occur. The reason for this is that the jet flow on the low end (and hence momentum contribution to the reaction force) is severely reduced on contact with the ground, whereas the jet on the high end faces a minimum of back pressure, has a relatively large momentum, and hence a relatively high reaction force.

The base plus jet center of pressure shift of the  $45^\circ$  inclined jet model is shown in Figure 14. Stable slopes exist to higher values of  $h/b$  than for the vertical jet model. Again, the base contribution to the stability is the large one and the stability of the model is represented to a first approximation by the base contribution. The tendency for the base to become increasingly stable at the higher pitch angles may be observed in Figure 15. The jet contribution (Figure 16) is larger than it was for the vertical jet model and varies from neutral at small angles to unstable at larger pitch angles.

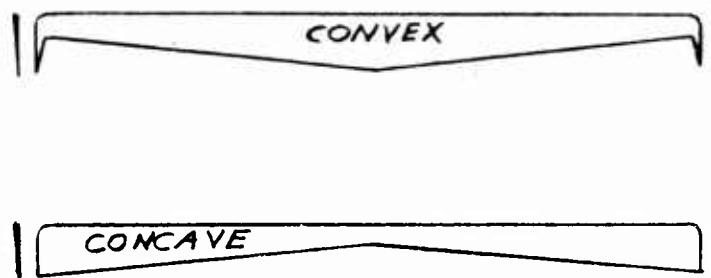
The static longitudinal stability derivative (for small angles)  $\partial C_M / \partial \alpha$  is shown in Figure 17 for the vertical jet and for the  $45^\circ$  inclined jet models as a function of the height in percent of length. The derivative is expressed in percent center of pressure shift per degree of tilt to obtain larger numbers than would occur if a pure decimal system were used. A value of  $-.2$  means that  $5^\circ$  of tilt would result in a shift of the center of pressure 1% of the length off the centerline toward the low side. The two models have identical values at  $h/b = .05$  and  $.20$ . The  $45^\circ$  jet model is clearly superior at all intermediate height values. In particular, the  $45^\circ$  jet does not go unstable until  $h/b$  exceeds  $.107$ , whereas the vertical jet becomes unstable at  $h/b = .075$ .

The boundaries of pitch angle and height for stability are compared for the two models by Figure 18. These simple peripheral jet models are stable at all angles at the lower heights but have the peculiar characteristic of regaining stable slopes at high angles of pitch at those higher heights

where they are unstable for small pitch angles. This tendency has been previously reported by the NASA tests of annular jet models with length-width ratios greater than one (Reference 5). The superiority of the  $45^\circ$  jet model at  $h/b = .13$  and  $\alpha \geq 10^\circ$  is clearly indicated.

b. Shaped Bases

Two-dimensional stability investigations conducted previously at Aeronutronic<sup>†</sup> suggested that proper shaping of the base profile might (in the presence of cross flow) produce a more stable base pressure distribution. Two variations were investigated utilizing the simple vertical peripheral jet model. In the concave version the base sloped to a central recessed point. In the Convex version the base was recessed just inboard of the inner jet wall and sloped back to a central point which lay in the plane of the jet exit.



The magnitude of the recess was in each case 5% of the model length or 10% of the width.

<sup>†</sup> Reference 1



The comparison of these configuration, base plus jet center of pressure shifts with that of the flat base is given in Figures 19 and 20. The convex base was stable at  $h/b = .05$  and neutral at  $h/b = .075$  similar to the flat base. At  $h/b = .10$  all three configurations were very nearly alike. At  $h/b = .15$  and  $.20$  the convex was least unstable, and the concave base was intermediate between the convex base and the flat base. At these heights all three configurations were unstable.

Both the concave and the convex base exhibited increasing instability at the larger pitch angles in contrast to the flat base which exhibited improved stability at the larger pitch angles. These experiments, although very brief, do not hold out much hope for base shaping as a method of obtaining hovering static stability.

c. Skirted and Flap Segmented Models

Aeronutronic is actively studying the flexible skirt concept as a means of reducing required flow quantities and power requirements. If this should prove practical, it will be of interest to know what influence the skirt will have on the stability problem. If a long flexible peripheral flap is practical, it should also be possible to segment the base with long flexible flaps. These could perhaps replace base segmenting jets as a means of improving hovering stability.

A rigid skirt of length = 5% of the model length was added to the model as an extension of the outer nozzle wall. In addition, the base was segmented by various rigid flaps. All stability runs were conducted at height (measured to the model base) of either 7.5% or 10% of the model length. The clearance beneath the skirt is therefore either 2.5% or 5%. The skirt reaches either two-thirds or one half the way to the ground.

The base plus jet center of pressure shift is compared for several configurations in Figure 21. The addition of the skirt alone did not markedly improve the static stability.

The concentric flap changed the neutral stability at  $h/b = .075$  to slightly stable, but was not adequate to provide stability at  $h/b = .10$ . The corner lobe and centerline base segmenting flaps provided static stability at  $h/b = .075$  and  $.10$ . The centerline flaps were superior to the other types. The magnitude of the C. P. shift was small because the long skirt limited the pitch angles to modest values. The jet contribution is small and the base contribution describes to a first approximation the stability behavior of the model. In general the stability improves at the higher pitch angles.

The stability derivative  $\partial C_M / \partial \alpha$  for small angles is shown in Figure 22. The degree of static stability for the skirted and flapped models is seen to decrease rapidly with increasing height similar to the basic model. The order of improvement in stability from the basic to the concentric to the corner lobe to the centerline configuration is clearly indicated. In general, the flap is very effective when it extends two-thirds of the way to the ground, and is losing effectiveness rapidly when it extends only half way to the ground.

#### d. Jet Segmented Models

Jet segmentation of the base is the accepted method of augmenting the static hovering stability of annular jet air-cushion vehicles (Reference 6). The most general formulation of the problem would be, "What is the geometry of jet segmentation which will provide a given level of static stability at high values of  $h/b$  while retaining the highest possible performance". Several problems are immediately apparent. It is not clear what level of stability is desirable. If a level is arbitrarily decided upon, one must still define what is meant by performance. Air-cushion vehicles (for a variety of reasons) do not

employ peripheral jets which are optimized for hovering performance. The percent change in performance due to segmenting jets will vary depending on how close or far one is from optimum hovering geometry. It is not possible at present to compute the amount of jet segmentation required to provide a given level of stability. The lift and power of a jet segmented configuration is likewise not accurately predictable.

In view of the above dilemma, a simple experimental program was employed to gain some working experience with the problem and to provide inputs for follow-on analytical work which might eventually provide a general solution.

The basic 40" by 20" rectangular vertical peripheral jet was used as the reference model. The base was replaced with centerline, corner lobe, and concentric, segmenting jet bases in succession. All models had one-inch wide peripheral and segmenting jets and the total pressure in the jet was set at 41.5 pounds per square foot.

The base plus jet center of pressure shift is given in Figure 23 for the centerline jet segmented model. The stability for small angles is high at low and moderate heights and becomes lower at the higher heights. Instability occurs at large angles. This change from stable for small angles to unstable at large angles is the reverse of the situation for the basic model at high heights where the model had an unstable slope at low angles and became stable at high angles. It should be noted that the centerline jet segmented model is stable in pitch (at small angles) at all heights tested including 20% of the model length. The base center of pressure shift curves given in Figure 24 are very similar to the total C. P. curves except that the decrease in stability at large angles is less pronounced. The jet contribution given in Figure 25 shows little effect up to moderate angles but a significant de-stabilizing tendency at high angles.

The base plus jet center of pressure shift is given for the corner lobe jet segmented model in Figure 26.

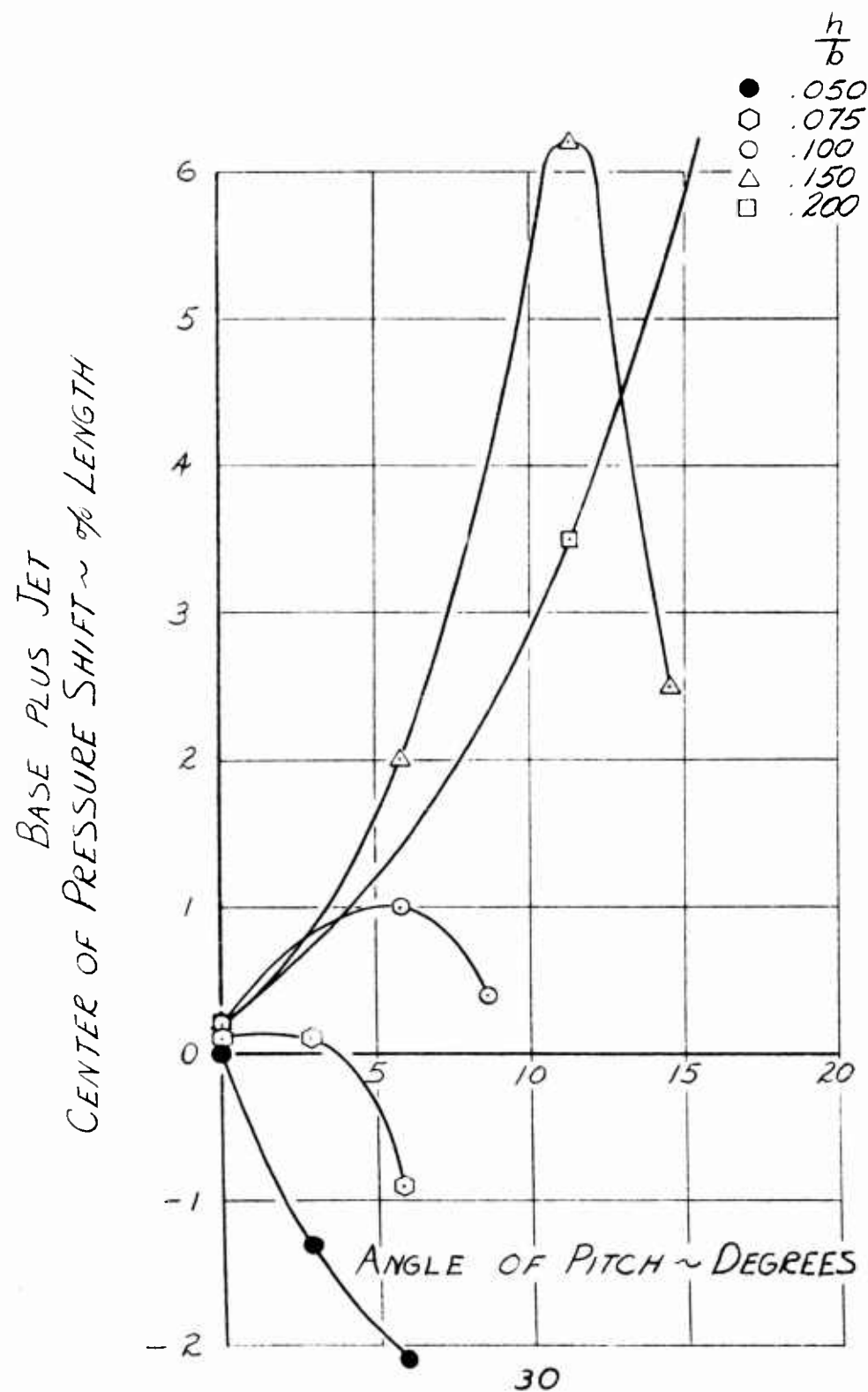
The nature of the curves are very similar to those of the centerline jet segmented model but the stability is not as high. Instability again appears at high tilt angles at high heights. The base contribution (Figure 27) and jet contribution (Figure 28) tell a very similar story to the centerline jet segmented model.

The base plus jet center of pressure shift is given for the concentric jet segmented model in Figure 29. The model is stable at all heights although the degree of stability is lower than demonstrated by the two previous jet segmented models. The concentric jet goes unstable at the highest height angle combination. The base contribution is shown by Figure 30 to be the stabilizing term and the jet contribution of Figure 31 exhibits a large unstable contribution at large  $h$  and  $\alpha$ .

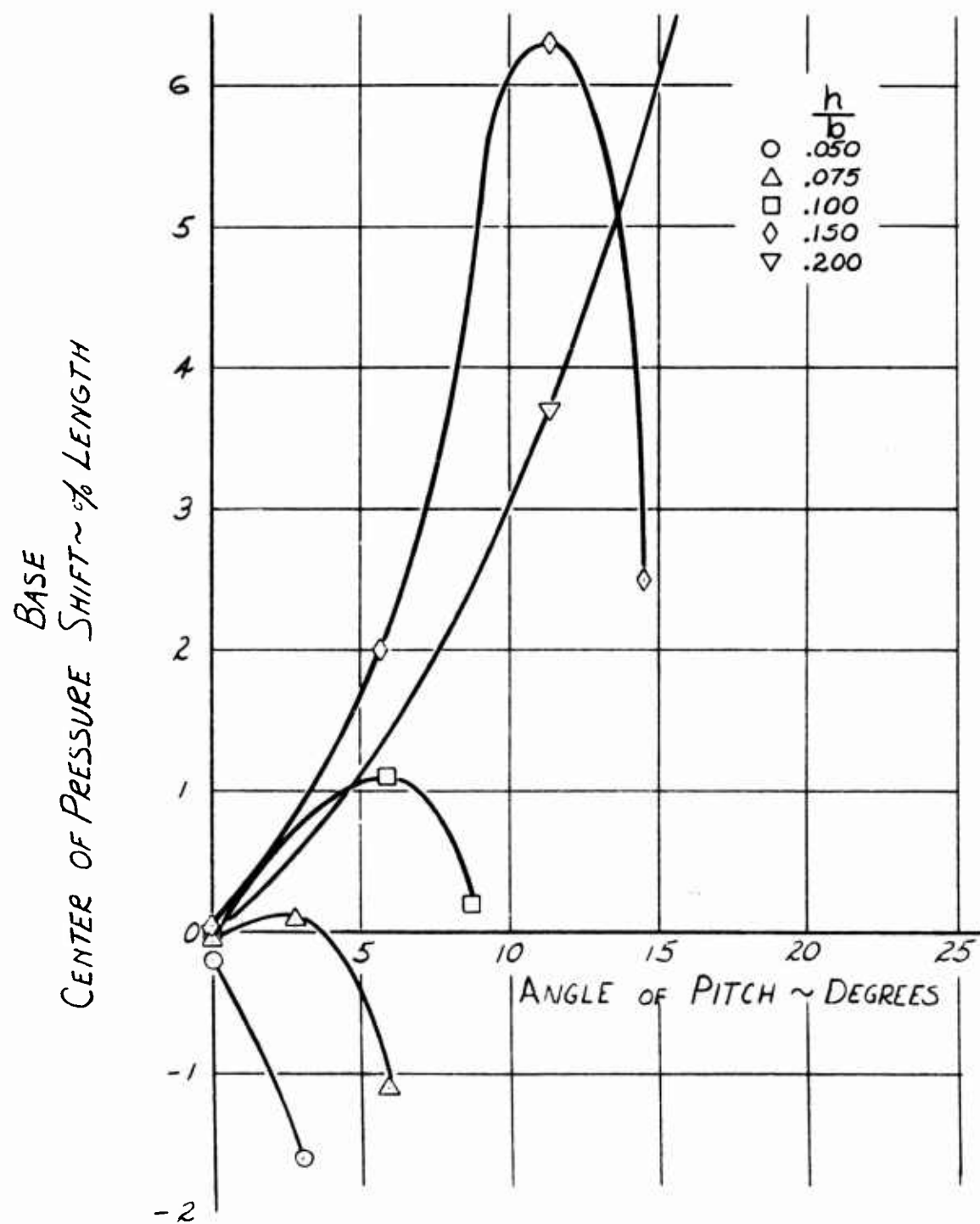
The small angle stability data for the jet segmented models is summarized in Figure 32. All three configurations are stable at all heights tested through 20% of the model length. The concentric jet had the lowest stability, the corner lobe configuration had somewhat higher stability, and the centerline jet configuration had the highest stability.

The effect of jet segmentation on height-pitch angle stability boundaries is illustrated by Figure 33. High tilt angle instability is encountered on the centerline jet model at  $h/d > .08$ , on the corner lobe model at  $h/d > .12$ , and on the concentric jet model at  $h/d > .16$ . Thus, we see that order of preference on high tilt angle stability is just the reverse of the order of preference on the magnitude of the low tilt angle stability.

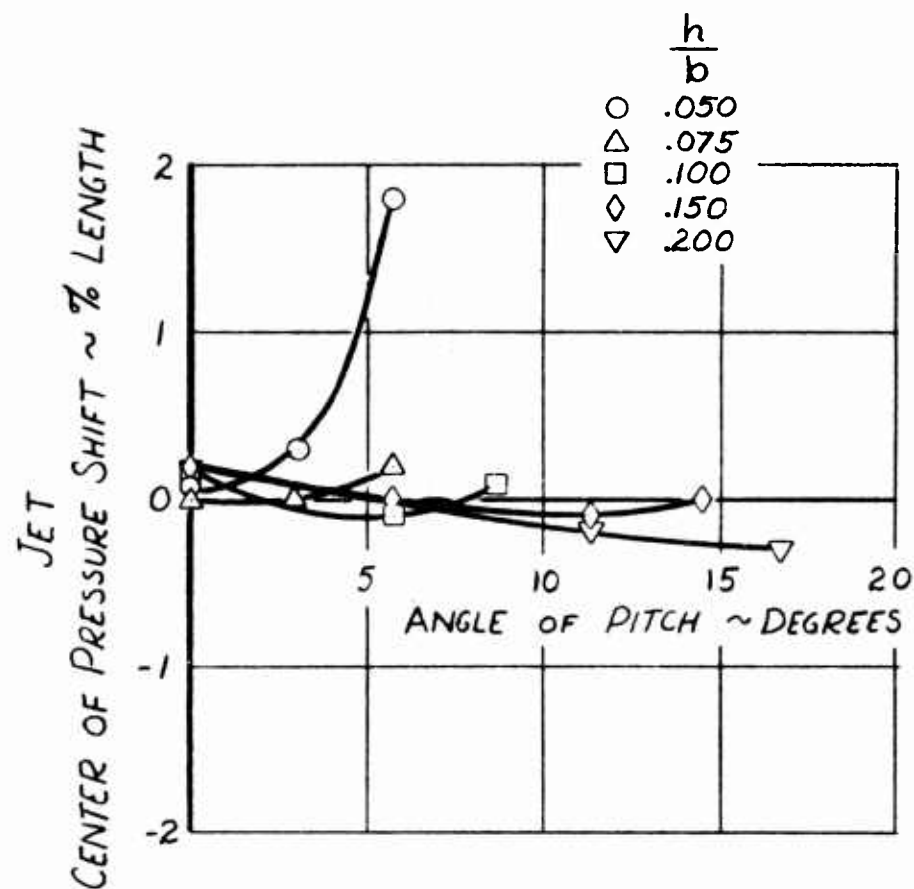
VERTICAL PERIPHERAL JET MODEL  
BASE PLUS JET  
CENTER OF PRESSURE SHIFT



VERTICAL PERIPHERAL JET MODEL  
BASE CENTER OF PRESSURE SHIFT

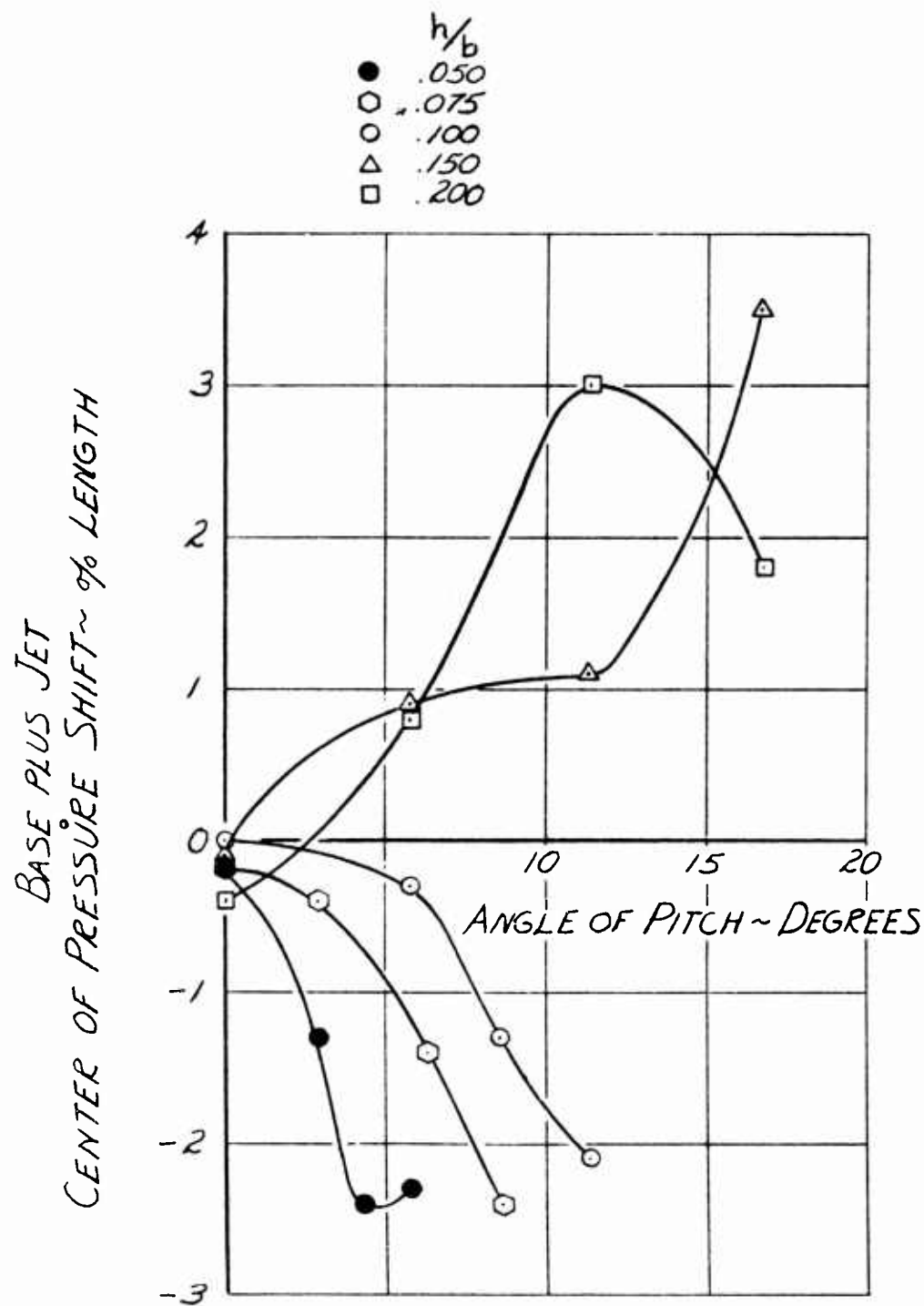


VERTICAL PERIPHERAL JET MODEL  
JET CENTER OF PRESSURE SHIFT



45° INCLINED PERIPHERAL JET MODEL  
BASE PLUS JET  
CENTER OF PRESSURE SHIFT

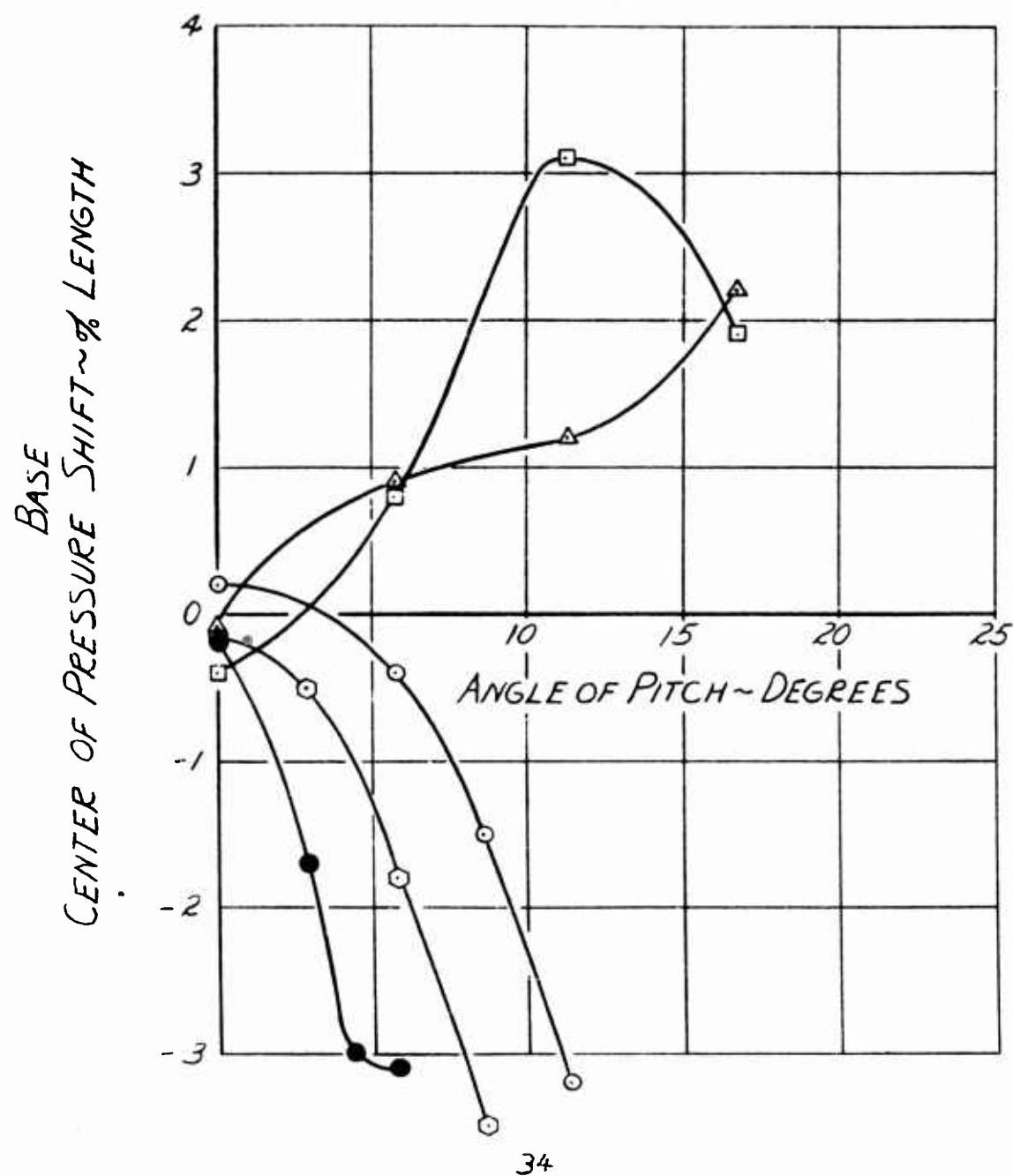
Figure 14





45° INCLINED PERIPHERAL JET MODEL  
BASE  
CENTER OF PRESSURE SHIFT

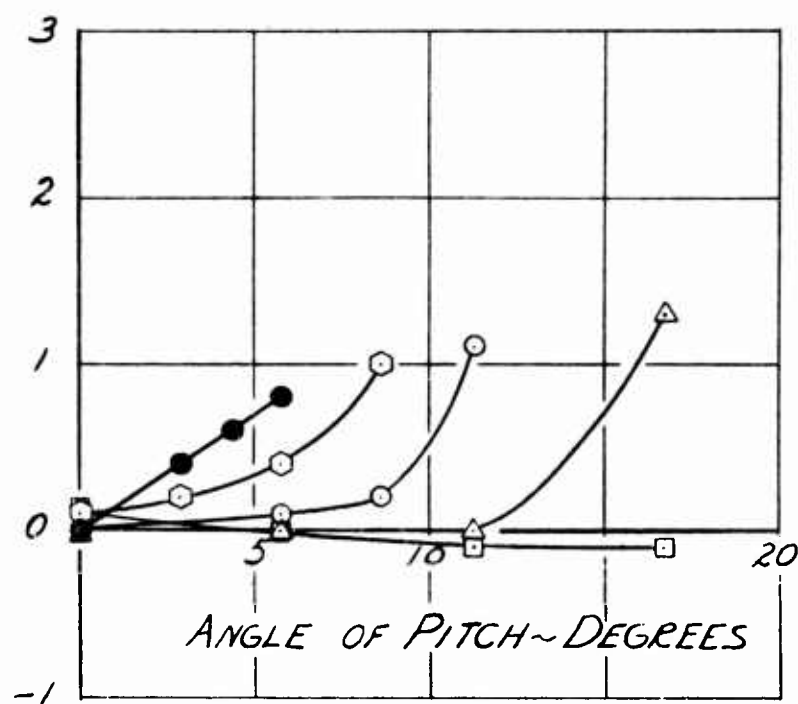
- $h/b$   
 ● .050  
 ○ .075  
 ○ .100  
 △ .150  
 □ .200



45° INCLINED PERIPHERAL JET MODEL  
JET  
CENTER OF PRESSURE SHIFT

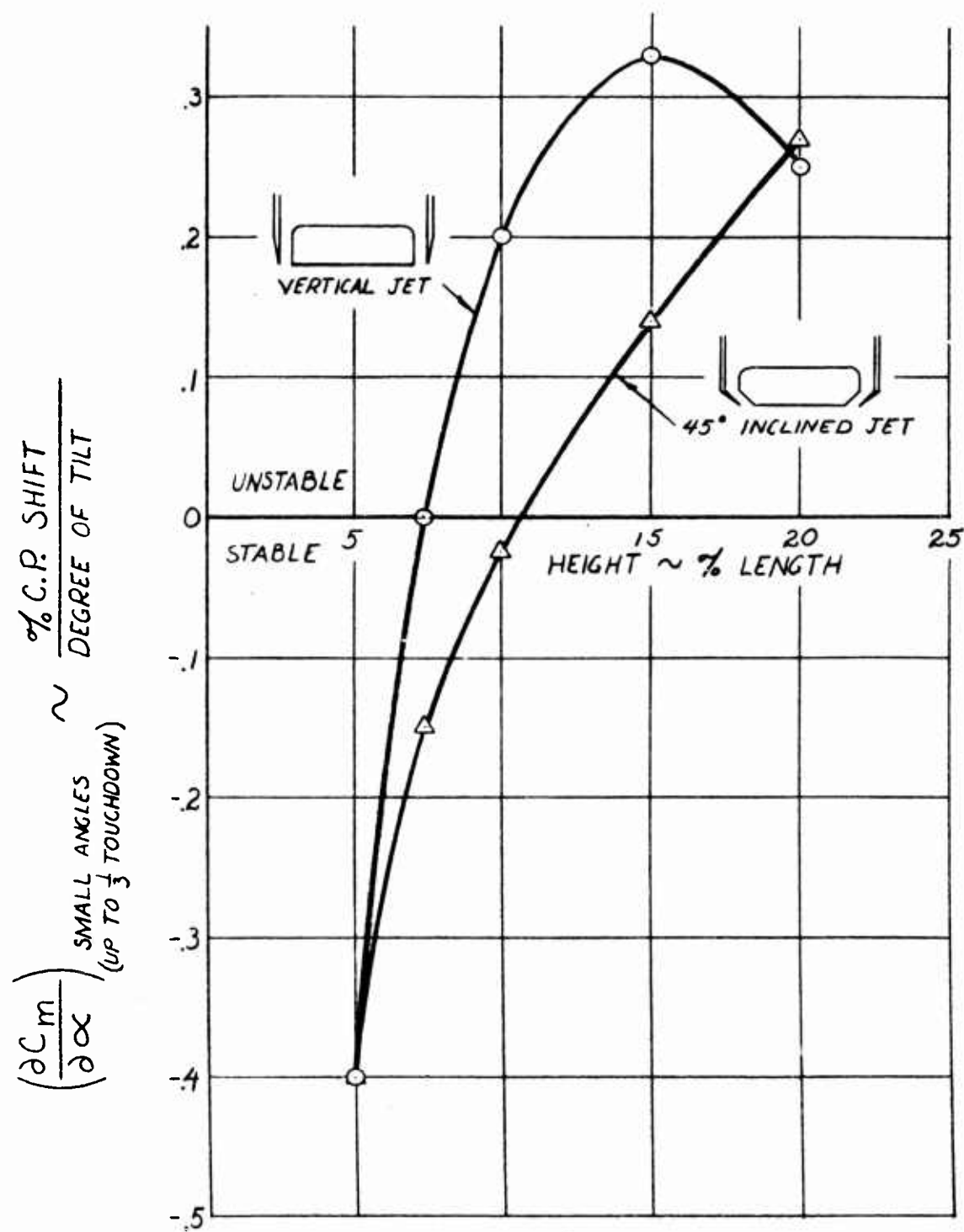
- $h/b$   
 ● .050  
 ○ .075  
 ○ .100  
 △ .150  
 □ .200

JET  
 CENTER OF PRESSURE SHIFT ~ % LENGTH

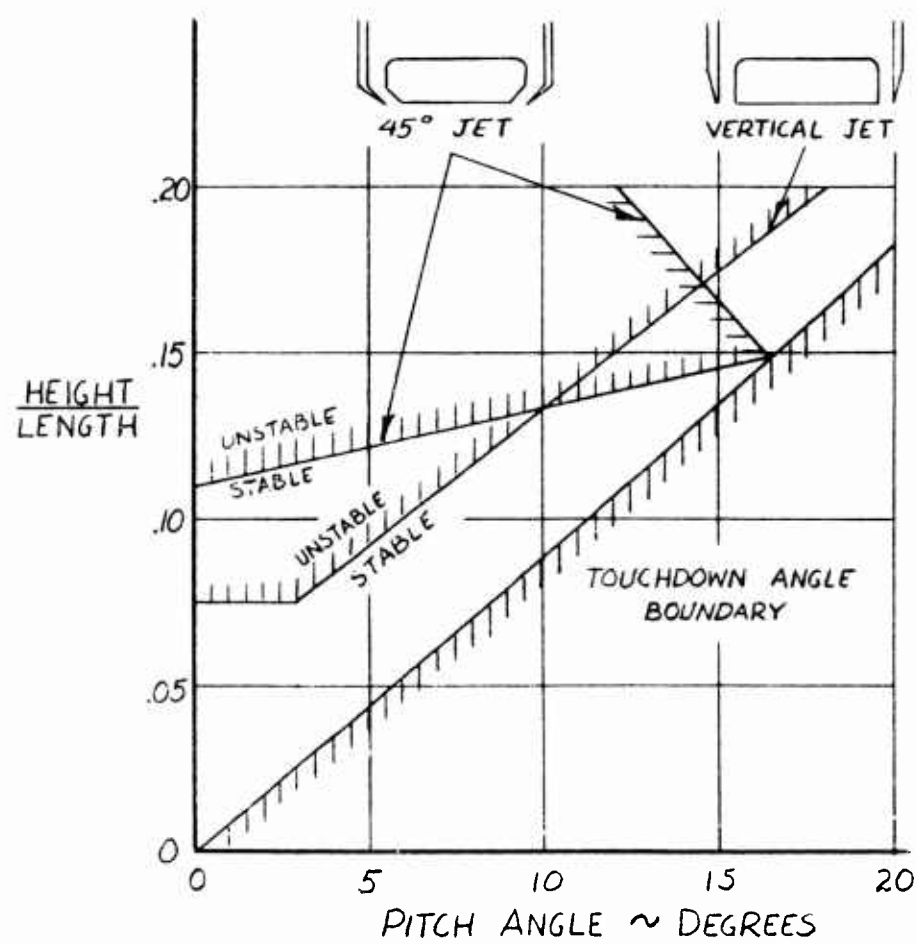


# STATIC LONGITUDINAL HOVERING STABILITY

VERTICAL vs. 45° INCLINED JET



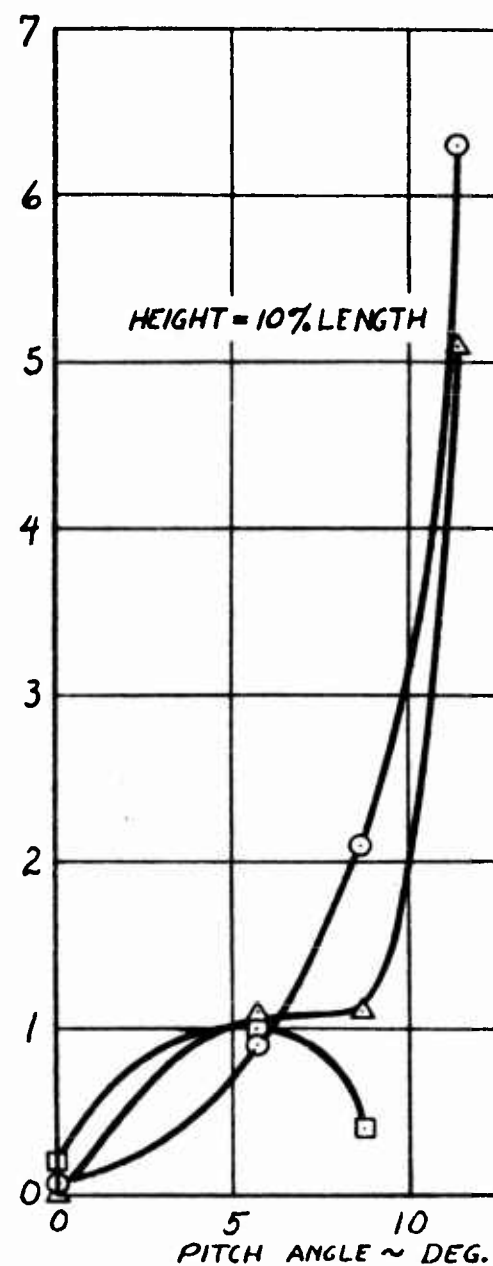
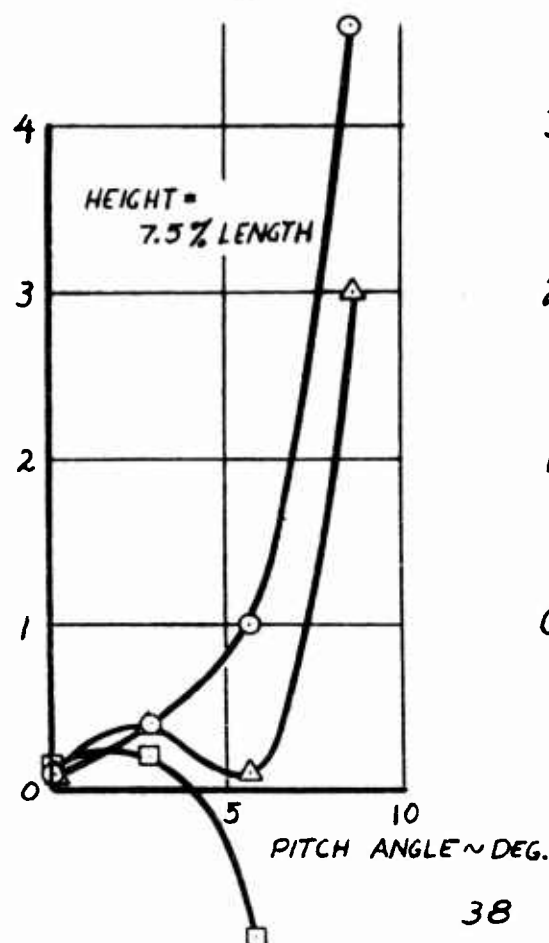
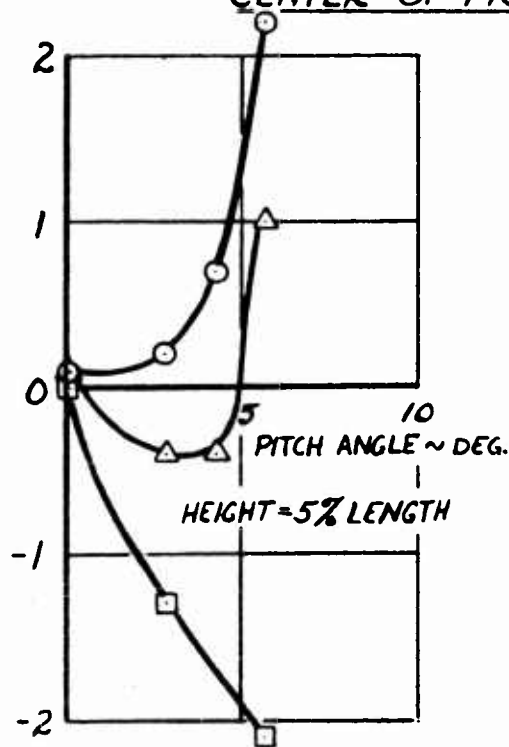
HEIGHT-PITCH ANGLE STABILITY BOUNDARIES  
VERTICAL vs 45° INCLINED JET



# EFFECT OF BASE SHAPING ON BASE PLUS JET CENTER OF PRESSURE SHIFT

Figure 19

C.P. SHIFT ~ % LENGTH



# EFFECT OF BASE SHAPING ON BASE PLUS JET CENTER OF PRESSURE SHIFT

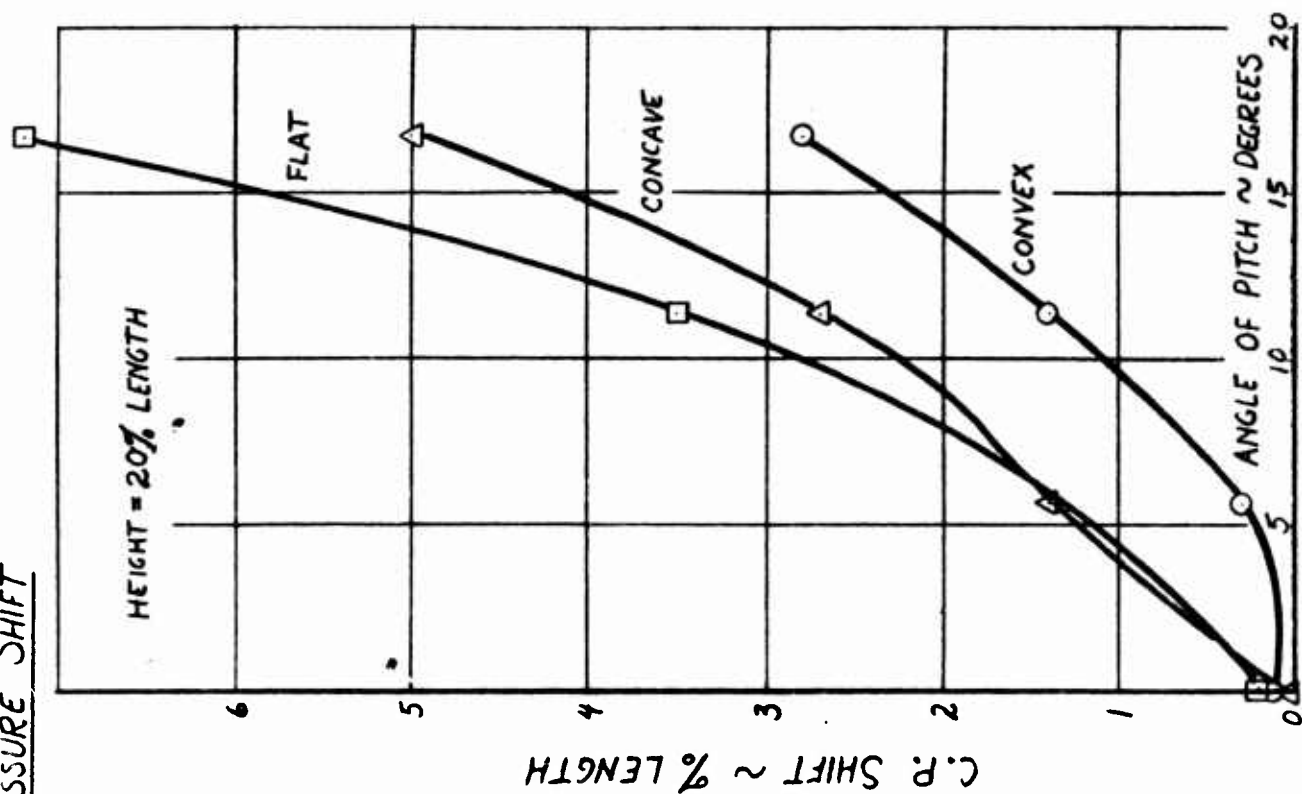
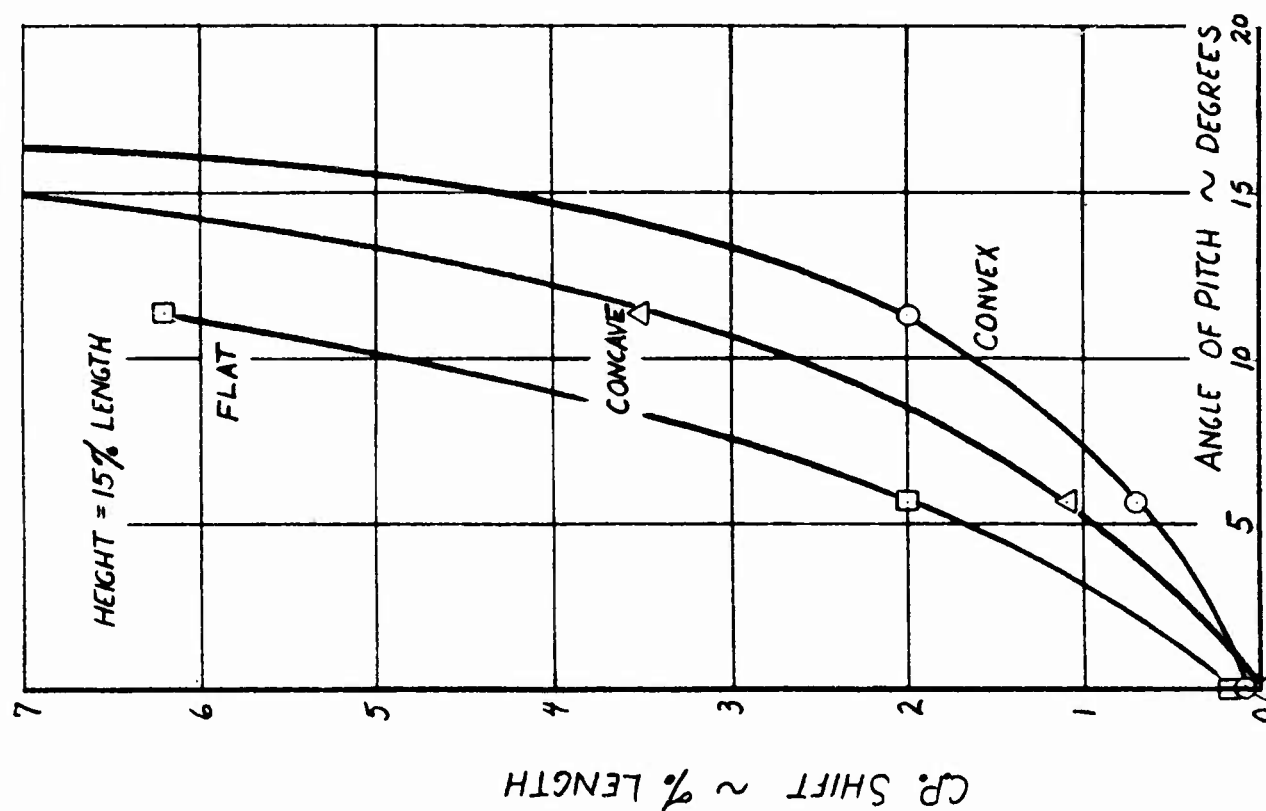
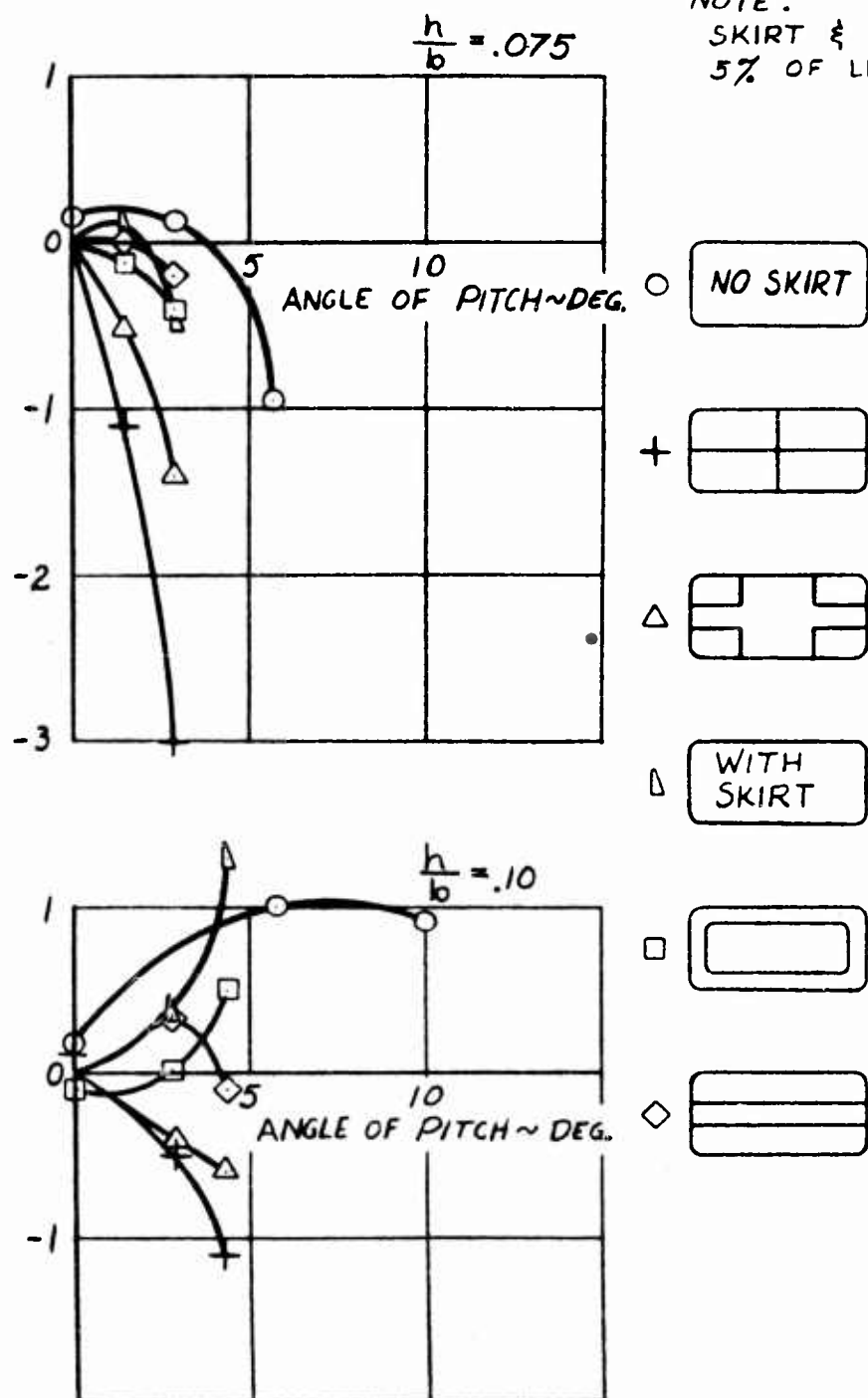


Figure 20

# EFFECT OF SKIRT AND FLAPS ON BASE PLUS JET CENTER OF PRESSURE SHIFT

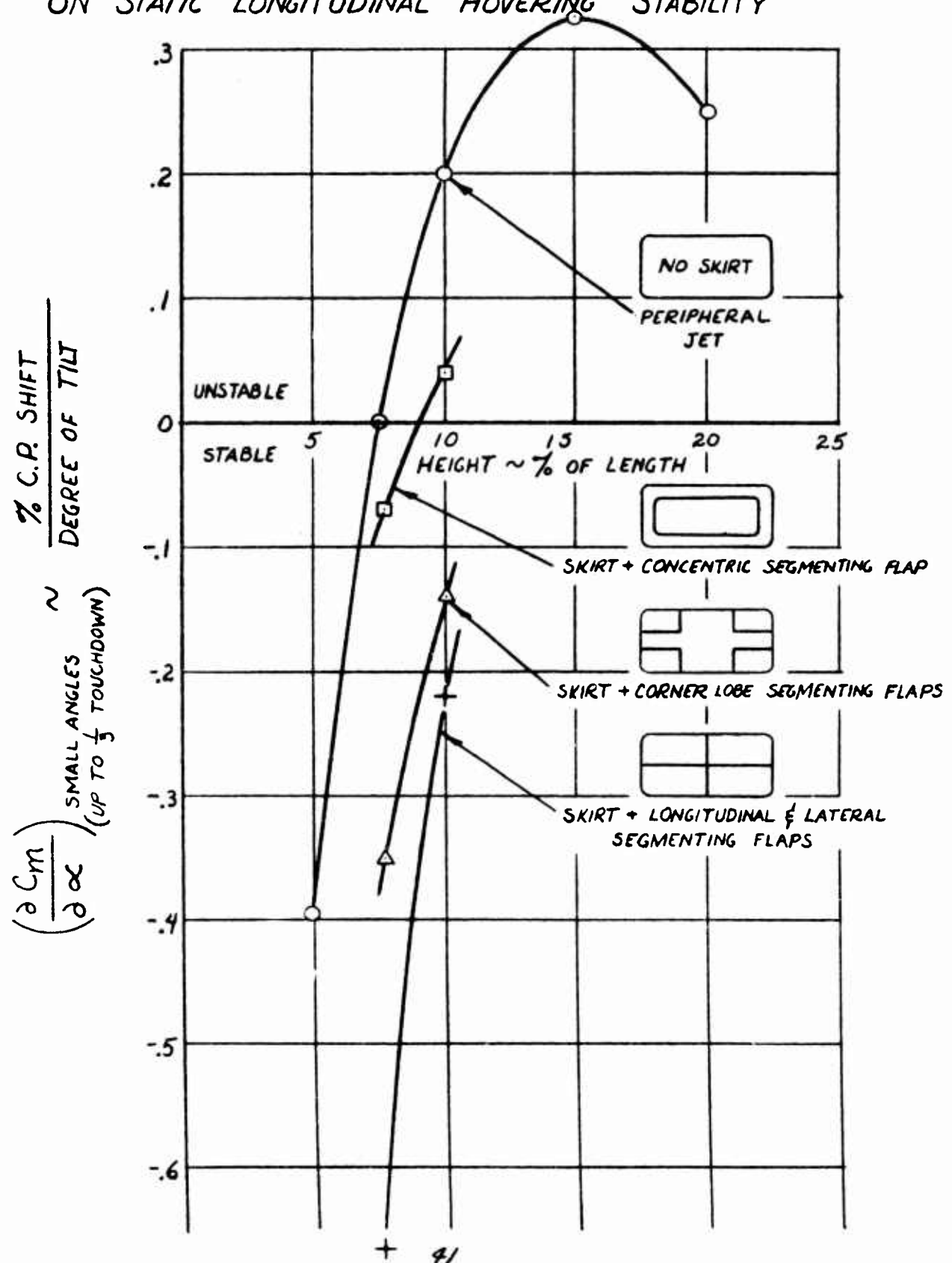
Figure 21

C.P. SHIFT  $\sim \frac{1}{2}$  LENGTH



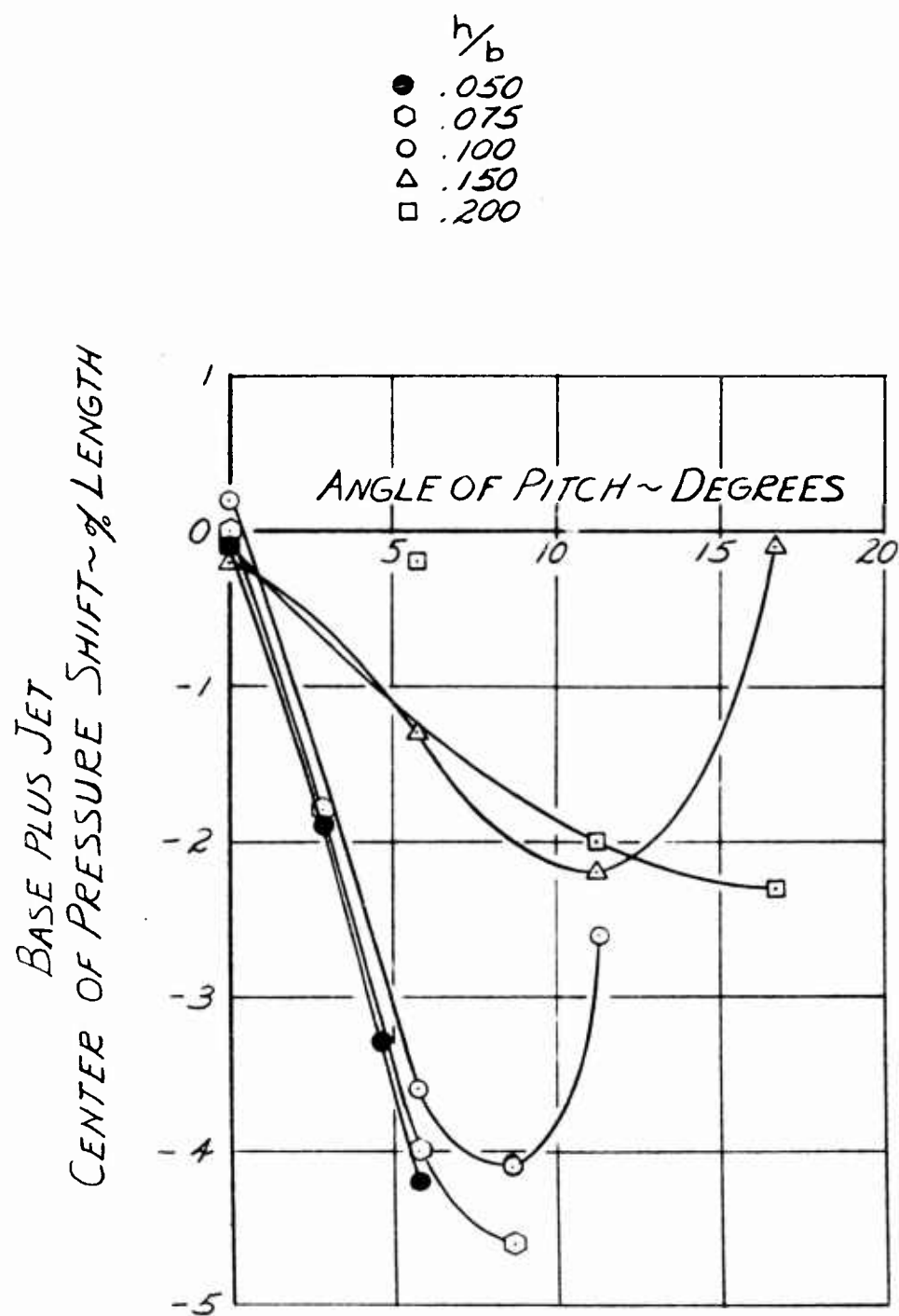
# EFFECT OF 5% LENGTH SKIRT AND FLAPS ON STATIC LONGITUDINAL HOVERING STABILITY

Figure 22





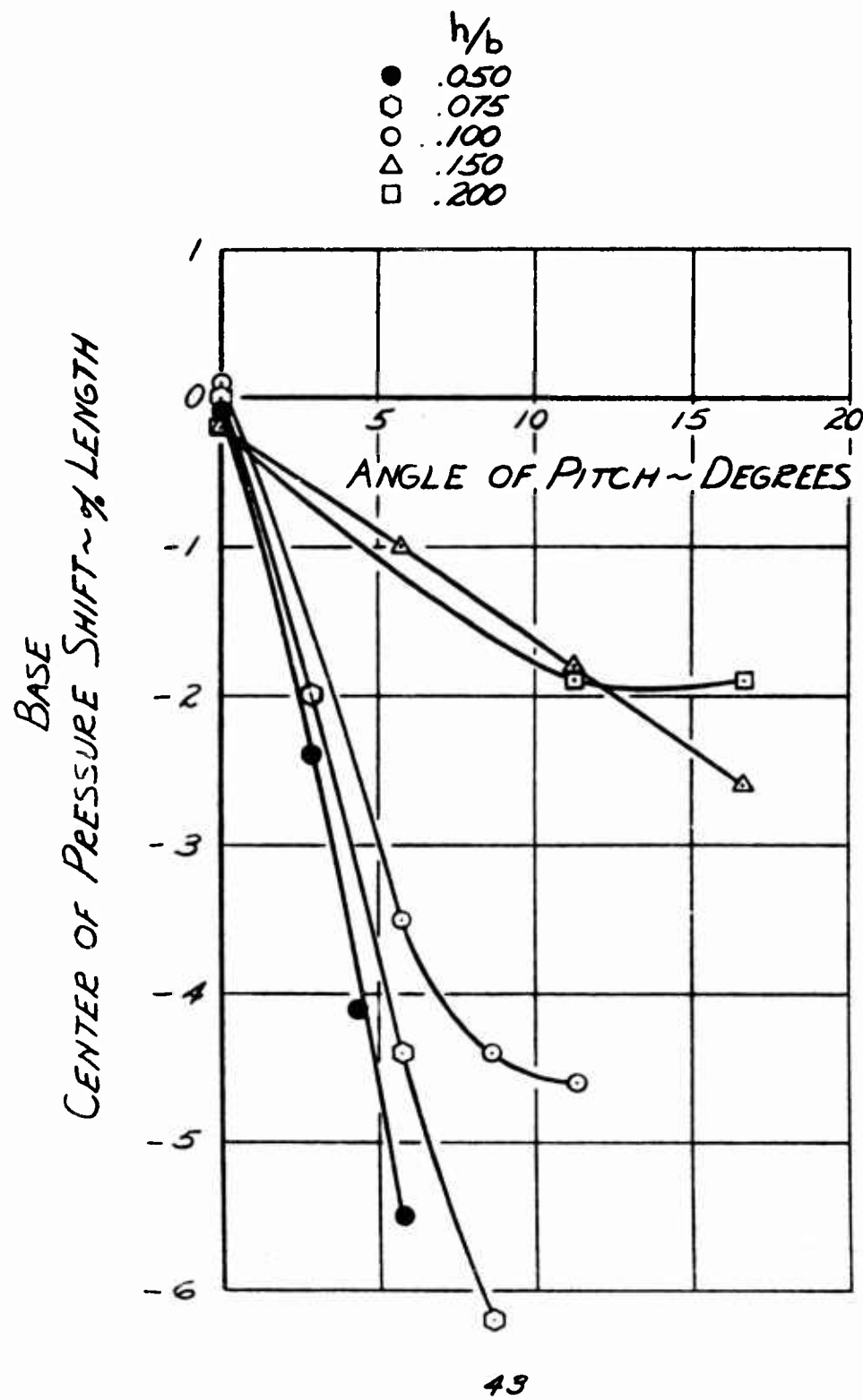
CENTERLINE JET SEGMENTED MODEL  
BASE PLUS JET  
CENTER OF PRESSURE SHIFT



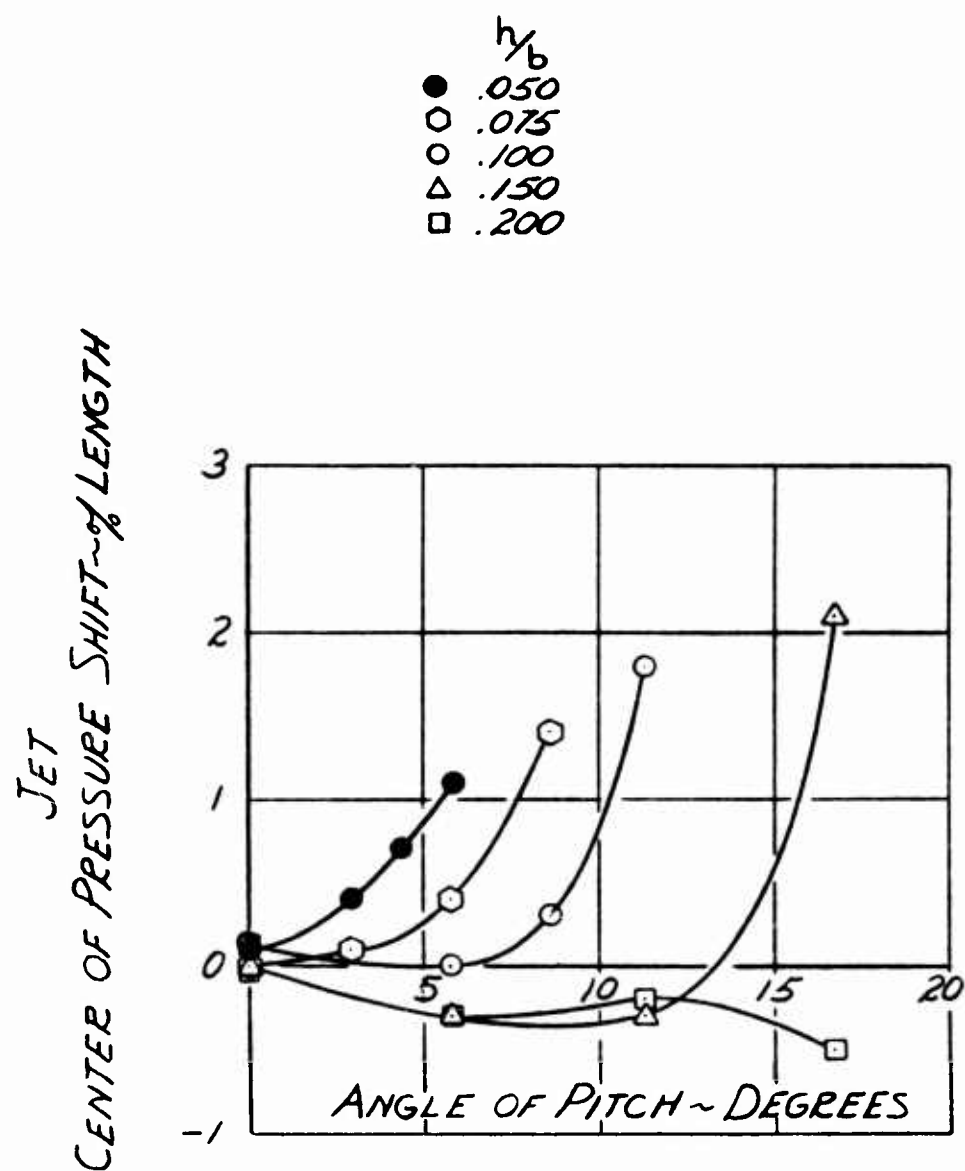
# CENTERLINE JET SEGMENTED MODEL

Figure 24

## BASE CENTER OF PRESSURE SHIFT



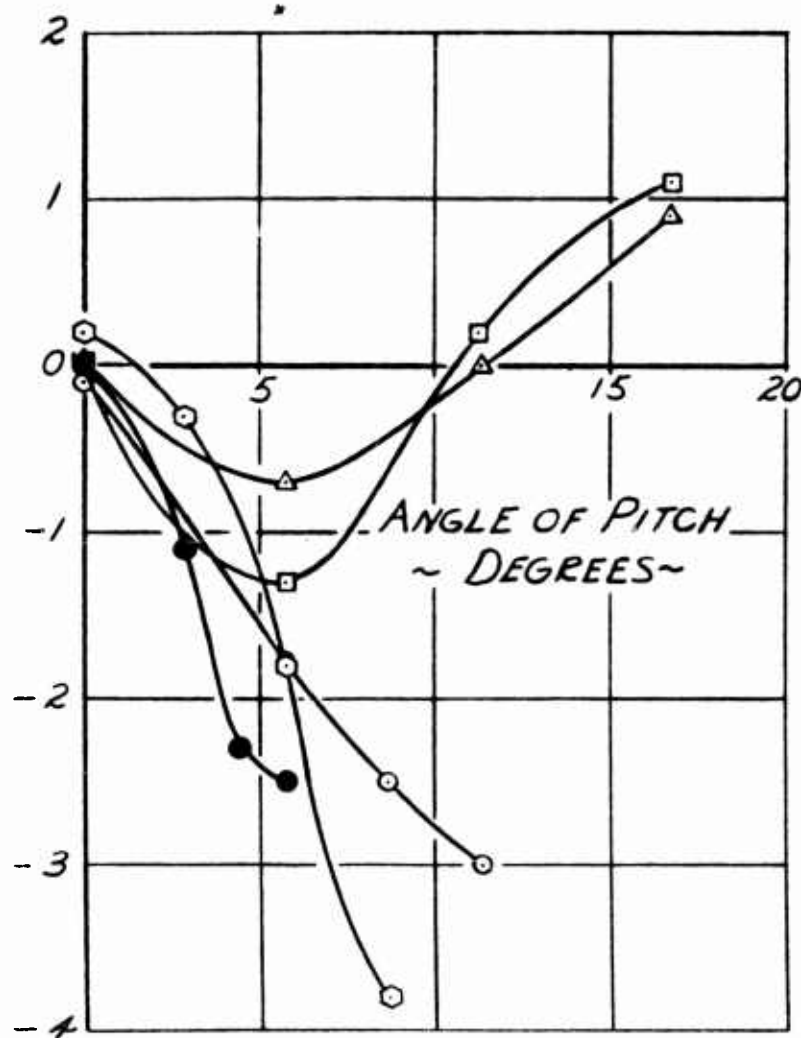
CENTERLINE JET SEGMENTED MODEL  
JET  
CENTER OF PRESSURE SHIFT



CORNER LOBE JET SEGMENTED MODEL  
BASE PLUS JET  
CENTER OF PRESSURE SHIFT

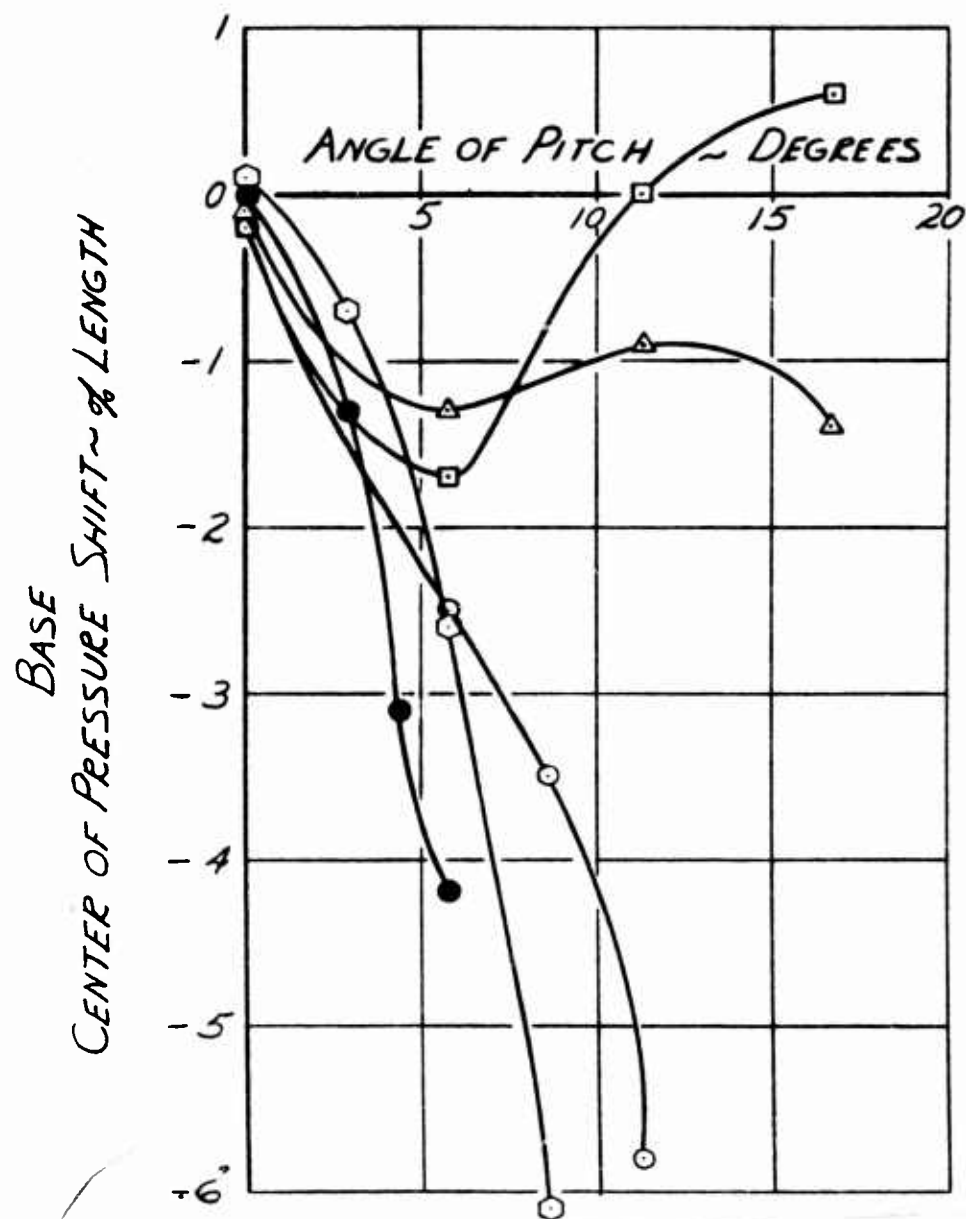
$h/b$   
 ● .050  
 ○ .075  
 ○ .100  
 △ .150  
 □ .200

BASE PLUS JET  
 CENTER OF PRESSURE SHIFT ~ % LENGTH



BASE  
CENTER OF PRESSURE SHIFT

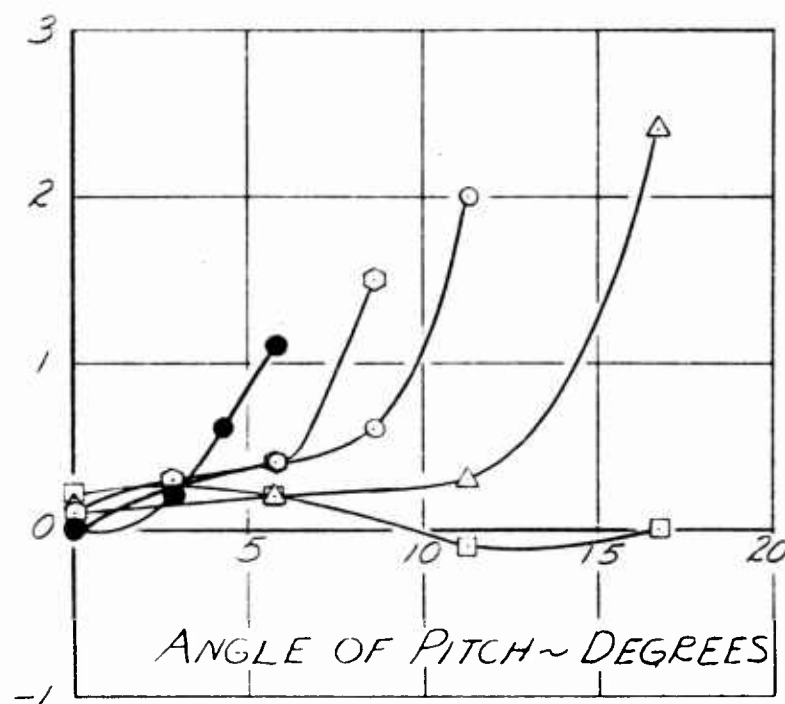
- $h/b$
- .050
  - .075
  - .100
  - △ .150
  - .200



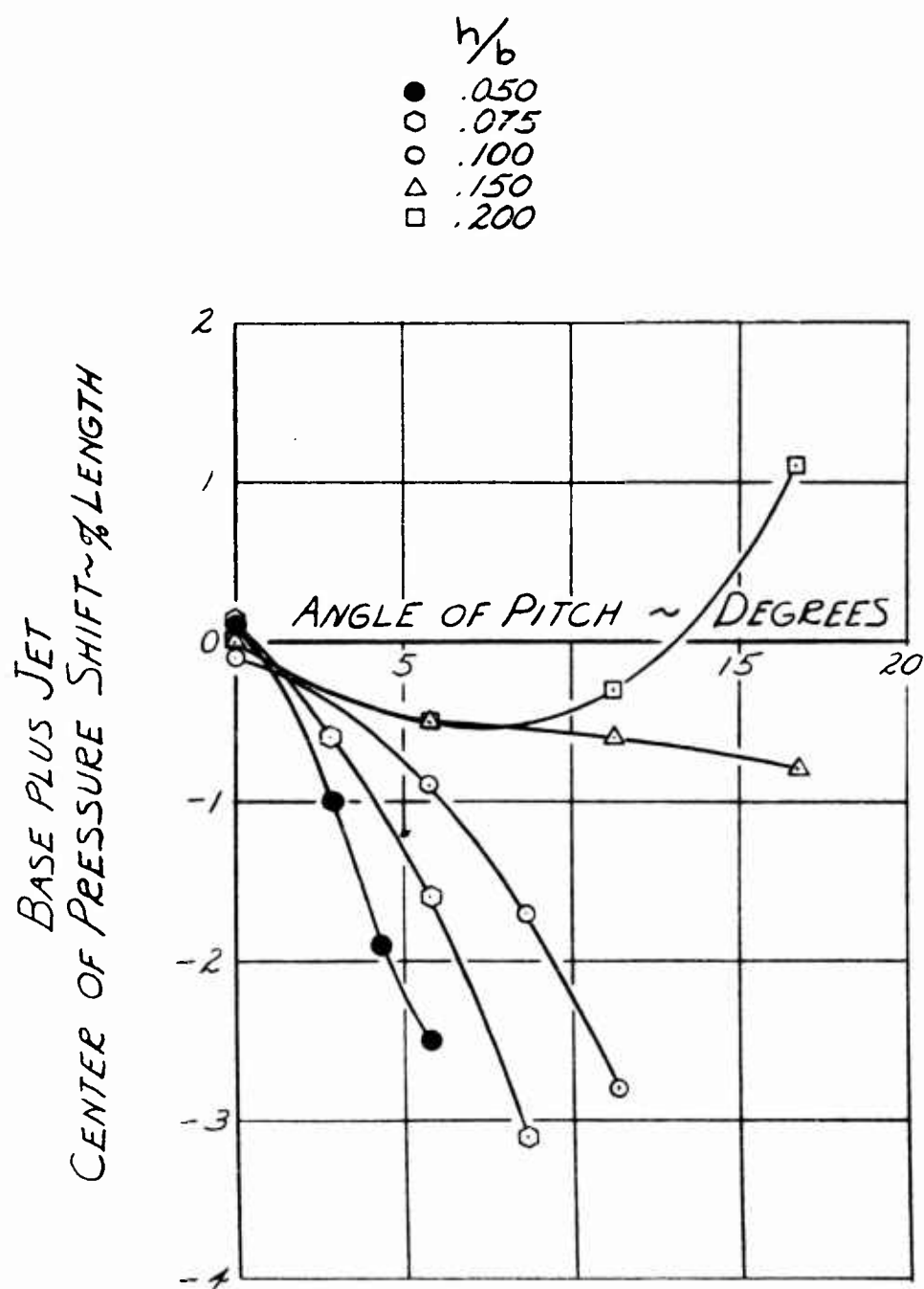
CORNER LOBE JET SEGMENTED MODEL  
JET  
CENTER OF PRESSURE SHIFT

$h/b$   
 ● .050  
 ◻ .075  
 ○ .100  
 △ .150  
 □ .200

JET  
 CENTER OF PRESSURE SHIFT ~ % LENGTH



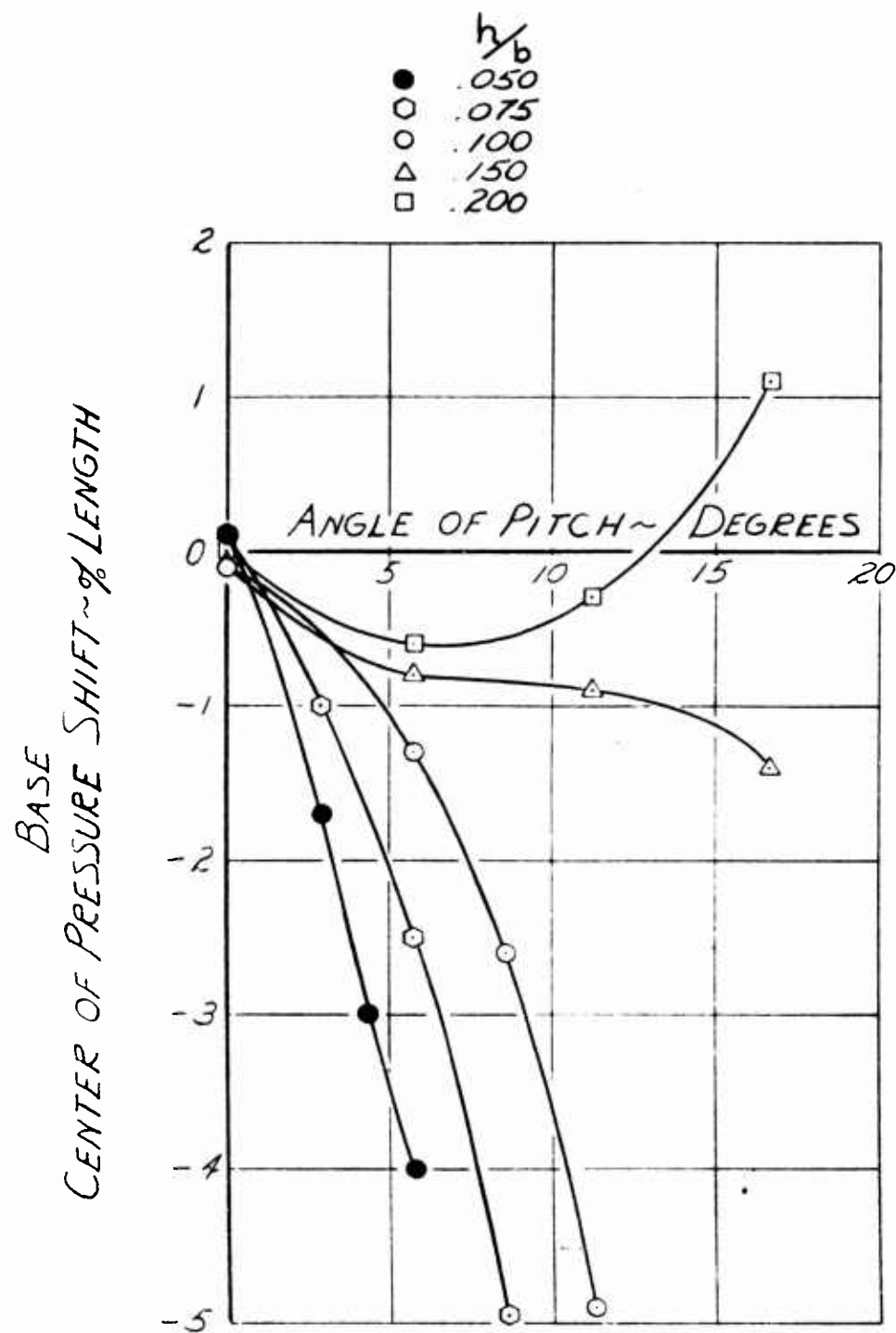
CONCENTRIC JET SEGMENTED MODEL  
BASE PLUS JET  
CENTER OF PRESSURE SHIFT



CONCENTRIC JET SEGMENTED MODEL

Figure 30

BASE  
CENTER OF PRESSURE SHIFT

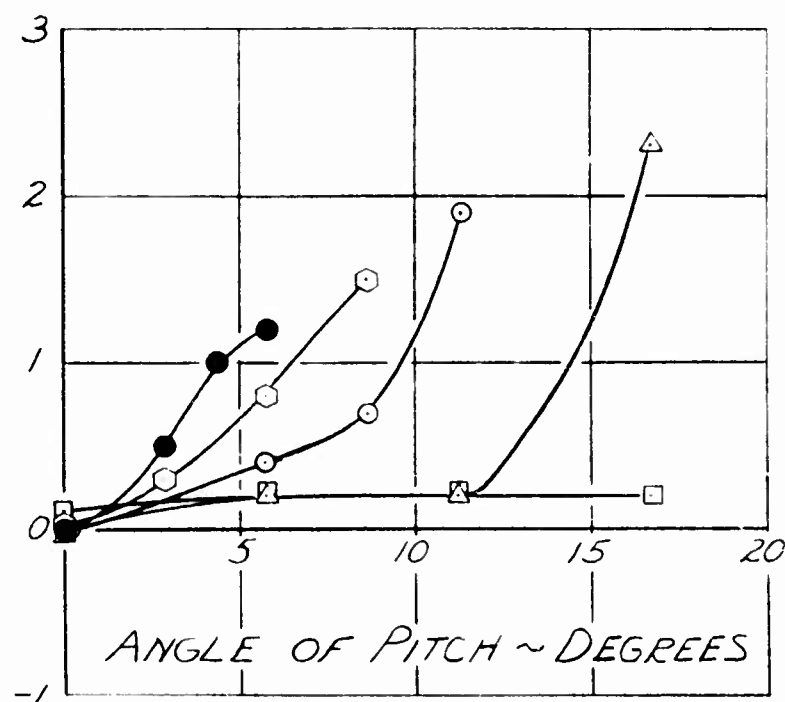




CONCENTRIC JET SEGMENTED MODEL  
JET  
CENTER OF PRESSURE SHIFT

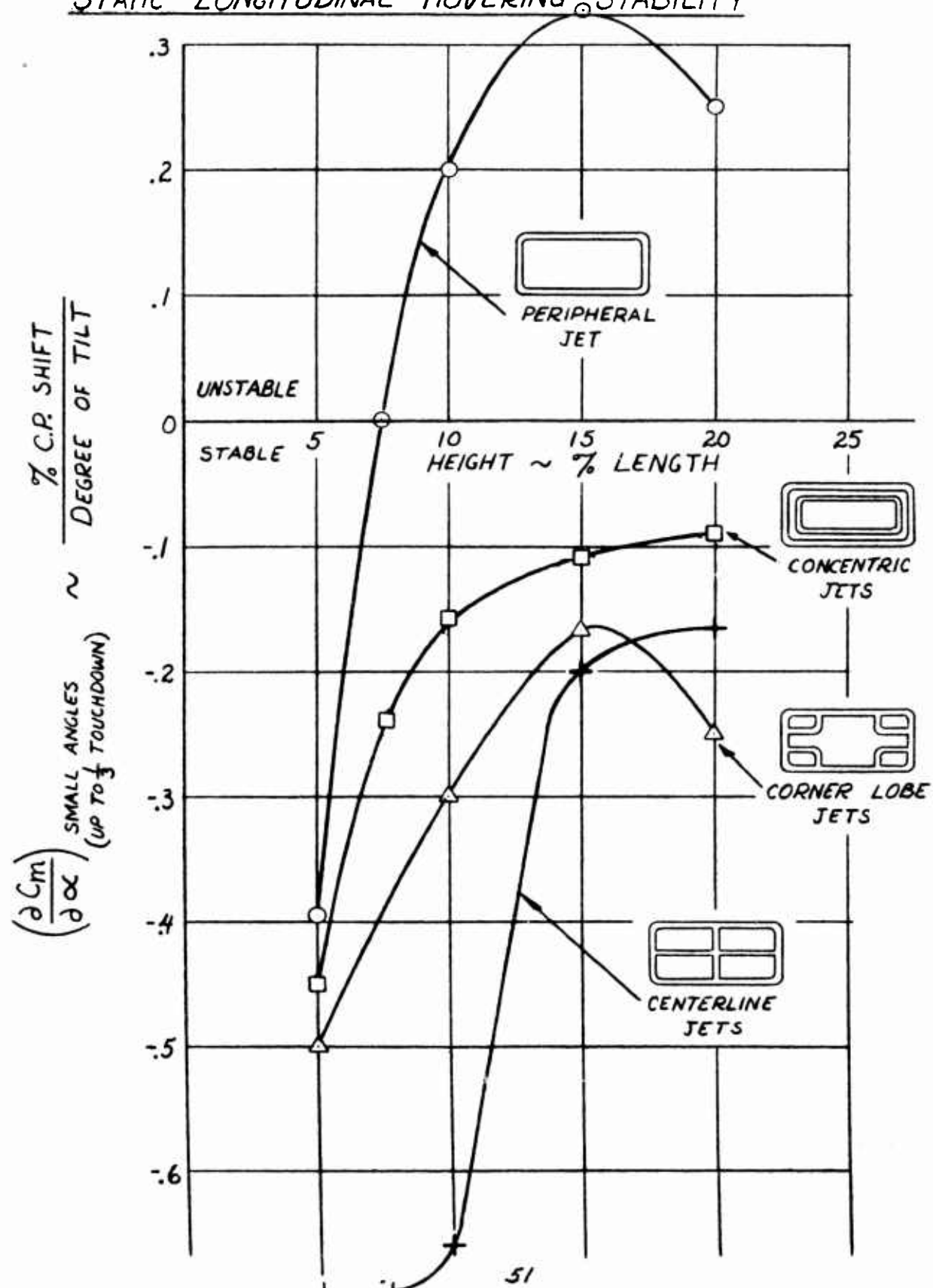
$h/b$   
 ● .050  
 ○ .075  
 ○ .100  
 △ .150  
 □ .200

JET  
 CENTER OF PRESSURE SHIFT ~ % LENGTH

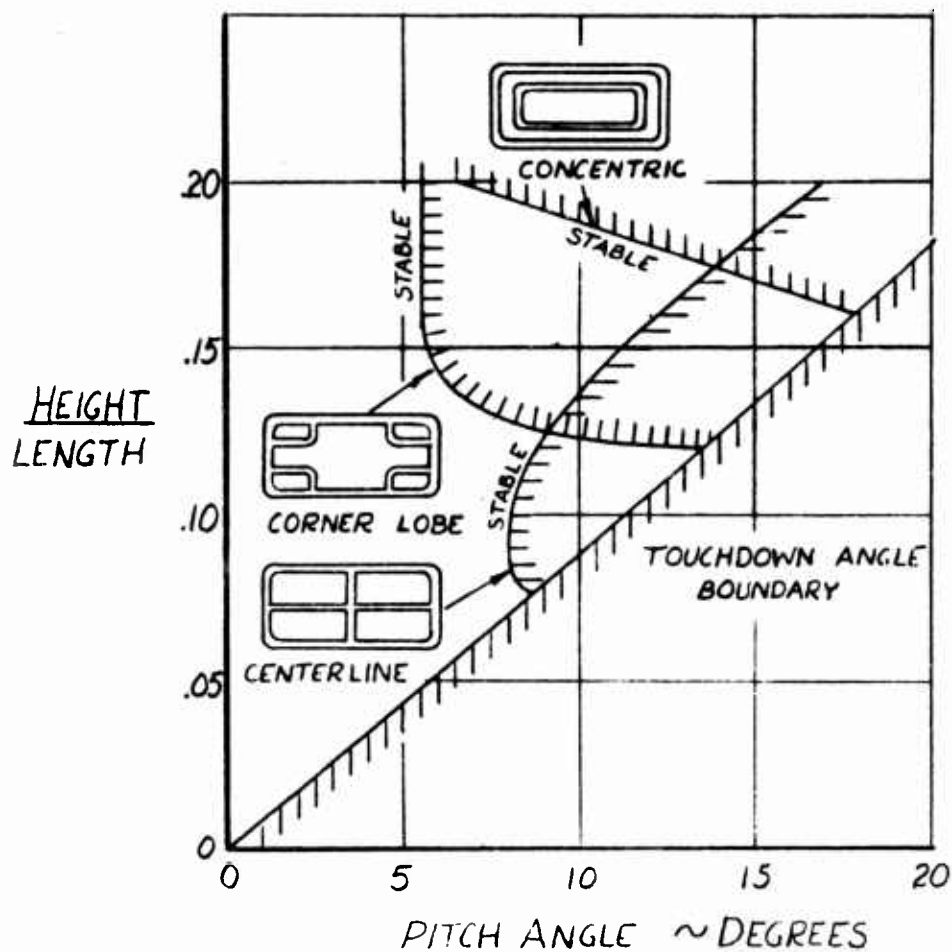


# EFFECT OF JET SEGMENTATION ON STATIC LONGITUDINAL HOVERING STABILITY

Figure 32



EFFECT OF JET SEGMENTATION  
ON HEIGHT-PITCH ANGLE STABILITY BOUNDARIES



## 2. Lateral Stability

### a. Simple Peripheral Jet Models

The base plus jet center of pressure shift of the vertical peripheral jet model is shown in Figure 34. This configuration is unstable in roll at small angles at all heights and tends to become more unstable at large tilt angles. The model was unstable in roll at heights where it was stable in pitch. Since the model width is only half the model length, the minimum physical height point was halved in order to amount to the same percentage of characteristic length as in the pitch case. This height =  $5\% w = 2.5\% b$  still produced an unstable slope. It would appear that long narrow models have near two-dimensional flow patterns in roll. Aeronutronic experiments (Reference 1) indicated instability at all heights and angles for two-dimensional flow.

The base center of pressure shift of Figure 35 is very similar to the base + jet curves. There is, however, a decrease of base instability at large tilt angles and low heights. The jet contribution is small for all cases except at tilt angles near touchdown at low heights as shown in Figure 36.

The base + jet center of pressure shift of the  $45^\circ$  inclined peripheral jet model as shown in Figure 37 is either unstable or neutrally stable over the entire height range. The degree of instability at both small and large tilt angles is less for the  $45^\circ$  inclined jet than for the vertical jet.

The base center of pressure shift as given in Figure 38 is very similar to the base + jet shift. The jet contribution is small but becomes increasingly unstable as tilt angles approach touchdown as shown in Figure 39.

The small angle lateral stability of the vertical and  $45^\circ$  inclined jet are compared in Figure 40. The  $45^\circ$  inclined jet is less unstable at low to moderate heights. There is little difference at the larger height.

b. Effect of Base Shaping

The effect of shaping the base (in an effort to change the base pressure distribution under crossflow condition) was almost negligible as shown in Figure 41 and 42.

c. Skirted and Flap Segmented Models

The addition of a peripheral skirt alone did not change the instability in roll of the basic model to any extent as shown in Figure 43. The concentric flap was also not very helpful. The corner lobe flaps were somewhat more effective but still did not stabilize the model at either height. (15% and 20% of the width.) The single and double longitudinally running flaps stabilized the model at the lower height where they extended two-thirds of the way to the ground but failed to provide stability at the 20% height where they extended only half way to the ground.

The small angle stability slopes are compared for the various flap arrangements in Figure 44. In order of increasing improvement they are: concentric, corner lobe, single longitudinal, and double longitudinal. As mentioned before, the basic model instability in the lateral mode is more severe than in the longitudinal mode. It also appears to be more difficult to rectify the situation with segmenting flaps.

d. Jet Segmented Models

The base + jet center of pressure shift of the centerline jet segmented model is shown in Figure 45. Good small angle stability is available at all heights and holds up to 12 degrees of tilt angle. The model becomes unstable at large tilt angles at virtually all heights.

The base center of pressure shift shown in Figure 46 appears similar to the base + jet curves but retains a stable slope to higher angle-height combinations. The jet contribution is seen in Figure 47 to be responsible for the high angle instability of the base + jet.

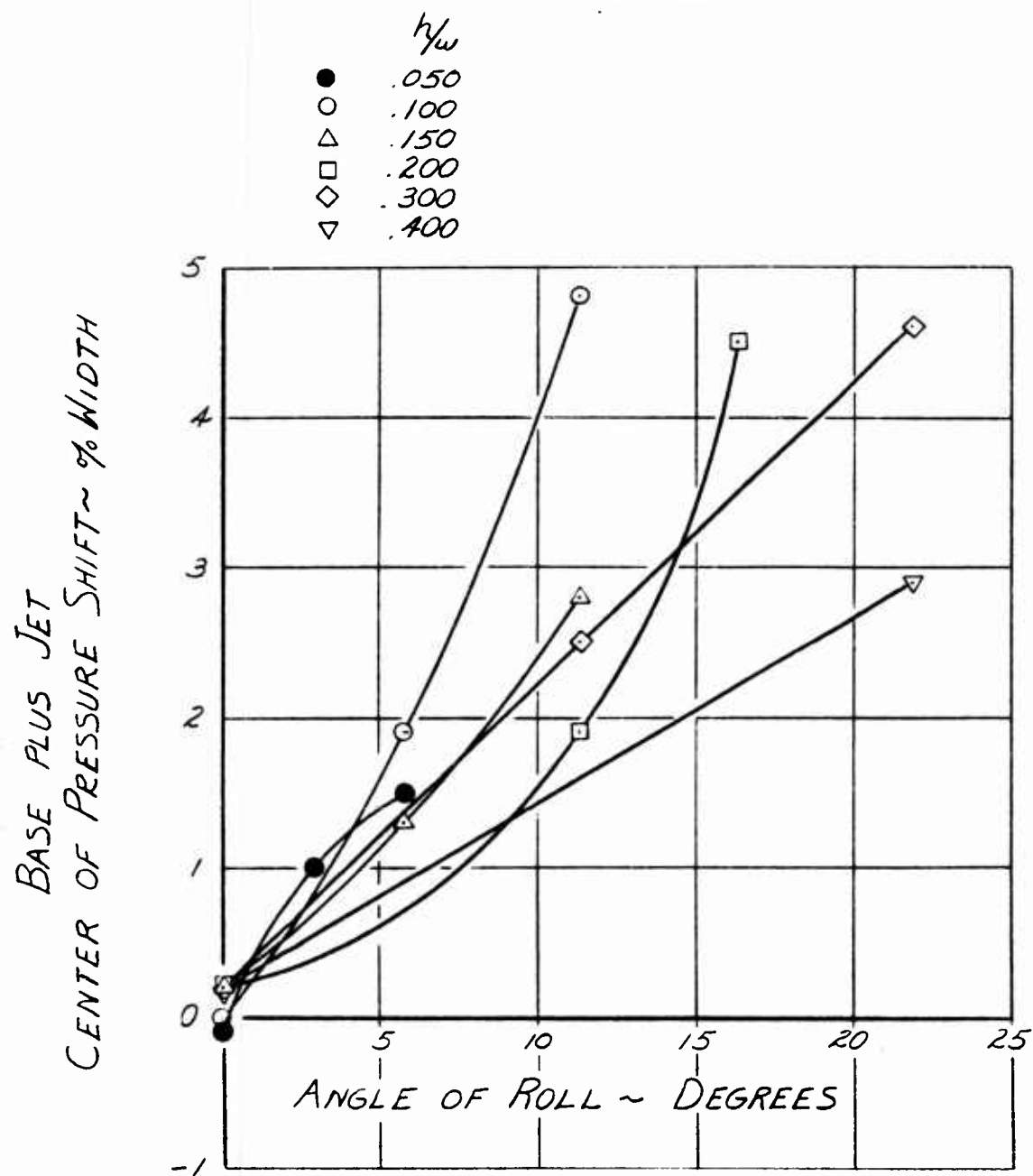
The base + jet center of pressure shift of the corner lobe jet segmented model is shown in Figure 48. Small angle stability exists to a height of 20% of the width with instability occurring at higher heights. High angle instability is present at all height values. The base center of pressure shift curves presented in Figure 49 exhibit the same trends but have a lower degree of high angle instability. Figure 50 demonstrates the unstable contribution from the jets at tilt angles approaching touchdown.

The base + jet center of pressure shift of the concentric jet segmented model is shown by Figure 51 to exhibit almost neutral stability at all heights. The base contribution of Figure 52 is moderately stable at all heights and practically throughout the range of tilt angles. There is of course the usual decrease in magnitude of base stability contribution with increasing height. The jet contributions of Figure 53 are more unstable than for other configurations, even at small angles where neutral or slightly positive stability has been the rule. This effect was also present for the concentric jet in pitch. This could be expected since the two branches of the concentric arrangement will magnify the momentum choking on the low side.

The small angle stability of the jet segmented models is compared in Figure 54. The concentric model is slightly stable below 20% h/w and neutrally stable above this height. The corner lobe model is somewhat more stable below this crossover and slightly unstable at higher heights. The centerline jet segmented model is stable at all heights up through the maximum tested height of 40% of the width!

The height-roll angle stability boundaries are compared in Figure 55. The concentric and corner lobe boundaries are very similar and the centerline jet segmented model shows a clear superiority. It should be emphasized that even the centerline jet segmented model is unstable at very large tilt angles.

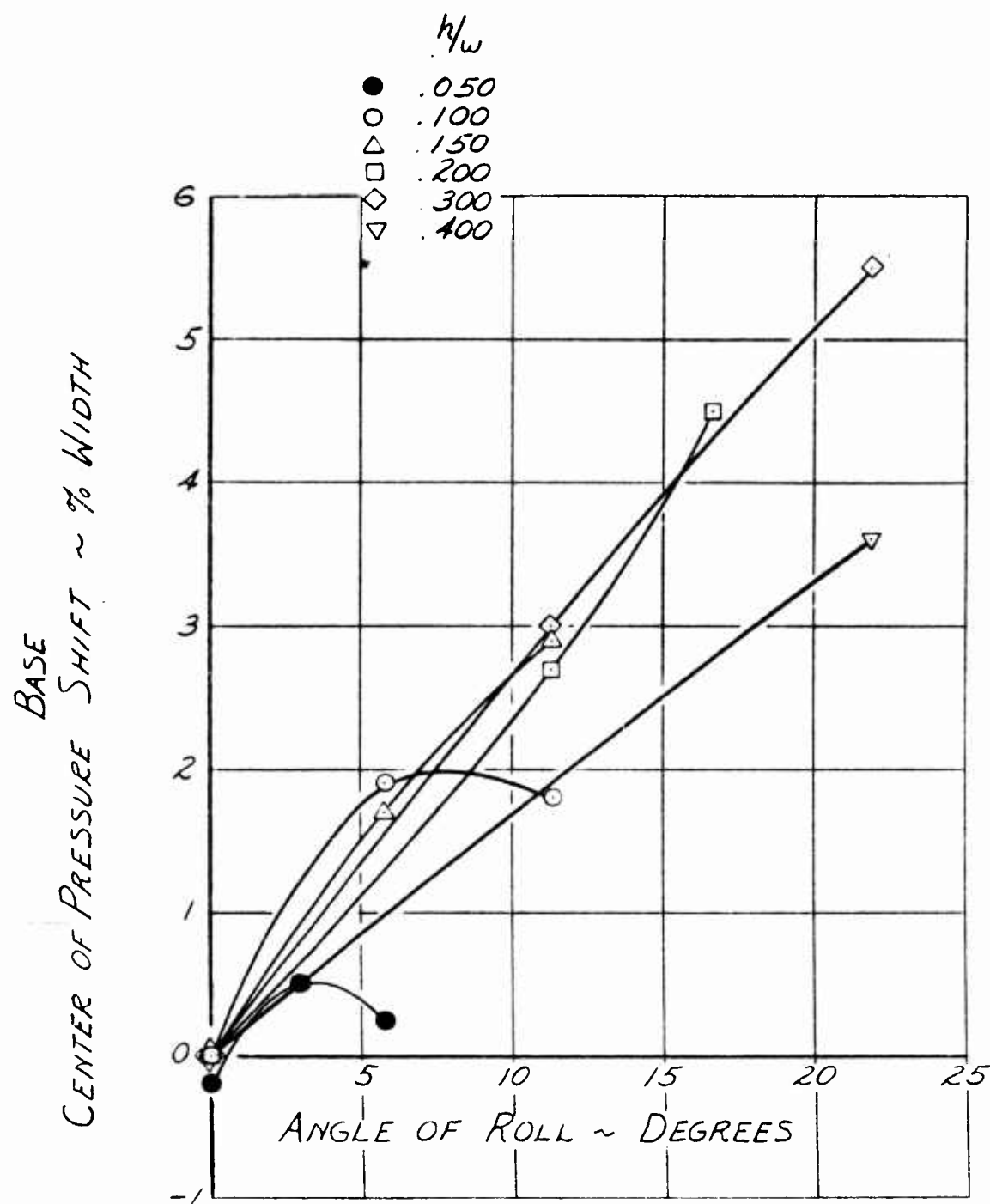
VERTICAL PERIPHERAL JET MODEL  
BASE PLUS JET  
CENTER OF PRESSURE SHIFT



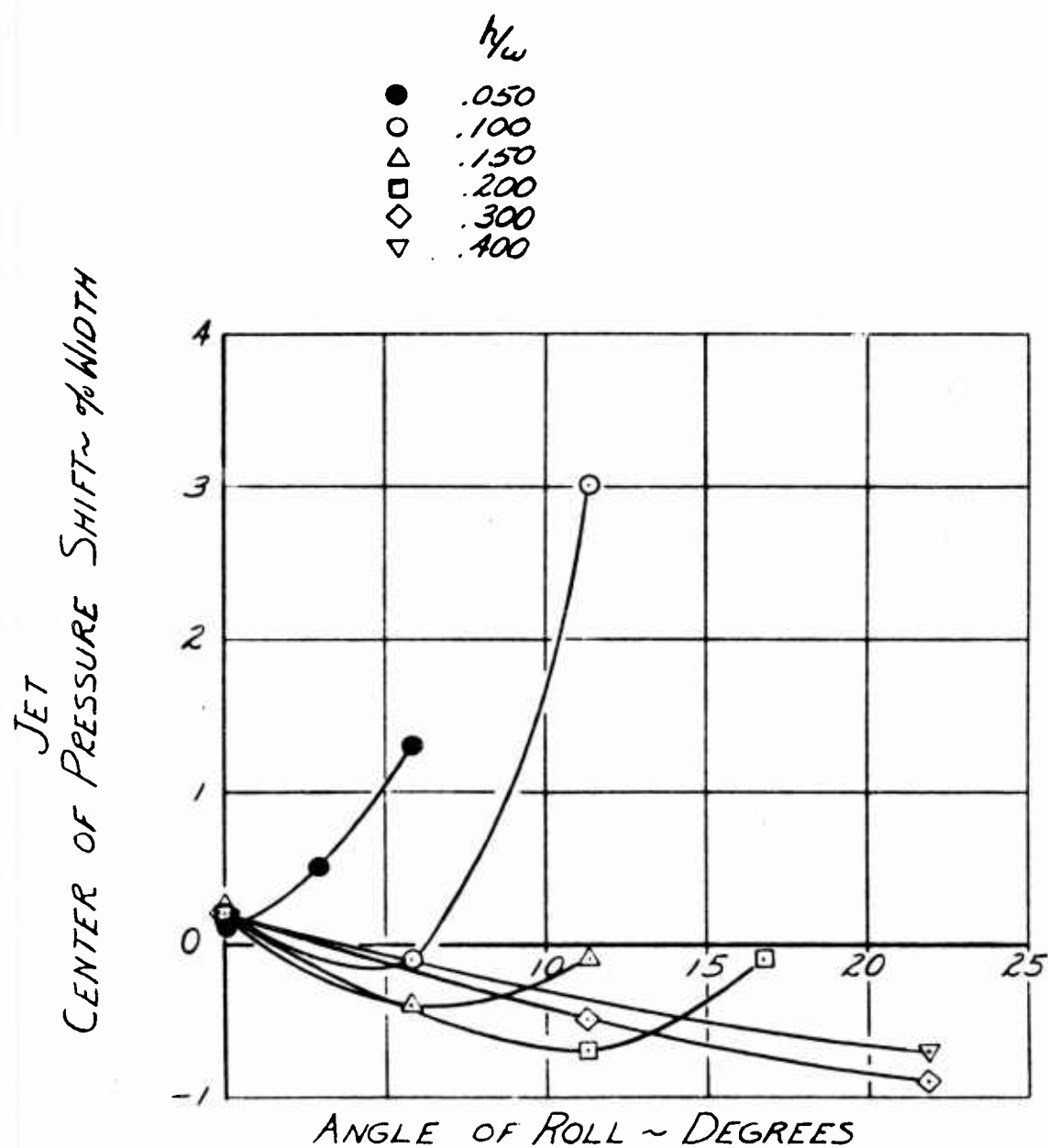


VERTICAL PERIPHERAL JET MODEL  
BASE  
CENTER OF PRESSURE SHIFT

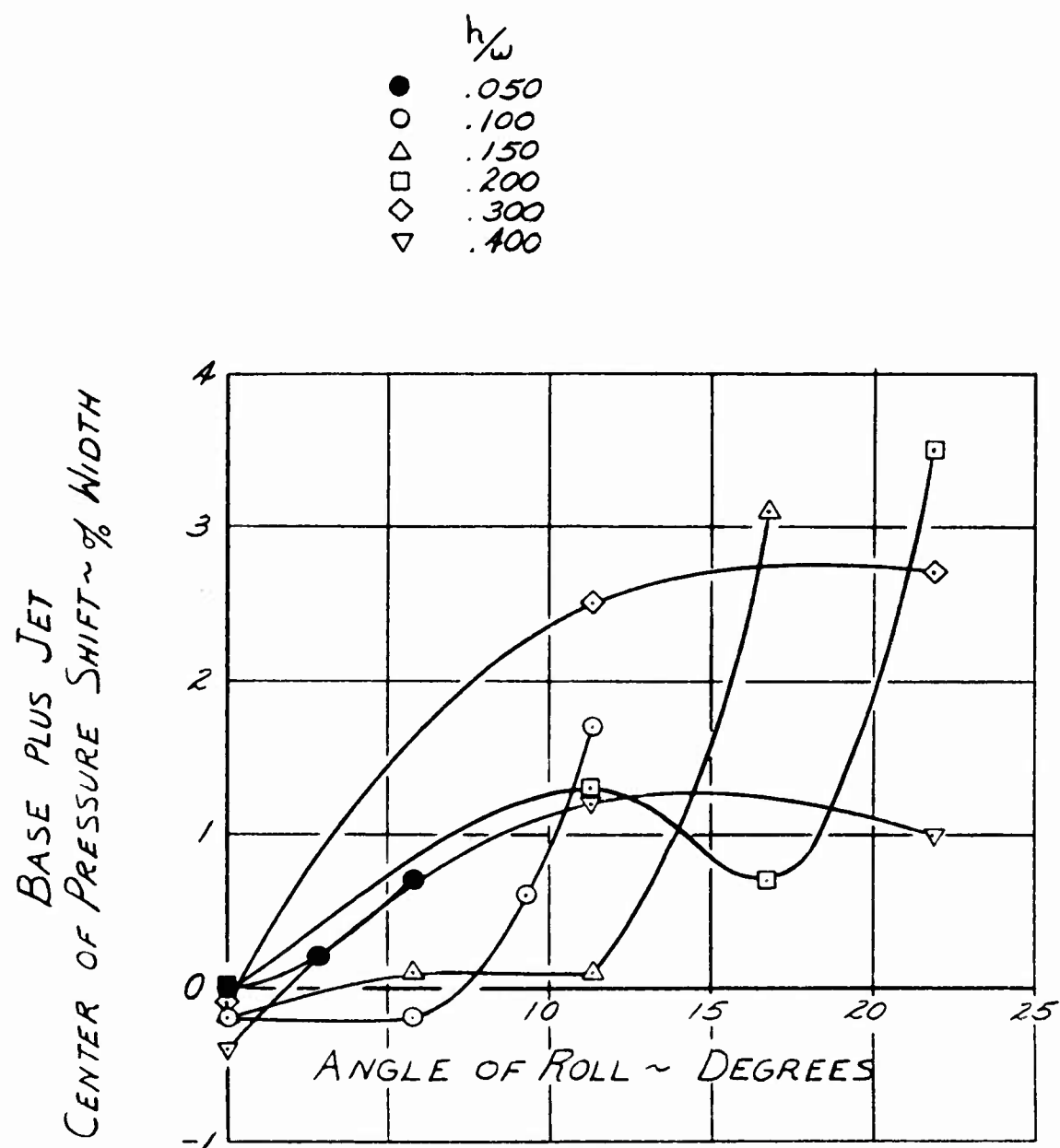
Figure 35



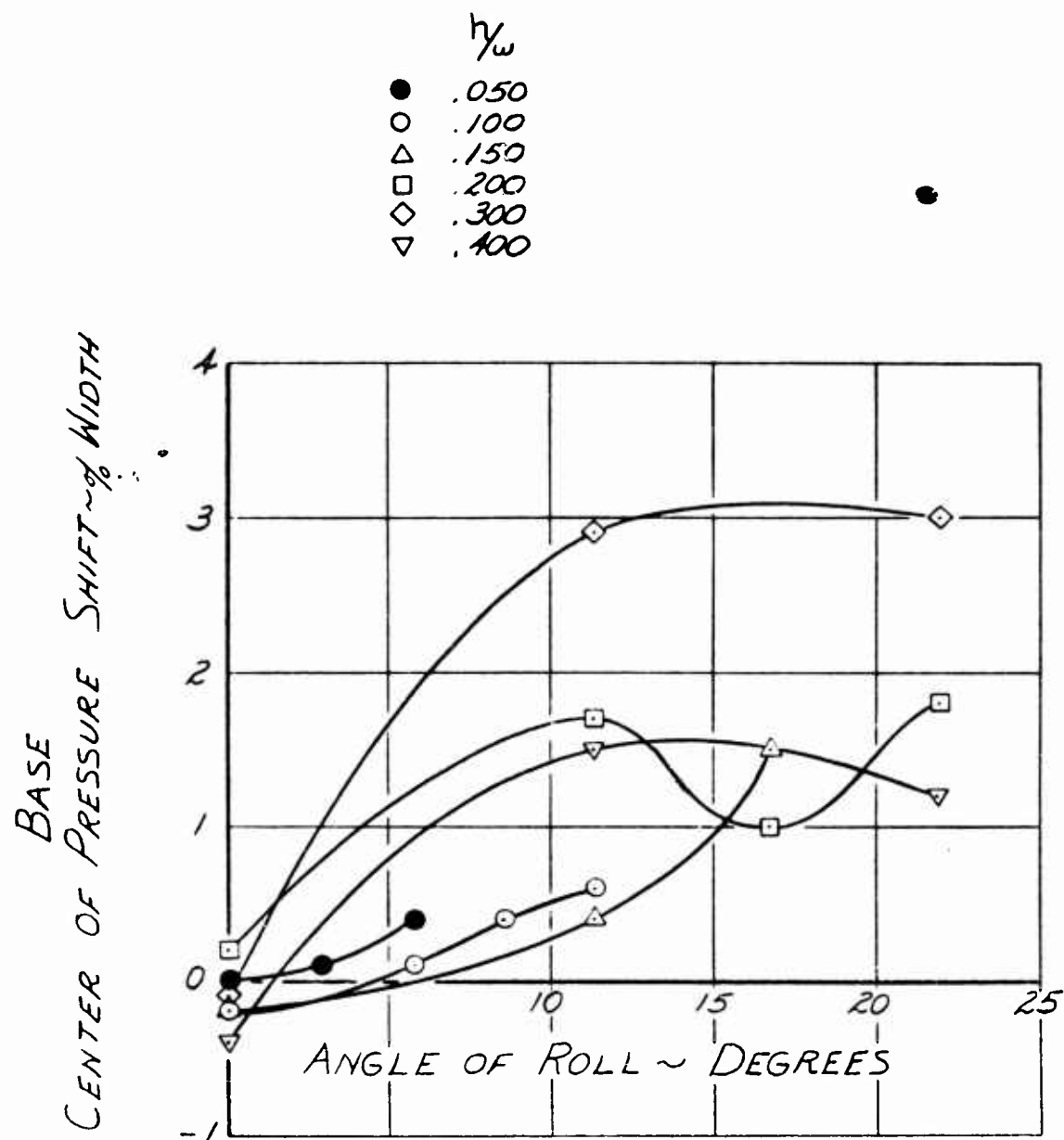
VERTICAL PERIPHERAL JET MODEL  
JET  
CENTER OF PRESSURE SHIFT



45° INCLINED PERIPHERAL JET MODEL  
BASE PLUS JET  
CENTER OF PRESSURE SHIFT

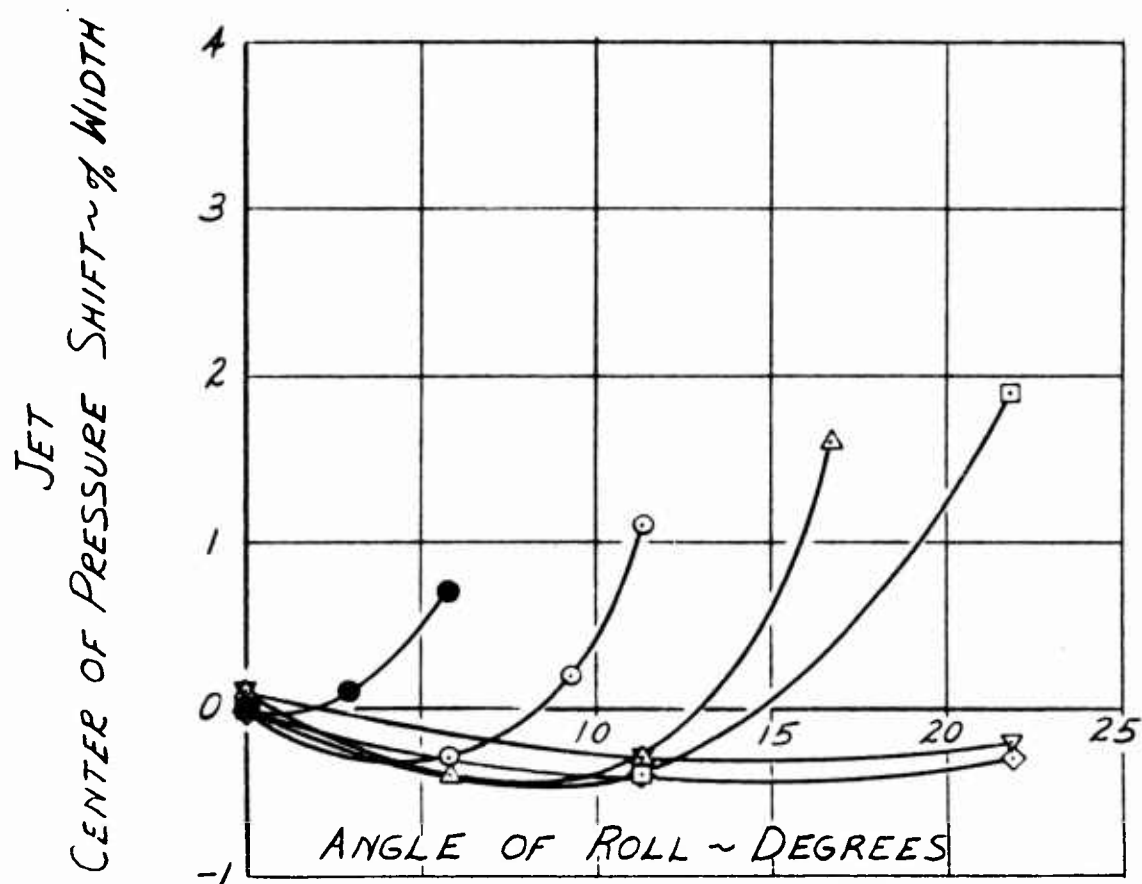


45° INCLINED PERIPHERAL JET MODEL  
BASE  
CENTER OF PRESSURE SHIFT



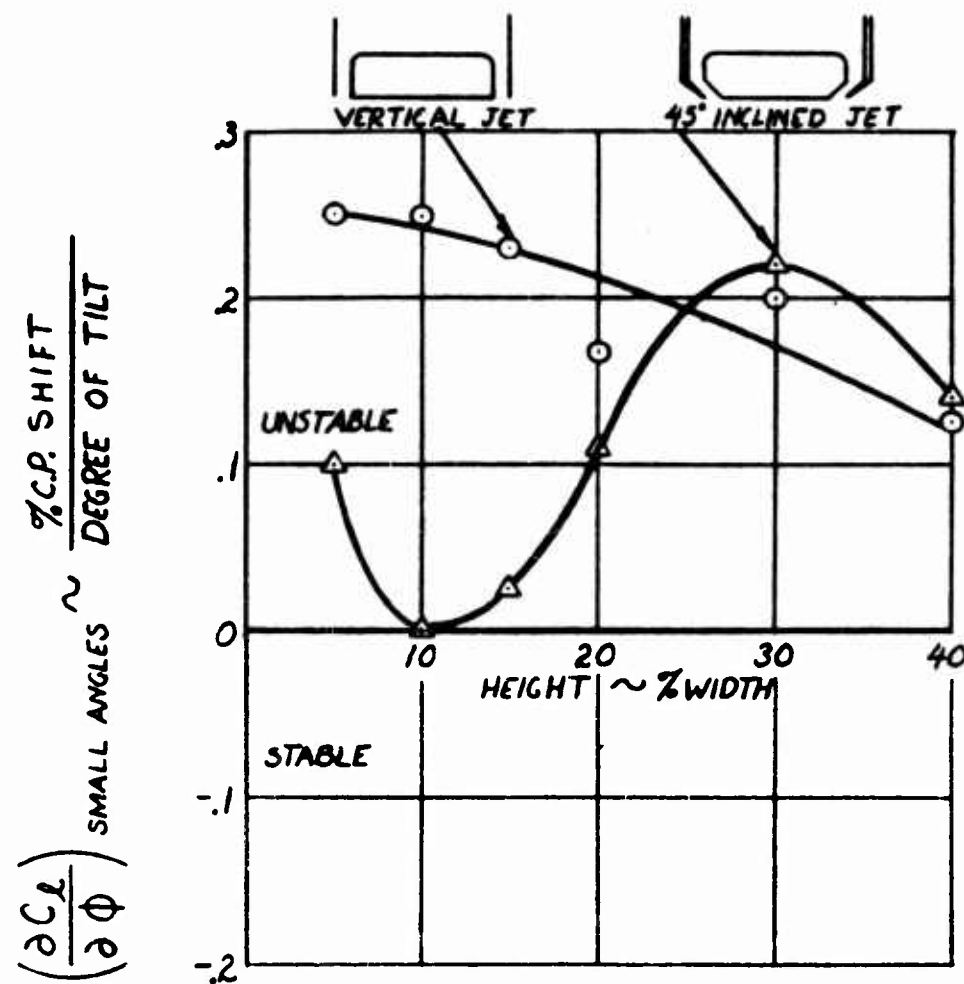
45° INCLINED PERIPHERAL JET MODEL  
JET  
CENTER OF PRESSURE SHIFT

$h/w$   
 ● .050  
 ○ .100  
 △ .150  
 □ .200  
 ◇ .300  
 ▼ .400

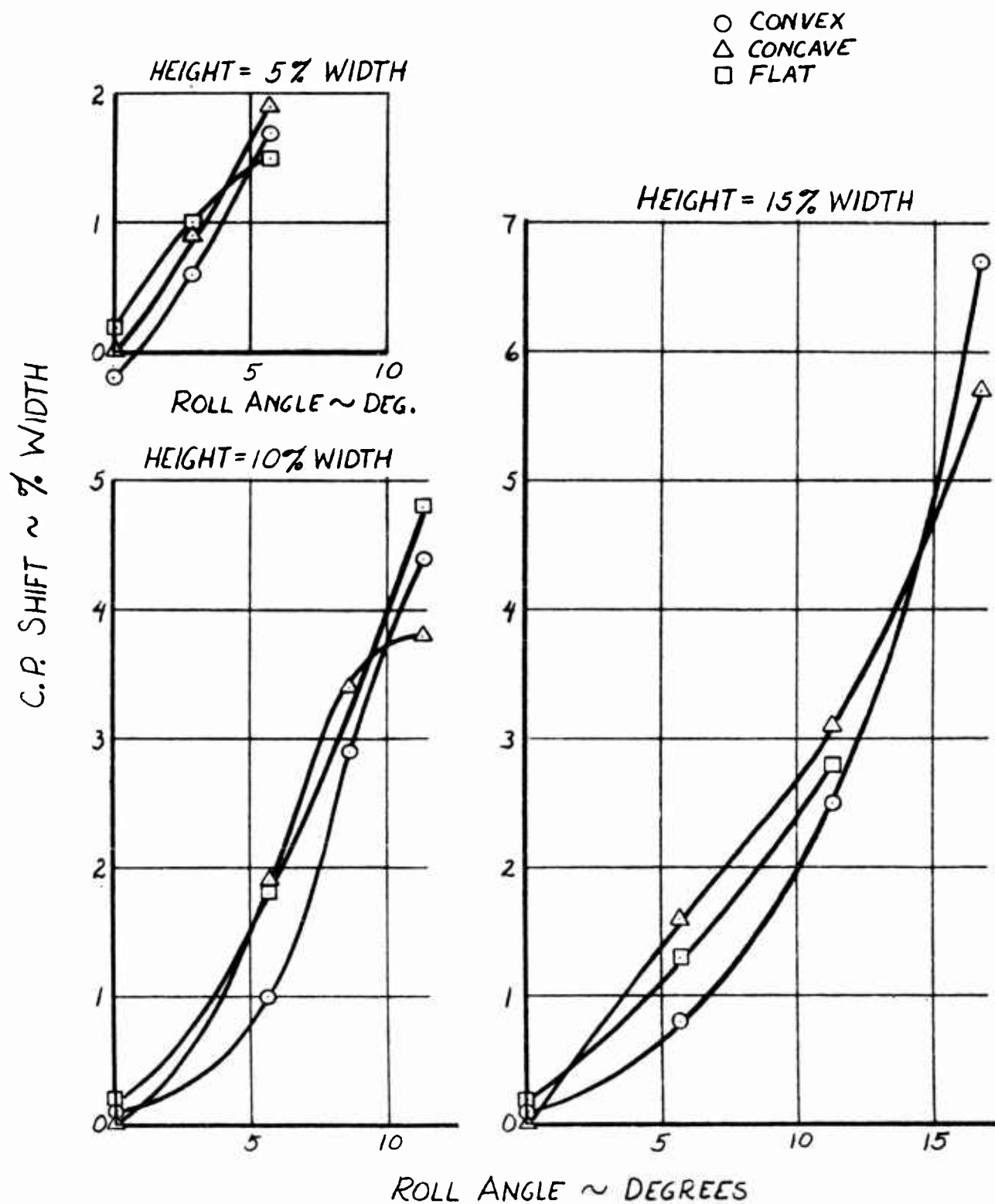


# STATIC LATERAL HOVERING STABILITY

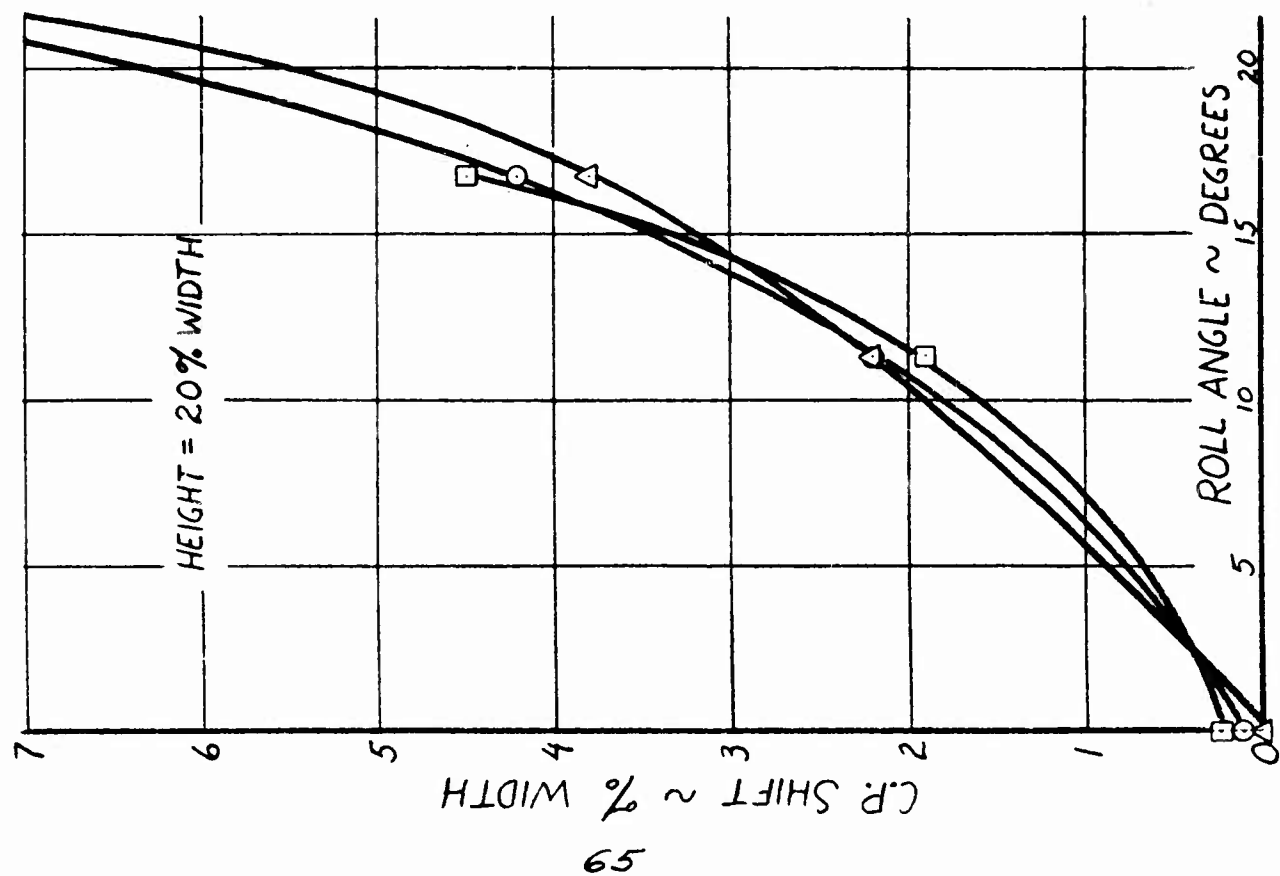
VERTICAL vs. 45° INCLINED JET



EFFECT OF BASE SHAPING ON BASE PLUS JET  
CENTER OF PRESSURE SHIFT



# CENTER OF PRESSURE SHIFT



○ CONVEX  
△ CONCAVE  
□ FLAT

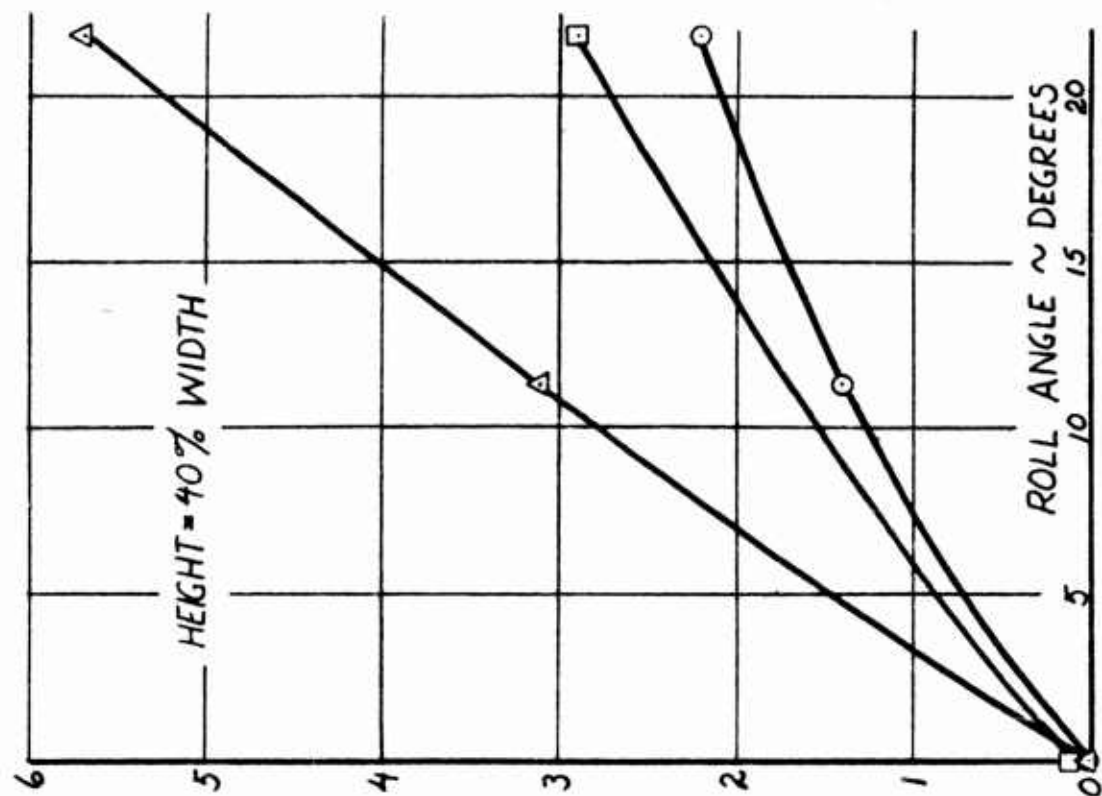


Figure 42



# EFFECT OF SKIRT AND FLAPS ON BASE PLUS JET CENTER OF PRESSURE SHIFT

Figure 43

C.P. SHIFT ~ % WIDTH

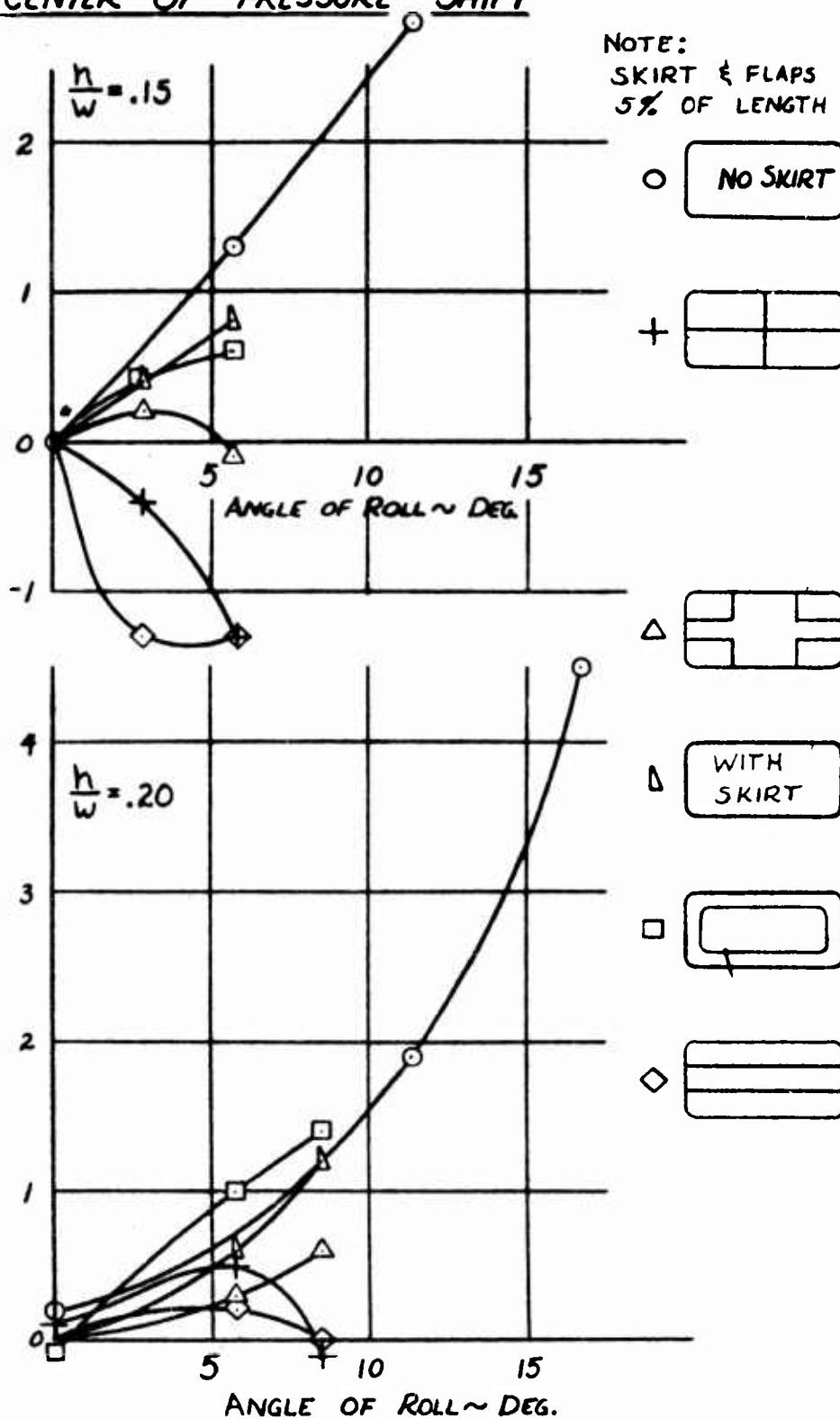
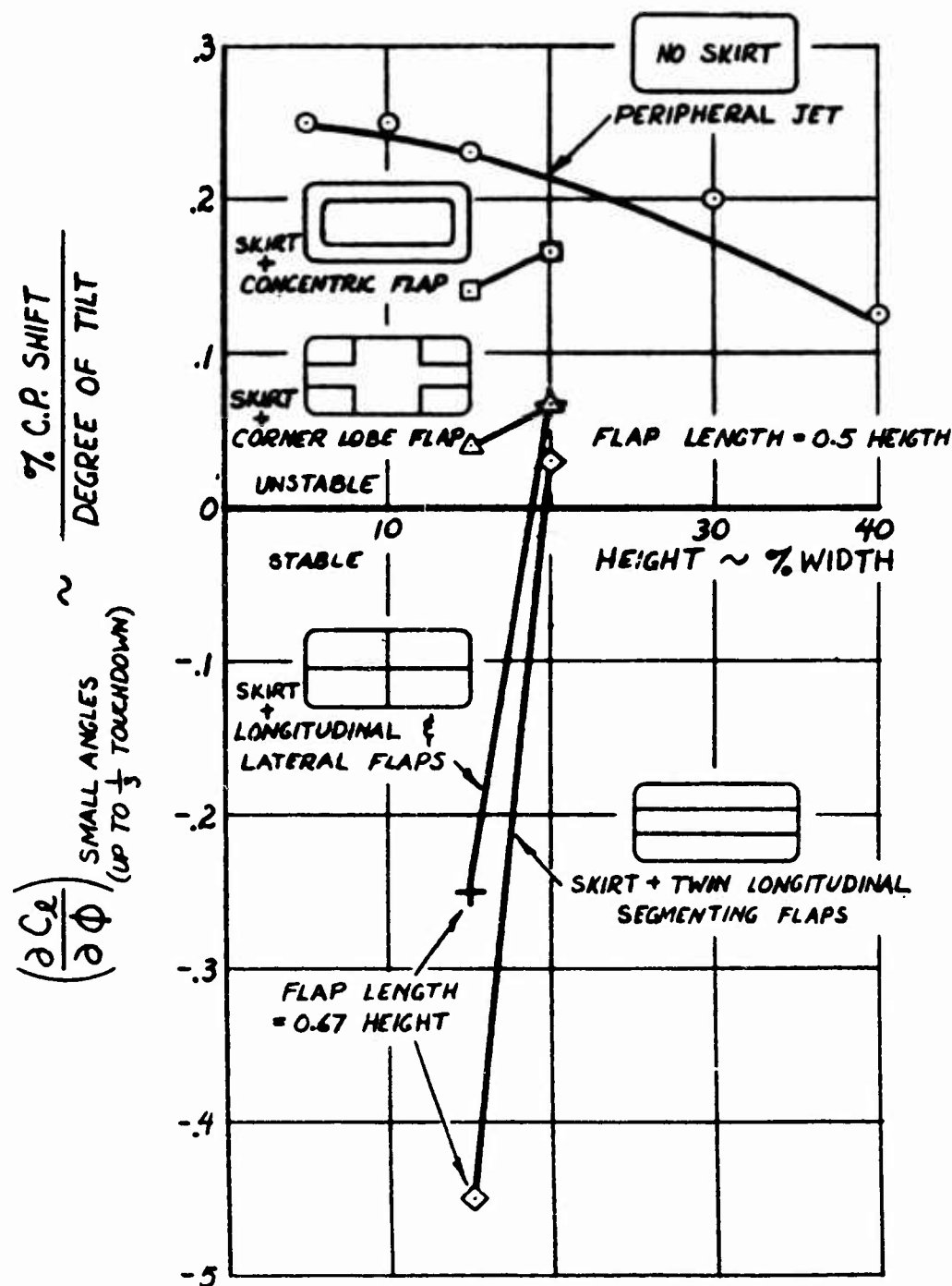


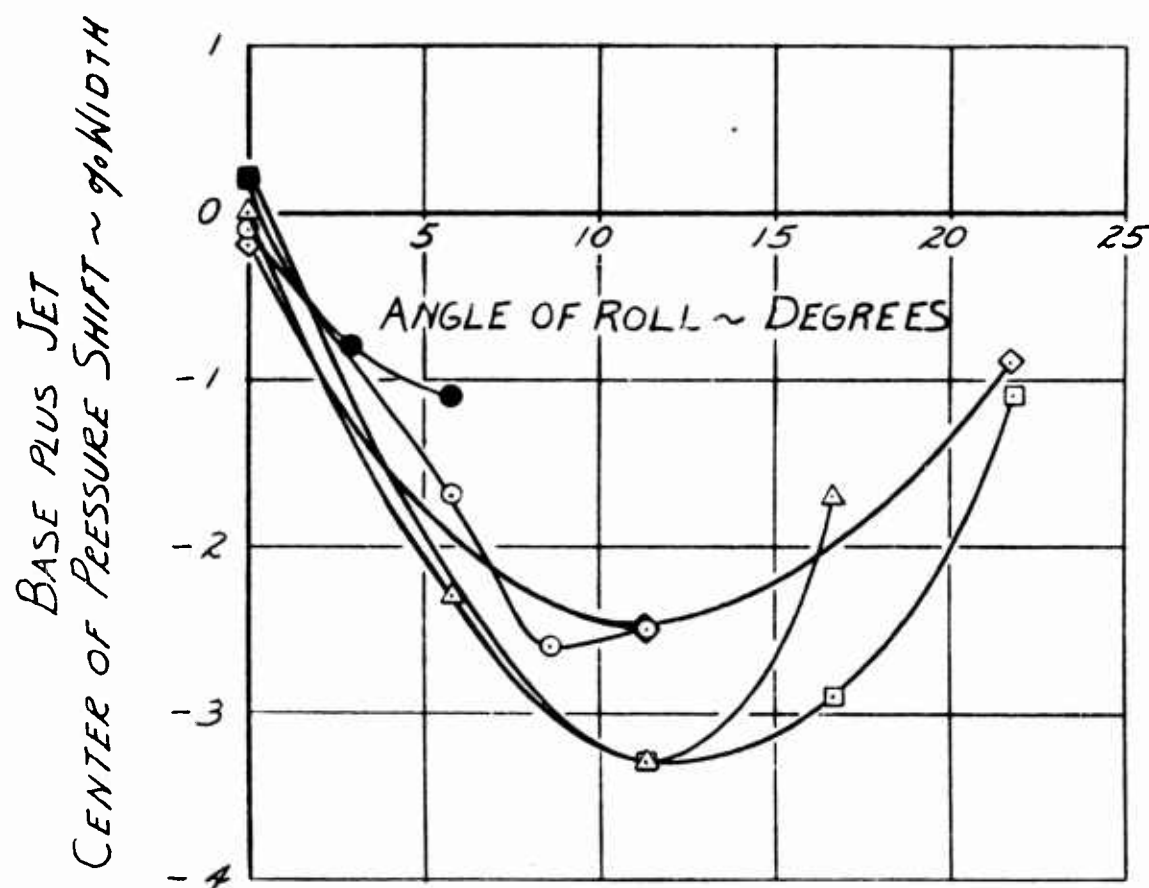
Figure 44

# EFFECT OF 5% LENGTH SKIRT AND FLAPS ON STATIC LATERAL HOVERING STABILITY

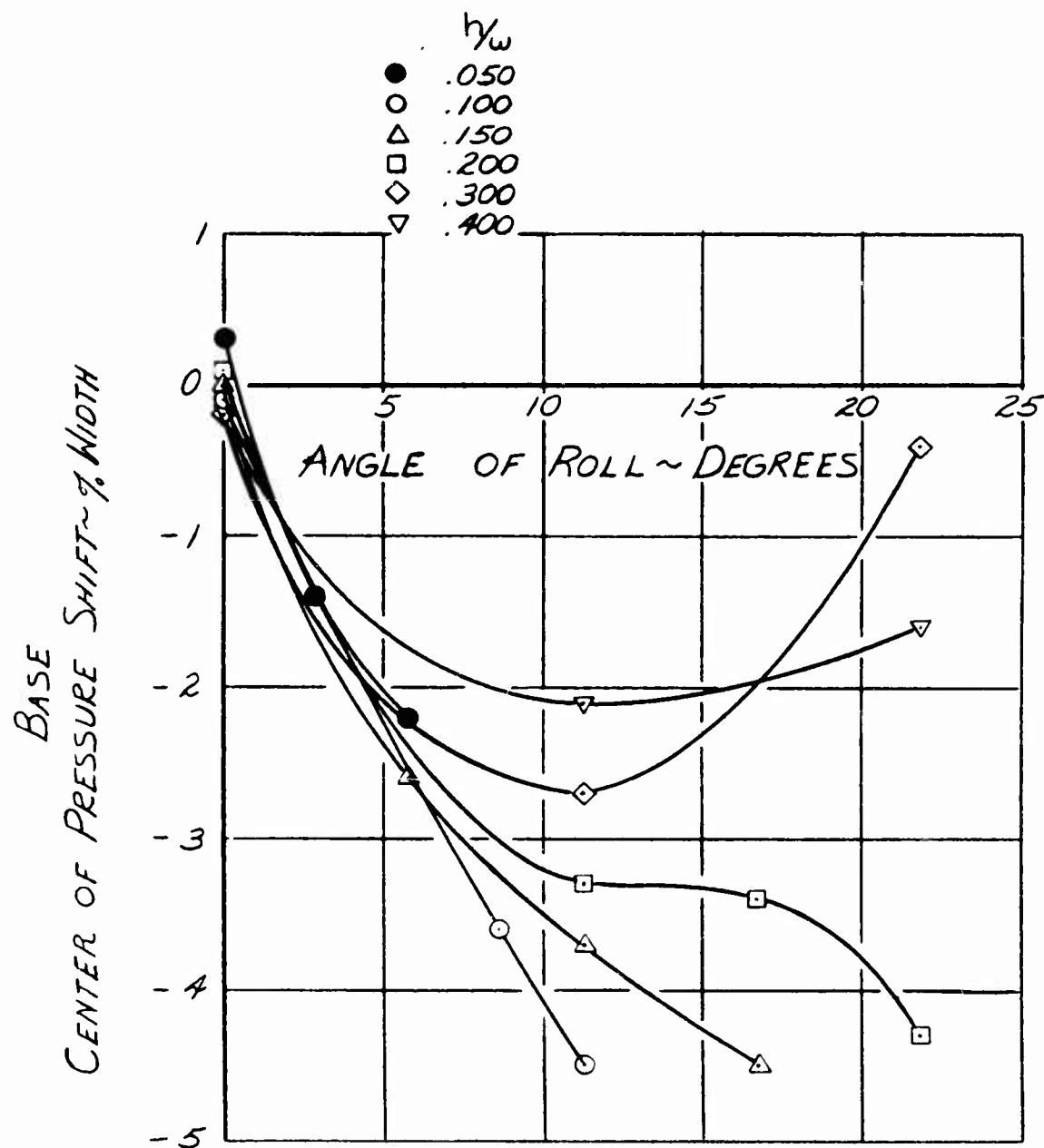


CENTERLINE JET SEGMENTED MODEL  
BASE PLUS JET  
CENTER OF PRESSURE SHIFT

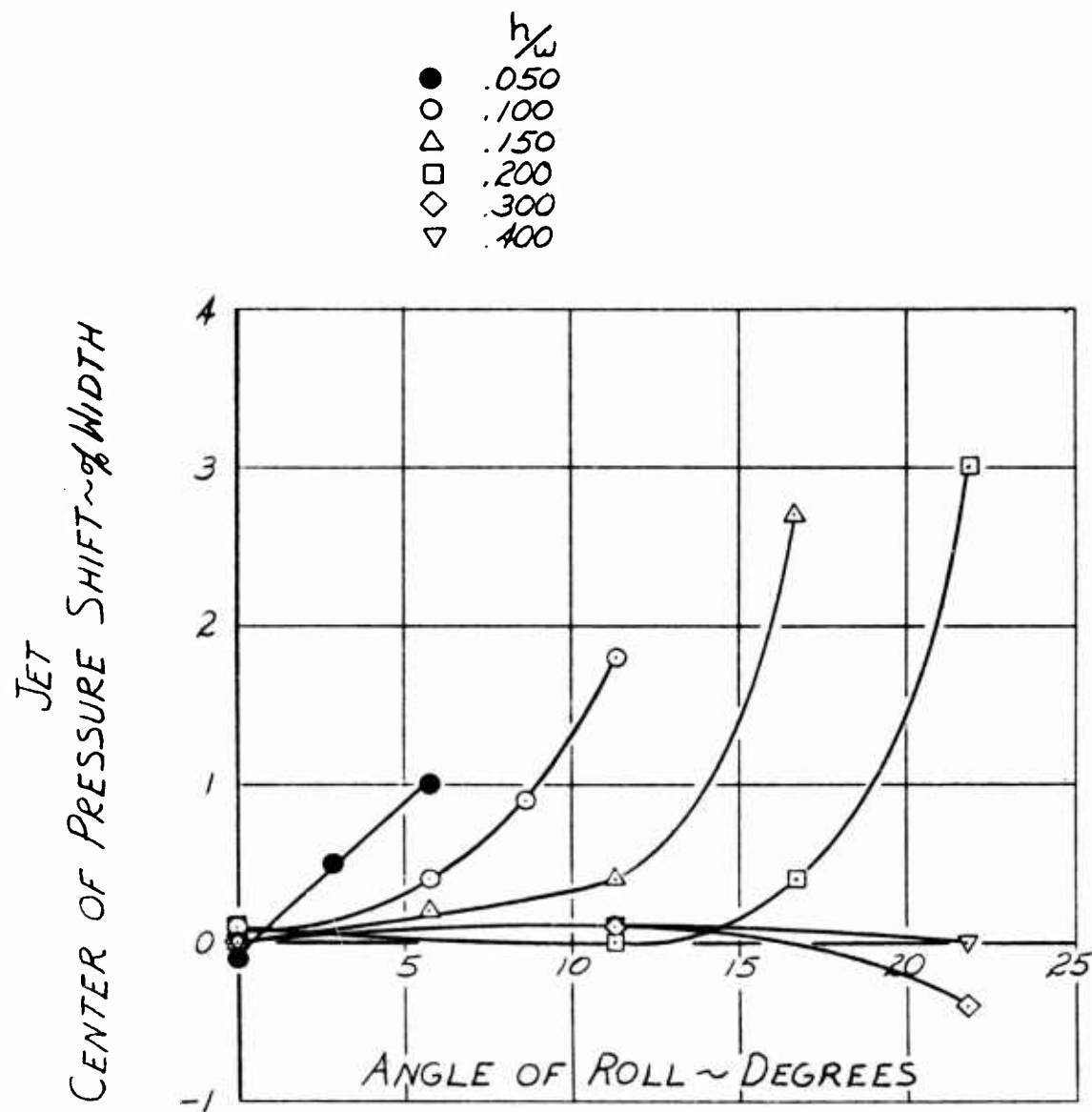
- $h_w$
- .050
  - .100
  - △ .150
  - .200
  - ◇ .300
  - ▽ .400



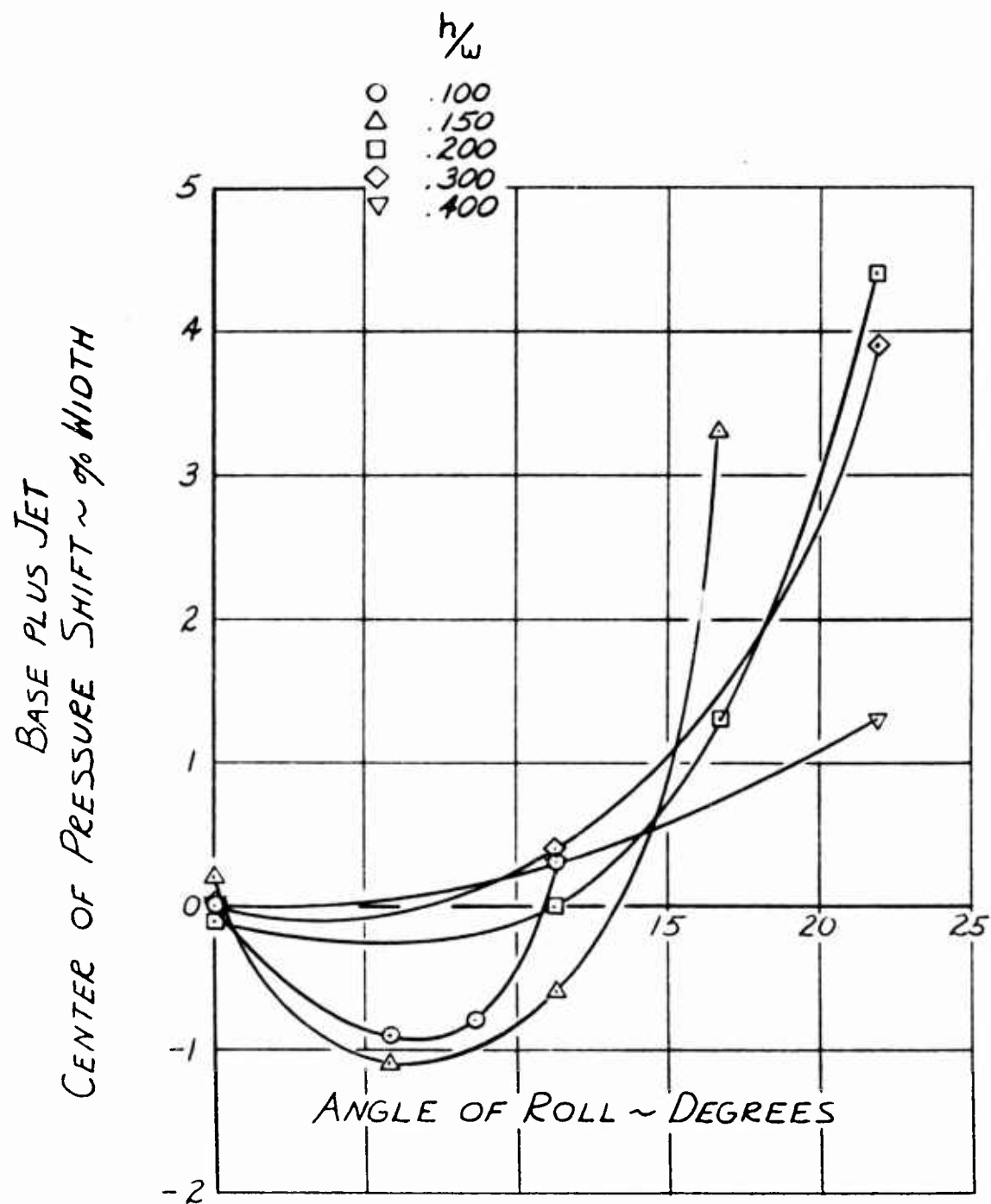
CENTERLINE JET SEGMENTED MODEL  
BASE  
CENTER OF PRESSURE SHIFT



CENTERLINE JET SEGMENTED MODEL  
JET  
CENTER OF PRESSURE SHIFT

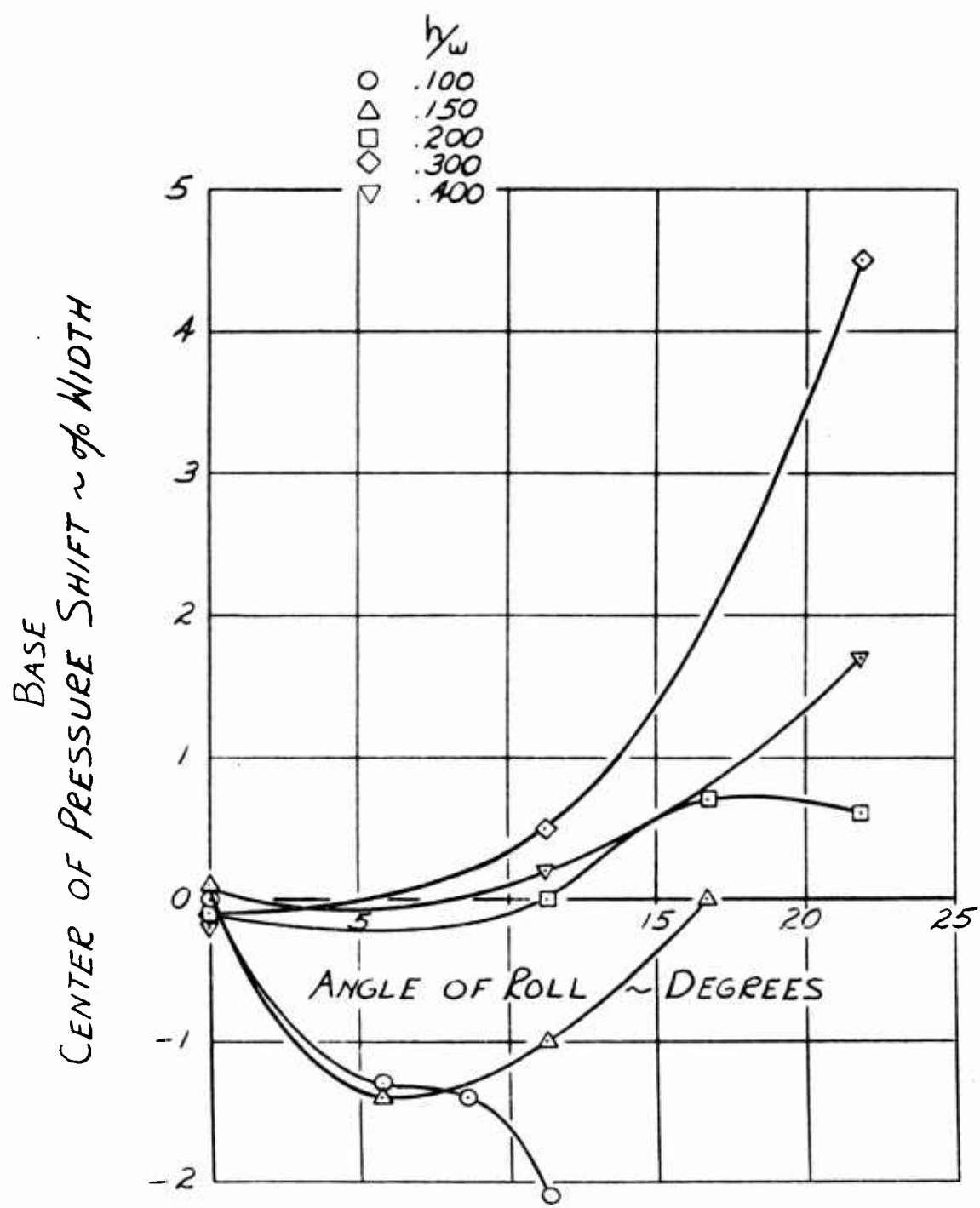


CORNER LOBE JET SEGMENTED MODEL  
BASE PLUS JET  
CENTER OF PRESSURE SHIFT

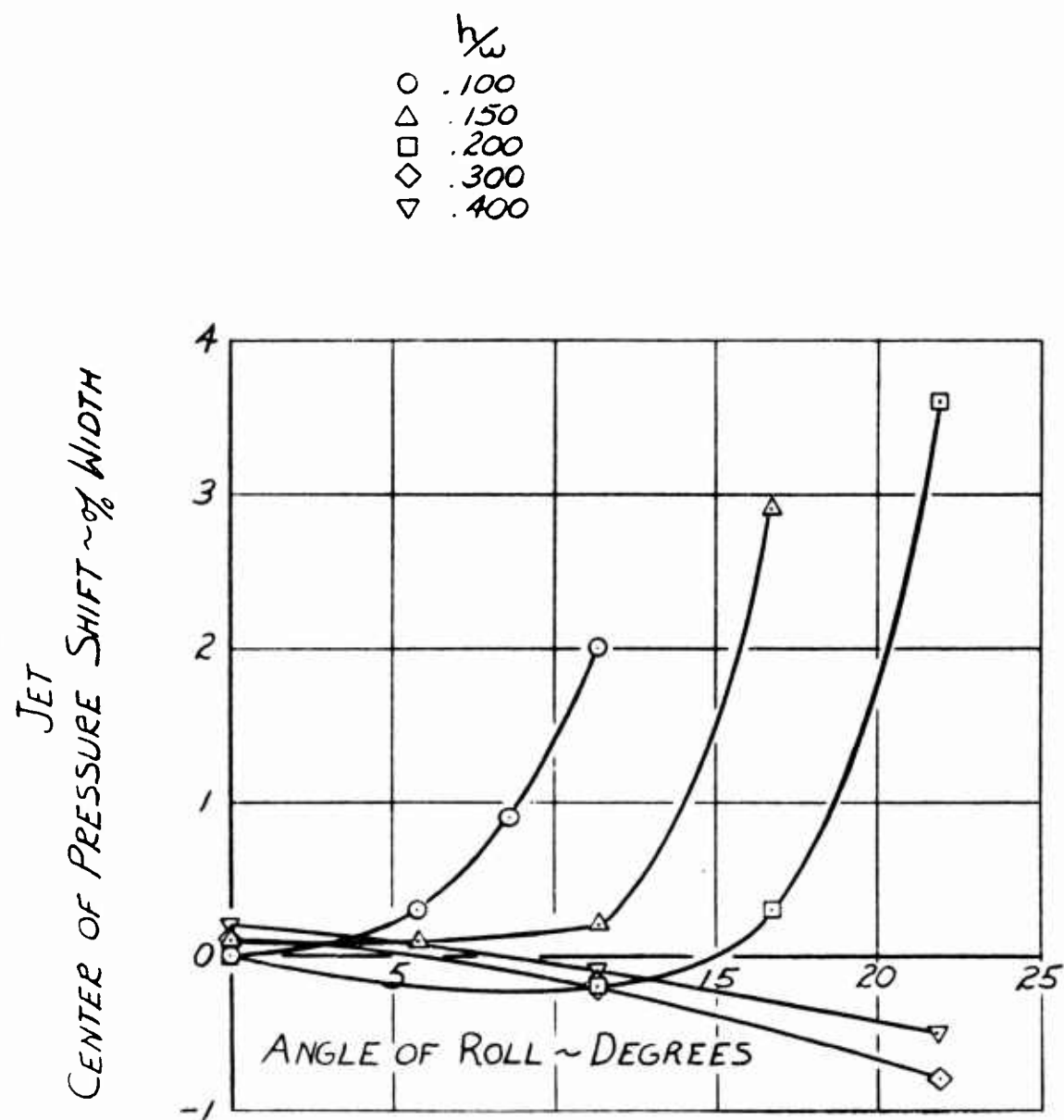


CORNER LOBE JET SEGMENTED MODEL

BASE  
CENTER OF PRESSURE SHIFT

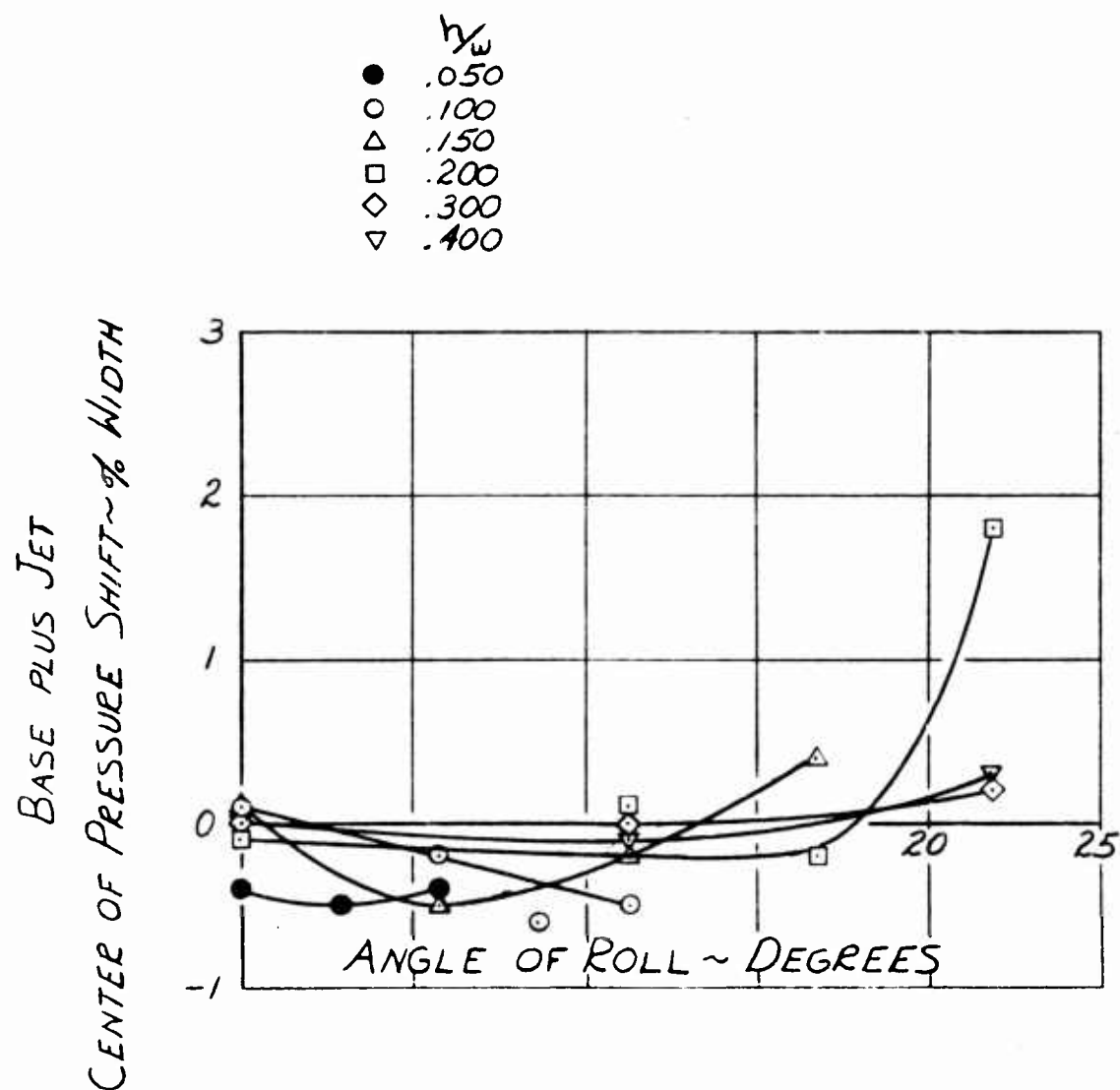


CORNER LOBE JET SEGMENTED MODEL  
JET  
CENTER OF PRESSURE SHIFT





CONCENTRIC JET SEGMENTED MODEL  
BASE PLUS JET  
CENTER OF PRESSURE SHIFT



CONCENTRIC JET SEGMENTED MODEL  
BASE  
CENTER OF PRESSURE SHIFT

- .050
- .100
- △ .150
- .200
- ◇ .300
- ▽ .400

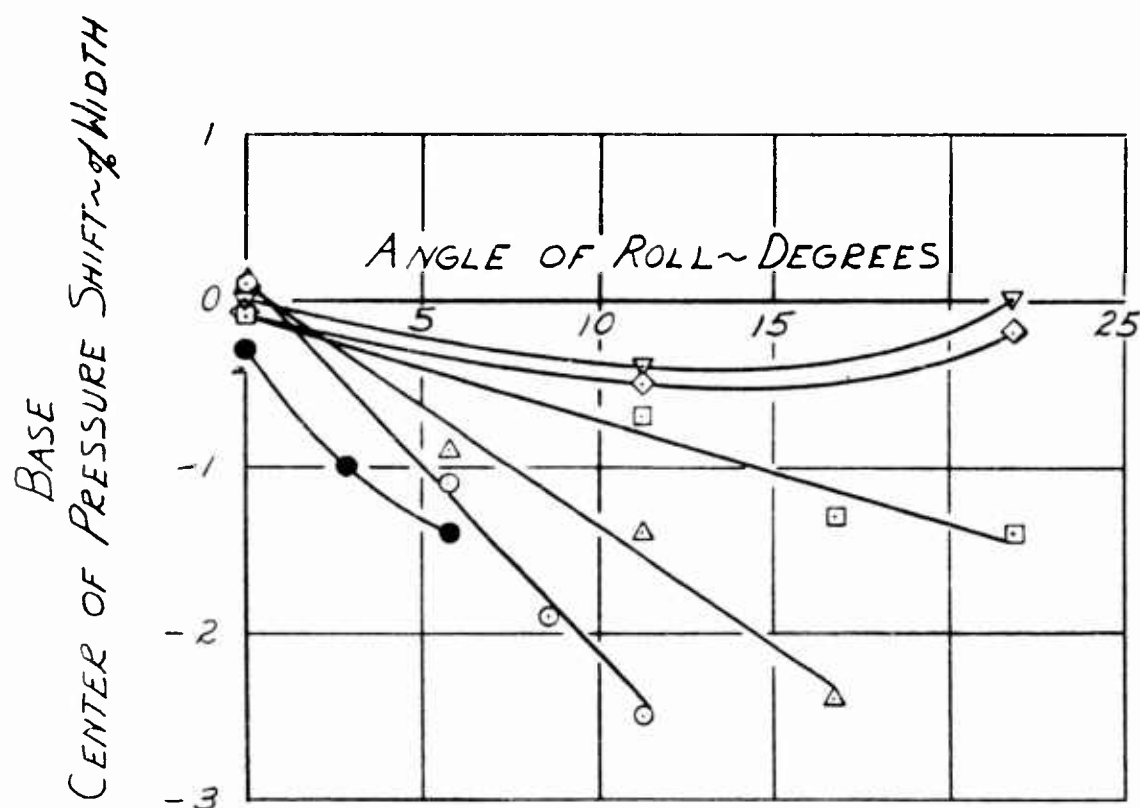


Figure 53

CONCENTRIC JET SEGMENTED MODEL  
JET  
CENTER OF PRESSURE SHIFT

- .050
- .100
- △ .150
- .200
- ◇ .300
- ▽ .400

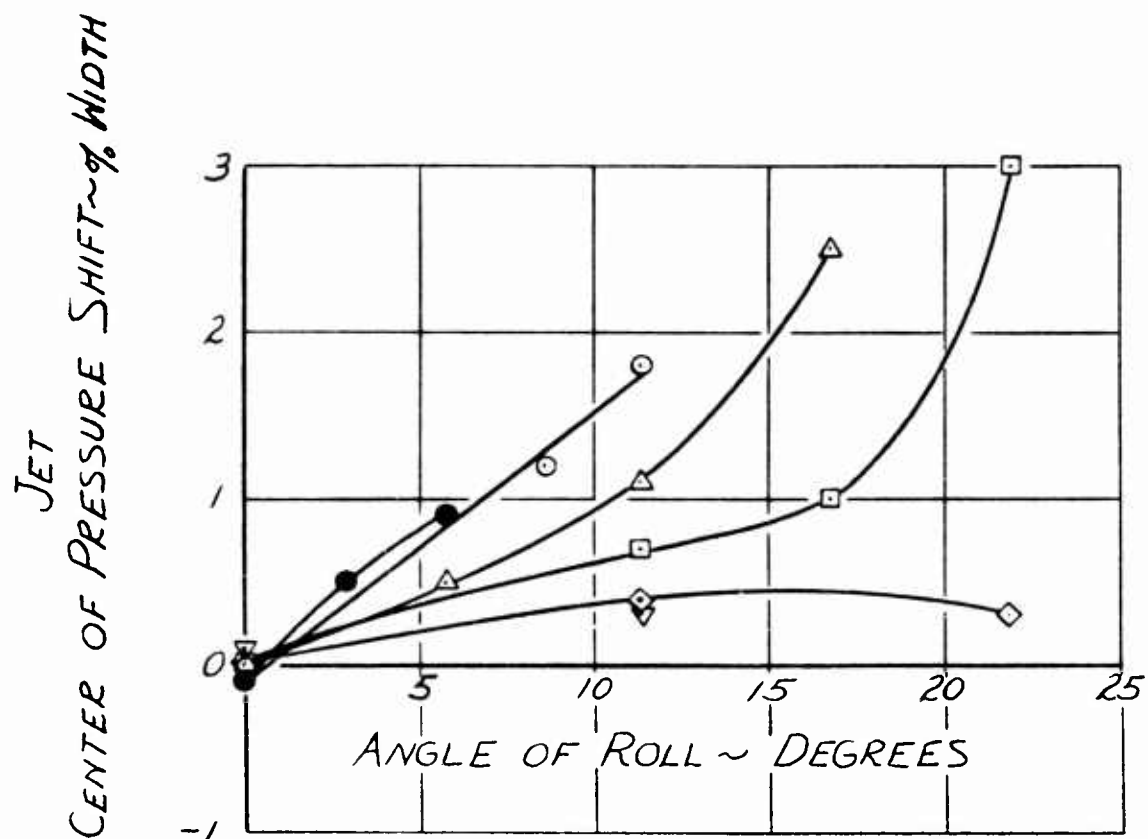
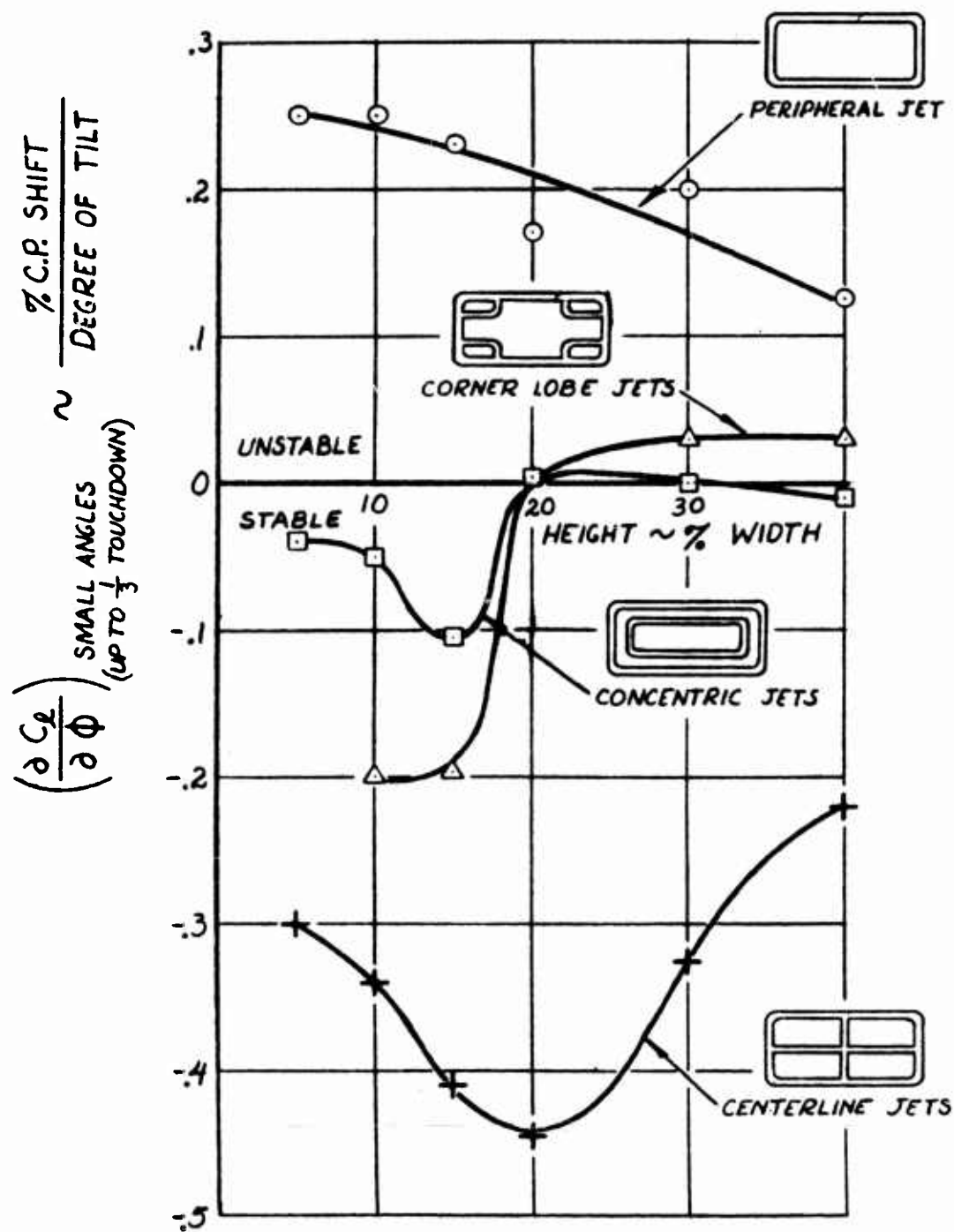
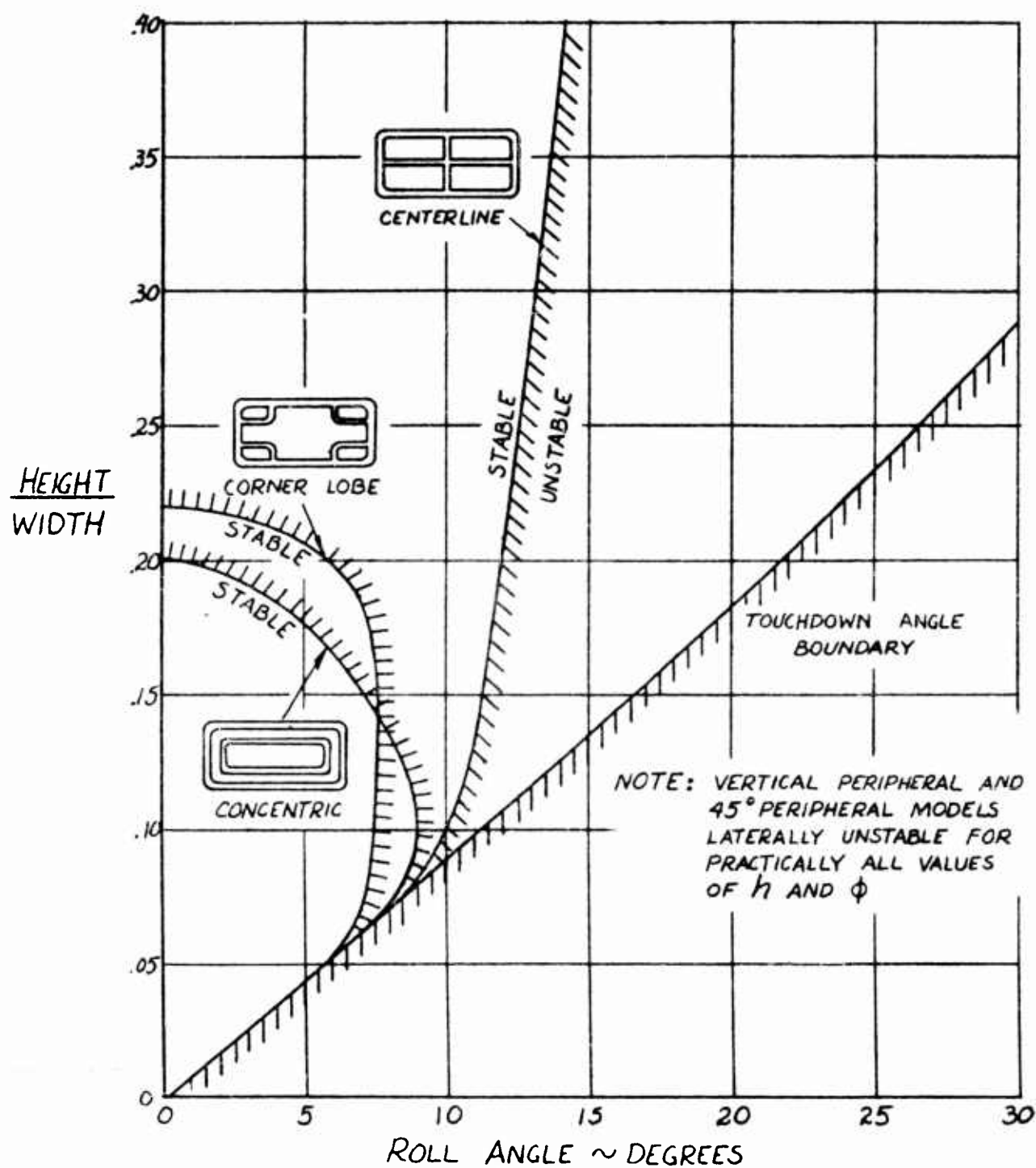


Figure 54

# EFFECT OF JET SEGMENTATION ON STATIC LATERAL HOVERING STABILITY



EFFECT OF JET SEGMENTATION  
ON HEIGHT-ROLL ANGLE STABILITY BOUNDARIES



### 3. Qualifications of the Stability Results

#### a. Response of the Flow Supply

It should be remembered that the results presented here are for a near ideal flow impeller and internal aerodynamic system. The Chicago Airfoil Centrifugal Fan output was not affected by model tilt. The internal aerodynamics were simple such that no unsymmetry in total head occurred due to tilt. The average total head on the low and high end of the models were within one-half of 1% of each other throughout the range of pitch and roll angles. This might not necessarily hold true of an actual air-cushion vehicle with an axial flow impeller and internal aerodynamics which are compromised because of space limitations.

#### b. Possible Contributions Not Measured in the Tests

The air loads which were integrated to provide the lift and moments in this work consisted of the load normal to the base and the reactions along the jets. Theoretical and experimental work on plenum chambers by Hunt of English Electric Company (Reference 7) has revealed a chord force in the plane of the base which can be appreciable for plenum chambers at large tilt angles. Unpublished recent experiments at Aeronutronic with a six-component force balance have indicated that although the chord force may be 10% of the normal force for a plenum chamber it does not exceed 2% of the normal force for a peripheral jet configuration. This was found to hold true for both simple and jet segmented models. Thus, it would appear that little, if any, inaccuracy has been introduced by the pressure integration method employed in these tests. It should be remembered that the moment center in these experiments was in the plane of the base. The center of gravity of any vehicle will be somewhat higher. Thus, chord forces, if present, will have an appreciable arm.

#### 4. Performance Aspects

##### a. Effect of Tilt of Lift

The stability data which has been presented was obtained with the model pitch axis at a fixed distance above the ground. In practice, the vehicle will lose lift and thus height as it tilts. It is therefore of interest to examine the rate at which the lift decreases with tilt angle.

The ratio of the lift (perpendicular to the ground) to the lift with model level was found for the vertical peripheral jet model to fall from 1.6 to 2.5% per degree of tilt. The lift loss is near the lower figure at very low and very high heights and near the high figure at intermediate heights. The range of values of lift loss per degree tilt is identical for the pitch and roll case.

The effect of several flap configurations on the lift loss at a base  $h/b = 0.10$  was examined. The concentric flap and twin longitudinal flap have the same rate of lift loss as the plain configuration. The corner lobe and centerline flap configurations reduce the rate of lift loss from 2.5%/deg to 2.0%/deg in both pitch and roll.

The effect of peripheral jet inclination and jet segmentation of the base on the lift loss at a base  $h/b = 0.10$  was also investigated. The basic vertical jet had a loss rate of 2.5% per degree, the  $45^\circ$  inclined peripheral jet and the concentric segmented jet models had a loss of 1.3% per degree, and the corner lobe and centerline jet segmented model had a loss of 0.4% per degree, in pitch. In roll, the curves are not as linear, but in general the rate varies from 1.0% per degree to 2.5% per degree. Increasing  $h/b$  to 0.15 or  $h/w$  to 0.30 reduces the loss rate in pitch and roll to 0.85 to 1.8%/deg.

b. Cost of Stabilization

Where special techniques of stabilization require power, it is of interest to determine the cost in performance.

The hovering performance of air-cushion vehicles is generally expressed as a power savings due to ground effect. This ground effect power factor  $G$  is the ratio of  $\frac{L}{P} \sqrt{\frac{L}{S}}$  of an ideal ducted rotor operating out of ground effect to that of the air-cushion vehicle in ground effect.

There are three possible ways to express the gain in hovering performance of an air-cushion vehicle compared to the ideal rotor out of ground effect once the value of  $G$  is given.

$$G = \frac{\frac{L^{3/2}}{P(s)^{1/2}} \text{ ideal}}{\frac{L^{3/2}}{P(s)^{1/2}} \text{ air-cushion}}$$

(1) Same Lift and Area

$$\frac{P_{AC}}{P_i} = G$$

(2) Same Power and Area

$$\frac{L_{AC}}{L_i} = \left(\frac{1}{G}\right)^{2/3}$$

(3) Same Power and Lift

$$\frac{S_{AC}}{S_i} = G^2$$

It should be noted that the results of comparison of  $G$  for the various configurations presented in the following paragraphs should not be generalized as the cost for hovering stabilization for all air-cushion vehicles. The configurations tested were compromised (with forward flight considerations in mind) away from optimum hovering values of jet thickness and angle. It is probable that the cost of hovering stabilization might come out differently

\* Jets were thinner and less inclined than optimum.



if one started with an optimum hovering configuration. The results presented here are believed of more practical interest, however, since the goal of air-cushion development effort is to produce a transportation system, not a hovering system. Considerable additional analysis work would be required to enable prediction of hovering performance and stability of a broad enough family of jet segmented planforms to permit analytical optimization.

A comparison of the experimental results obtained for the vertical peripheral jet with predicted results using the two-dimensional annular jet performance data and method of Reference 8 are presented in Figure 56. The agreement is quite good.

The vertical peripheral jet model requires only 30% of the ideal rotor power out of ground effect at  $h_l/S = 0.14$ . Above  $h_l/S = 0.63$  more power is required than for the ideal rotor out of ground effect. It should be remembered that this is exit power and does not include any internal flow losses. Actual air-cushion vehicles would become inferior to the ideal rotor at even lower values of  $h_l/S$ .

The skirted model data was also plotted vs.  $h_l/S$  where  $h$  was measured to the base, not the bottom of the skirt. Figure 56 shows that with the base at  $h_l/S = 0.42$ , the  $G$  was identical as the unskirted version at  $h_l/S = 0.14$ . The clearance to the bottom of the skirt  $h'/S$  was 0.14 when  $h_l/S$  was 0.42. This result indicates that at low skirt clearances the performance is as good as if the base were as low as the bottom of the skirt. At the higher height  $h_l/S = 0.56$ ,  $h'/S = 0.28$  the performance is close to, but not quite as good as if the base were at the bottom of the skirt.

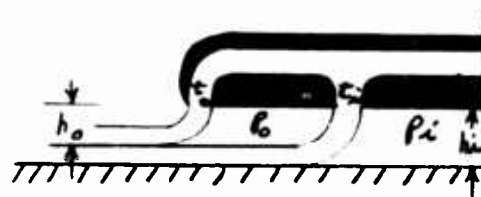
The  $G$  factors for the three types of jet segmented models are compared to the vertical peripheral jet model in Figure 57. The differences are very slight at  $h_l/S = 0.3$ .

At higher values of  $h_l/S$ , the corner lobe and centerline jet segmented models are inferior to the vertical peripheral jet model and become inferior to the ideal rotor out of ground effect at  $h_l/S = 0.58$ . The concentric vertical jet model is superior to the vertical peripheral jet model at all values of  $h_l/S$  and remains superior to the ideal ducted rotor out of ground effect up to  $h_l/S = 0.73$ . It was disappointing that the concentric jet did not do a better job of lateral stabilization, since its performance is superior to the other configurations. The penalty in  $L^{3/2}/\dot{p}$  for both the centerline and corner lobe jet segmented models was 8% at  $h_l/S = 0.6$  and only 4% at  $h_l/S = 1.0$ . The concentric jet exhibited an improvement in  $L^{3/2}/\dot{p}$  of 8% at  $h_l/S = 0.6$  and 11.5% at  $h_l/S = 1.0$ .

Comparative performance and stability of the vertical peripheral jet model and the centerline jet segmented model at two heights is presented in Figure 58. The centerline jet segmented model provided superior stability at the higher heights and the performance penalty was not severe.

The performance results for the concentric jet model were unusual enough to raise suspicion as to the experimental validity. The  $G$  values of the concentric jet model were more favorable than those for the basic peripheral jet.

A simple concentric theory was developed by the author to allow lift and power estimations based on the two-dimensional data and methods previously mentioned. The outer jet was assumed to flow out over the inner jet. The value



of  $p_o$  was based on  $t_o/h_o$  where  $h_o = h_i - t_i$ . The value for  $p_i = p_o + \Delta p_i$  where  $\Delta p_i$  was based on  $t_i/h_i$ . The

inner jet was assumed to face a back pressure of  $(p_o + p_i)/2$  and the outer jet was assumed to face a back pressure of  $p_o/2$ . Both jets were assumed to be at the same total pressure as in the experiment.

This simple theory at  $h_l/S = 0.56$  predicted 41% more lift for the concentric than for the simple peripheral jet, whereas the experiment produced 37% more. The theory predicted 45% more power for the concentric than for the basic, whereas the experiment produced 49% more power. The theoretical ratio of  $L^{3/2}/P$  was 15% larger for the concentric according to the simple theory, whereas it was only 8% larger in the experiment. At least the theory confirmed that the hovering performance of the simple non-optimum peripheral jet could be improved by increasing the jet thickness even with a concentric arrangement as indicated by the experiment. One should not infer from this, however, that optimum concentric jets are superior in performance to optimum simple peripheral jets. In fact, for the case of near optimum thickness, the pure peripheral jet will be superior in hovering performance to the concentric arrangement.

HOVERING PERFORMANCE  
VERTICAL PERIPHERAL JET

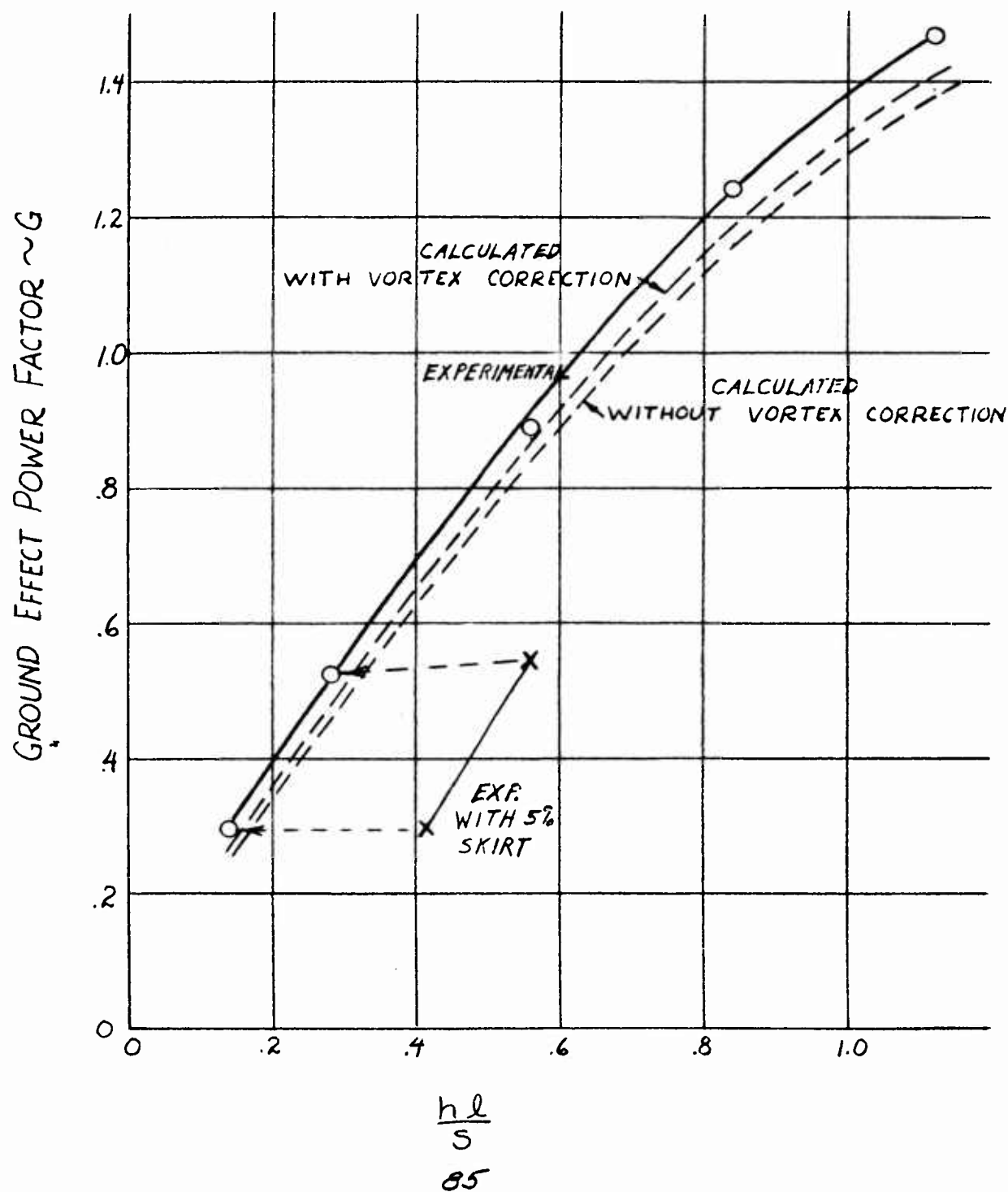
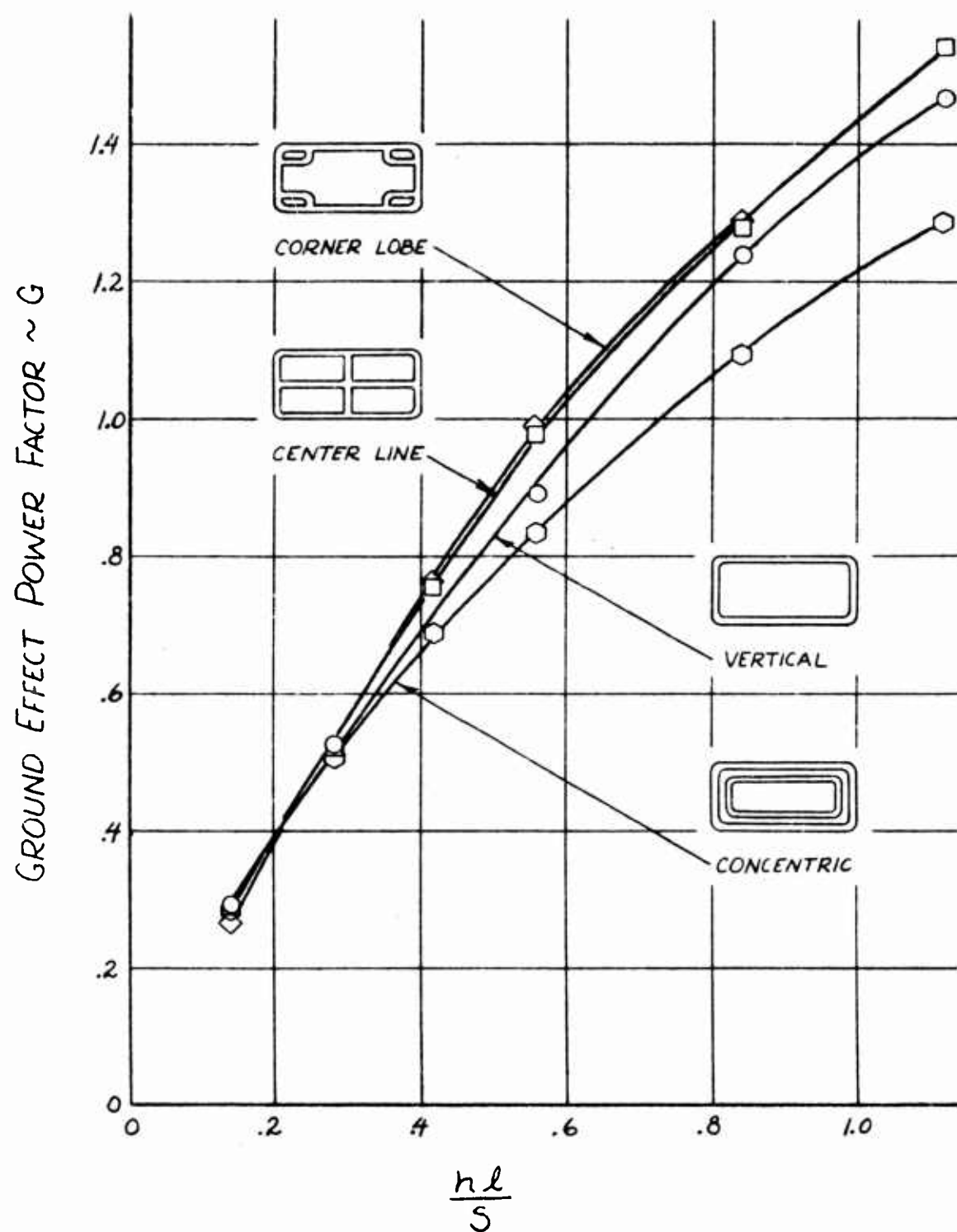




Figure 57

# HOVERING PERFORMANCE JET SEGMENTED MODELS



# STABILITY IMPROVEMENT AND PERFORMANCE COST DUE TO JET SEGMENTATION

	ITEM	PERIPHERAL JET	SEGMENTED JET
			
	PLANFORM AREA	1.0	1.0
	JET AREA	1.0	1.48
$\frac{\text{HEIGHT}}{\text{LENGTH}} = .10$	$\frac{\partial C_m}{\partial \alpha} \sim \frac{\% \text{C.P. SHIFT}}{\text{DEG. TILT}}$	.2 UNSTABLE	-.66 STABLE
	$\frac{\partial C_L}{\partial \phi} \sim \frac{\% \text{C.P. SHIFT}}{\text{DEG. TILT}}$	.2 UNSTABLE	-.45 STABLE
	LIFT / JET POWER	1.0	.835
	$(\text{LIFT})^{\frac{3}{2}} / \text{JET POWER}$	1.0	.915
$\frac{\text{HEIGHT}}{\text{LENGTH}} = .20$	$\frac{\partial C_m}{\partial \alpha} \sim \frac{\% \text{C.P. SHIFT}}{\text{DEG. TILT}}$	.25 UNSTABLE	-.17 STABLE
	$\frac{\partial C_L}{\partial \phi} \sim \frac{\% \text{C.P. SHIFT}}{\text{DEG. TILT}}$	.125 UNSTABLE	-.22 STABLE
	LIFT / JET POWER	1.0	.856
	$(\text{LIFT})^{\frac{3}{2}} / \text{JET POWER}$	1.0	.965

### ACKNOWLEDGEMENTS

The model designs were rapidly and ably executed by Mr. R. L. Noble. Mr. E. Bentzen installed the models on the hovering tower and conducted the experiments including photo recording of the data. The pressure integrations were performed on the Aeronutronic 709 Computer under the supervision of Mr. D. Stewart. Data reduction and curve plotting were accomplished by Mrs. K. Kuperus and Mrs. J. Herron. Report typing was by Mrs. A. Rasmussen.

## BIBLIOGRAPHY

1. Carmichael, B. H.  
Aeronutronic, a Division of Ford Motor Company  
HOVERING ANNULAR JET STABILITY EXPERIMENTS  
Aeronutronic Publication No. U-1057  
November 1960
2. Aeronutronic, a Division of Ford Motor Company  
STUDY OF STABILITY AND CONTROL OF AIR-CUSHION  
VEHICLES FOR OVERLAND USE (Proposal)  
VOLUME I OF II --- TECHNICAL APPROACH  
Aeronutronic Publication No. U-1039 - Proposal No. P-11570 (U)  
24 October 1960
3. Carmichael, B. H.  
Aeronutronic, a Division of Ford Motor Company  
PRE-TEST MEMORANDUM --- PHASE II Wind Tunnel Tests  
Contract No. DA 44-177-TC-709  
Aeronutronic Memo No. ACVD 61-122  
22 June 1961
4. Carmichael, B. H. and McNay, D. E.  
Aeronutronic, a Division of Ford Motor Company  
OVERLAND AIR-CUSHION VEHICLE STABILITY AND CONTROL  
WIND TUNNEL EXPERIMENTS  
Aeronutronic Publication No. U-1447  
10 November 1961
5. Kuhn, R. E. and Carter, A. W.  
RESEARCH RELATED TO GROUND EFFECT MACHINES  
Princeton Symposium  
October 1959
6. Higgins, H. C. and Martin, L. W.  
EFFECTS OF SURFACE GEOMETRY AND VEHICLE MOTION  
ON FORCES PRODUCED BY A GROUND PRESSURE ELEMENT  
Princeton Symposium  
October 1959



REFERENCES, continued...

7. Hunt, R. D. and Lopez, M. L.  
GEM STABILITY AND CONTROL EXPERIMENTAL RESULTS  
English Electric Aviation Limited Preliminary Report  
1961
8. Carmichael, B. H.  
Aeronutronic, a Division of Ford Motor Company  
HOVERING TWO-DIMENSIONAL ANNULAR JET PERFORMANCE  
EXPERIMENTS  
Aeronutronic Publication No. U-1053  
November 1960

# DISTRIBUTION

USAWC	1
USATMC(FTZAT), ATO	1
USAPRDC	1
DCSLOG	1
Rsch Anal Corp	1
ARO, Durham	2
OCRD, DA	2
Ofc of Maint Engr, ODDR&E, OSD	1
NATC	1
ARO, OCRD	1
DCSOPS	1
USAERDL	2
USAOTAC, Center Line	3
OrdBd	1
QMRECOMD	1
CofT	3
USATCDG	1
USATMC	19
USATSCH	4
USATRECOM	77
TCLO, USAERDL	1
TCLO, USAABELCTBD	1
USATRECOM LO, USARDG(EUR)	3
CNO	1
CNR	3
BUWEPS, DN	1
BUWEPS, DN (RA-4)	1
ACRD(OW), DN	1
USNSRDF	1
USNPGSCH	1
BUSHP, DN	1
USNOTS	1
Dav Tay Mod Bas	2
MCLFDC	1
MCEC	1
USASGCA	1
Canadian LO, USATSCH	3
BRAS, DAQMG(Mov&Tn)	4
USASG, UK	1
Langley Rsch Cen, NASA	3

NASA, Wash., D. C.	6
Ames Rsch Cen, NASA	2
Lewis Rsch Cen, NASA	1
USGPO	1
ASTIA	10
USAMRDC	1
HUMRRO	2
DDRE	1
Maritime Administration	1
Human Engineering Lab	1

Aeronutronic Division, Ford Motor Company, Newport Beach, California  
HOVERING STATIC STABILITY AND PERFORMANCE EXPERIMENTS ON THREEDIMENSIONAL ANNULAR JET MODELS, by B. H. Carmichael, D. E. McNay.  
Report No U-1447, November 1961 (Contract DA44-177-TC-709) Task 9R99-01-005-02. 90p. incl. illus. (TCREC Technical Report 62-36)

1. Fluid Dynamics, Aerodynamics
2. Stability & Control

Aeronutronic Division, Ford Motor Company, Newport Beach, California  
HOVERING STATIC STABILITY AND PERFORMANCE EXPERIMENTS ON THREEDIMENSIONAL ANNULAR JET MODELS, by B. H. Carmichael, D. E. McNay.  
Report No U-1447, November 1961 (Contract DA44-177-TC-709) Task 9R99-01-005-02. 90p. incl. illus. (TCREC Technical Report 62-36)

1. Fluid Dynamics, Aerodynamics
2. Stability & Control

#### Unclassified Report

The static stability in pitch, roll, and yaw of a generalized annular jet GEM has been determined in hover and (over)

Aeronutronic Division, Ford Motor Company, Newport Beach, California  
HOVERING STATIC STABILITY AND PERFORMANCE EXPERIMENTS ON THREEDIMENSIONAL ANNULAR JET MODELS, by B. H. Carmichael, D. E. McNay.  
Report No U-1447, November 1961 (Contract DA44-177-TC-709) Task 9R99-01-005-02. 90p. incl. illus. (TCREC Technical Report 62-36)

1. Fluid Dynamics, Aerodynamics
2. Stability & Control

Aeronutronic Division, Ford Motor Company, Newport Beach, California  
HOVERING STATIC STABILITY AND PERFORMANCE EXPERIMENTS ON THREEDIMENSIONAL ANNULAR JET MODELS, by B. H. Carmichael, D. E. McNay.  
Report No U-1447, November 1961 (Contract DA44-177-TC-709) Task 9R99-01-005-02. 90p. incl. illus. (TCREC Technical Report 62-36)

1. Fluid Dynamics, Aerodynamics
2. Stability & Control

#### Unclassified Report

The static stability in pitch, roll, and yaw of a generalized annular jet GEM has been determined in hover and (over)

Aeronutronic Division, Ford Motor Company, Newport Beach, California  
HOVERING STATIC STABILITY AND PERFORMANCE EXPERIMENTS ON THREEDIMENSIONAL ANNULAR JET MODELS, by B. H. Carmichael, D. E. McNay.  
Report No U-1447, November 1961 (Contract DA44-177-TC-709) Task 9R99-01-005-02. 90p. incl. illus. (TCREC Technical Report 62-36)

#### Unclassified Report

The static stability in pitch, roll, and yaw of a generalized annular jet GEM has been determined in hover and (over)

#### Unclassified Report

The static stability in pitch, roll, and yaw of a generalized annular jet GEM has been determined in hover and (over)

forward flight at ratios of  $h/d$  exceeding 0.1, the normal stability limit. The effects of modifications to the basic configuration, including full and partial skirting, were determined. In addition to stability data, control forces and some performance and pressure distribution data were obtained. The hovering and the forward flight investigations are presented in separate reports (TCREC Tech Rpts 62-35 and 62-36). A report, Vought Aeronautics LSWT 105, dated December 1961, containing basic wind tunnel test data is available, on loan, from the Research Reference Center, USA TRECOM.

forward flight at ratios of  $h/d$  exceeding 0.1, the normal stability limit. The effects of modifications to the basic configuration, including full and partial skirting, were determined. In addition to stability data, control forces and some performance and pressure distribution data were obtained. The hovering and the forward flight investigations are presented in separate reports (TCREC Tech Rpts 62-35 and 62-36). A report, Vought Aeronautics LSWT 105, dated December 1961, containing basic wind tunnel test data is available, on loan, from the Research Reference Center, USA TRECOM.

forward flight at ratios of  $h/d$  exceeding 0.1, the normal stability limit. The effects of modifications to the basic configuration, including full and partial skirting, were determined. In addition to stability data, control forces and some performance and pressure distribution data were obtained. The hovering and the forward flight investigations are presented in separate reports (TCREC Tech Rpts 62-35 and 62-36). A report, Vought Aeronautics LSWT 105, dated December 1961, containing basic wind tunnel test data is available, on loan, from the Research Reference Center, USA TRECOM.

forward flight at ratios of  $h/d$  exceeding 0.1, the normal stability limit. The effects of modifications to the basic configuration, including full and partial skirting, were determined. In addition to stability data, control forces and some performance and pressure distribution data were obtained. The hovering and the forward flight investigations are presented in separate reports (TCREC Tech Rpts 62-35 and 62-36). A report, Vought Aeronautics LSWT 105, dated December 1961, containing basic wind tunnel test data is available, on loan, from the Research Reference Center, USA TRECOM.

Aeronutronic Division, Ford Motor Company, Newport Beach, California  
HOVERING STATIC STABILITY AND PERFORMANCE EXPERIMENTS ON THREE-DIMENSIONAL ANNULAR JET MODELS, by B. H. Carmichael, D. E. McNay.  
Report No U-1447, November 1961 (Contract DA44-177-TC-709) Task 9R99-01-005-02. 90p. incl. illus. (TCREC Technical Report 62-36)

1. Fluid Dynamics, Aerodynamics

2. Stability & Control

Aeronutronic Division, Ford Motor Company, Newport Beach, California  
HOVERING STATIC STABILITY AND PERFORMANCE EXPERIMENTS ON THREE-DIMENSIONAL ANNULAR JET MODELS, by B. H. Carmichael, D. E. McNay.  
Report No U-1447, November 1961 (Contract DA44-177-TC-709) Task 9R99-01-005-02. 90p. incl. illus. (TCREC Technical Report 62-36)

1. Fluid Dynamics, Aerodynamics

2. Stability & Control

#### Unclassified Report

The static stability in pitch, roll, and yaw of a generalized annular jet GEM has been determined in hover and (over)

Aeronutronic Division, Ford Motor Company, Newport Beach, California  
HOVERING STATIC STABILITY AND PERFORMANCE EXPERIMENTS ON THREE-DIMENSIONAL ANNULAR JET MODELS, by B. H. Carmichael, D. E. McNay.  
Report No U-1447, November 1961 (Contract DA44-177-TC-709) Task 9R99-01-005-02. 90p. incl. illus. (TCREC Technical Report 62-36)

1. Fluid Dynamics, Aerodynamics

2. Stability & Control

Aeronutronic Division, Ford Motor Company, Newport Beach, California  
HOVERING STATIC STABILITY AND PERFORMANCE EXPERIMENTS ON THREE-DIMENSIONAL ANNULAR JET MODELS, by B. H. Carmichael, D. E. McNay.  
Report No U-1447, November 1961 (Contract DA44-177-TC-709) Task 9R99-01-005-02. 90p. incl. illus. (TCREC Technical Report 62-36)

1. Fluid Dynamics, Aerodynamics

2. Stability & Control

#### Unclassified Report

The static stability in pitch, roll, and yaw of a generalized annular jet GEM has been determined in hover and (over)

#### Unclassified Report

The static stability in pitch, roll, and yaw of a generalized annular jet GEM has been determined in hover and (over)

forward flight at ratios of  $h/d$  exceeding 0.1, the normal stability limit. The effects of modifications to the basic configuration, including full and partial skirting, were determined. In addition to stability data, control forces and some performance and pressure distribution data were obtained. The hovering and the forward flight investigations are presented in separate reports (TCREC Tech Rpts 62-35 and 62-36). A report, Vought Aeronautics LSWT 105, dated December 1961, containing basic wind tunnel test data is available, on loan, from the Research Reference Center, USA TRECOM.

forward flight at ratios of  $h/d$  exceeding 0.1, the normal stability limit. The effects of modifications to the basic configuration, including full and partial skirting, were determined. In addition to stability data, control forces and some performance and pressure distribution data were obtained. The hovering and the forward flight investigations are presented in separate reports (TCREC Tech Rpts 62-35 and 62-36). A report, Vought Aeronautics LSWT 105, dated December 1961, containing basic wind tunnel test data is available, on loan, from the Research Reference Center, USA TRECOM.

forward flight at ratios of  $h/d$  exceeding 0.1, the normal stability limit. The effects of modifications to the basic configuration, including full and partial skirting, were determined. In addition to stability data, control forces and some performance and pressure distribution data were obtained. The hovering and the forward flight investigations are presented in separate reports (TCREC Tech Rpts 62-35 and 62-36). A report, Vought Aeronautics LSWT 105, dated December 1961, containing basic wind tunnel test data is available, on loan, from the Research Reference Center, USA TRECOM.

forward flight at ratios of  $h/d$  exceeding 0.1, the normal stability limit. The effects of modifications to the basic configuration, including full and partial skirting, were determined. In addition to stability data, control forces and some performance and pressure distribution data were obtained. The hovering and the forward flight investigations are presented in separate reports (TCREC Tech Rpts 62-35 and 62-36). A report, Vought Aeronautics LSWT 105, dated December 1961, containing basic wind tunnel test data is available, on loan, from the Research Reference Center, USA TRECOM.

UNCLASSIFIED

UNCLASSIFIED